Study of the Rate-limiting Step on Extracellular Electron Transfer of *Shewanella oneidensis* MR-1

（*Shewanella oneidensis* MR-1 の細胞外電子伝達の律速段階に関する研究）

HUANG WENYUAN

Graduate School of Chemical Sciences and Engineering

Hokkaido University

2023

Table of contents

Chapter 1 Introduction

1.1 Extracellular electron transfer

The process of cellular respiration can be simplified to the electron transfer pathway (Fernie et al., 2004), in this process, electrons are transferred by the electron transfer proteins which are located on the mitochondria in the eukaryotic cells or cell inner membrane in prokaryotic cells (Bennett & San, 2017; Fontanesi). An amount of adenosine triphosphate (ATP) was produced in this process (Raymond et al., 1985). Aerobic respiration is a widely used way for cells, the electron acceptor is oxygen, which is coupled with energy generation (Dilling & Cypionka, 1990; Pedersen et al., 2012). However, under lacking oxygen, anaerobic respiration was mainly used to produce energy (Lovley & Coates, 2000), a diversity of electron acceptors instead of oxygen were used in anaerobic respiration (Gregory et al., 2004; Hedderich et al., 1998; Lovley et al., 1999). Electrons are accepted by the endogenous intermediate metabolites in the fermentation process, which is related to microbial metabolism (Schäpper et al., 2009). Extracellular electron transfer is one type of cellular respiration under an oxygen-limited environment, metal can be an electron acceptor to anaerobic respiration in dissimilatory metal-reducing bacteria (DMRB), the most common metals are iron and manganese (Fe^{3+} to Fe^{2+}, Mn^{4+} to Mn^{2+}) (Nealson & Saffarini, 1994). In the process of metal reduction, the electron from inside of cells was transferred to the outside by the extracellular electron transfer (EET) pathway, which coupled with cell growth and cell metabolism (Keogh et al., 2018; Rosenbaum et al., 2011). Clarifying the mechanism and influencing factors of extracellular electron transfer will effectively promote new energy development, earth element circulation, and pollutant degradation (Huang et al., 2022; Jiang et al., 2019; Xie et al., 2021).

Extracellular electron transfer was first studied in 1911, Prof. Potter found that the current could be produced by *E-coli* and yeast with glucose as substrate (Potter, 1911). Until 1987 years, the *Geobacter* genus was isolated in Norman USA by Prof. Lovely (Lovley et al., 1987), subsequently, *Shewanella* was discovered at Lake Oneida by Prof. Nealson (Myers & Nealson,

1988). Nowadays, a diversity of electrochemically active bacteria (EAB) was discovered. EAB not only was found in gram-negative bacteria but in gram-positive bacteria (Light et al., 2018; Pankratova et al., 2019), besides, it was found in bacteria, fungi, and archaea(Gao & Lu, 2021; Youn et al., 1995). With the development of microbial electrochemistry, the technology based on EET was applied in many fields, such as microbial fuel cells, the treatment of heavy metals in sewage (Yuan et al., 2021), biosensor (Simonte et al., 2017) and microbial electrochemical synthesis (Gong et al., 2020) , and so on.

Over the past few decades, extracellular electron transfer has made great progress in many fields, and the mechanism of EET in different bacteria was discovered a lot. However, due to the limitations of many aspects like throughput of electrochemical measurement and operando microbio-electrochemical measurement and so on, the mechanism of EET still needs to be explored more.

1.2 Microorganism capable of extracellular electron transfer

Under natural environments like the deep sea and mineral-rich soil, bacteria can utilize the solid electron acceptor as their respiratory endpoint for their survival where the extracellular electron transfer pathway was employed. Due to the current production generated in this process, this kind of bacteria was called electrochemical active bacteria (EAB). Wastewater, sludge, and sediment even primate gut containing a large number of microorganisms can be used as a screening source for electrogenic microorganisms (Sacco et al., 2017). In terms of the entire microbial system of the huge family, there are still many electricity-producing microorganisms waiting to be discovered. So far, electrogenic microorganisms have been found in bacteria, archaea, and fungi (Figure 1-1). EABs are mainly from *Proteobacteria* and *Firmieutes* (Ishii et al., 2017). This kind of bacteria can utilize extracellular electron acceptors under anaerobic conditions instead of using oxygen to produce energy, where the outer membrane cytochromes were employed to transfer electrons to the outside (Tanaka et al., 2018). The muti-heme cytochromes were expressed in the inner membrane periplasm and out membrane, forming an electron transfer pathway to transfer electrons from organic matter metabolism in gram-negative bacteria such as *Geobacter* and *Shewanella* (Breuer, Rosso,

Blumberger, et al., 2015; Ueki, 2021). Apart from cytochromes, a diversity of electron transfer protein was found, flavin-protein was found to transfer electrons to the extracellular acceptor in gram-positive *Listeria monocytogenes* (Light et al., 2018). Cable bacteria such as *Desulfobulbaceae* can produce even 1 cm conductive cable to transfer electrons from the anaerobic and aerobic surfaces (Kjeldsen et al., 2019). Even the super small bacteria *Cellulomonas sp.* strain NTE-D12 less than 0.22 μM could produce current (Ihara et al., 2022). Fungi as the Eukarya also can produce current production under the electrode, specifically members of the order *Saccharomycetaceae* (Sarma et al., 2021). For Archaea, the EET ability is less than the reported bacteria such as *Shewanella*. In addition, some archaea microbes could generate electricity under high temperatures even 90 °C, and, methanogenic archaea are also frequently found in MFC.

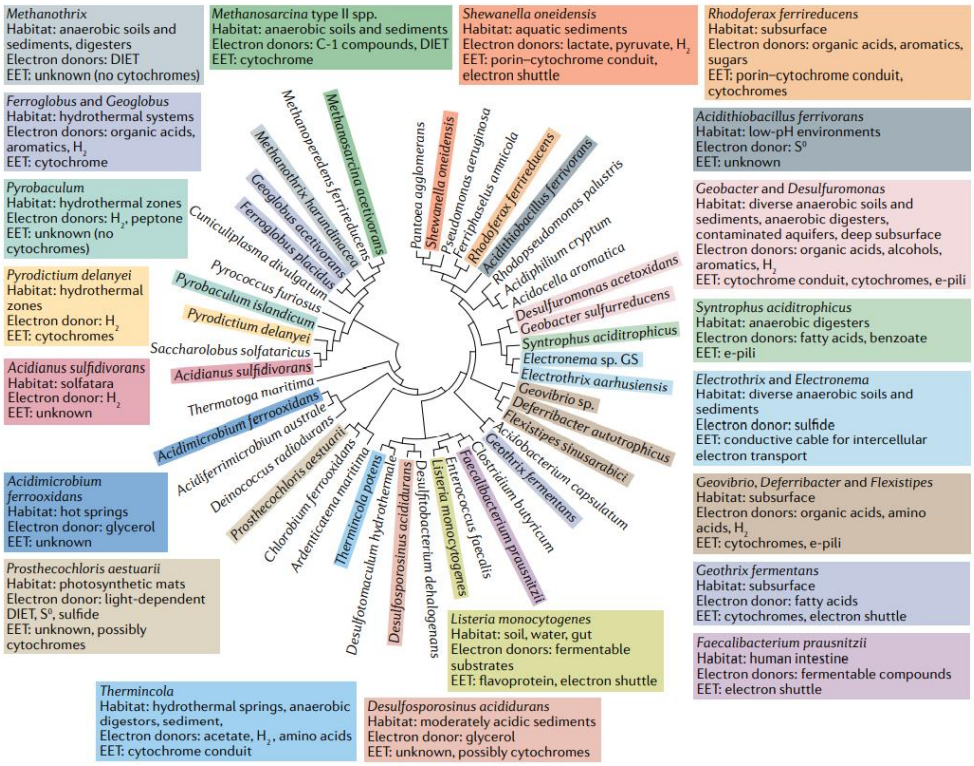

Figure 1-1 Phylogenetic diversity of electroactive microorganisms(Lovley & Holmes, 2022)

Shewanella species is a gram-negative proteobacteria with a size of 2-3 μM and it is widely distributed in many places, including oceans, lakes and even wastewater (Hau & Gralnick, 2007). In addition, it was found in spoiled food as well (Ge et al., 2017). Until now over 70 genera of *Shewanella* were discovered (Yu et al., 2022). In addition to iron and manganese,

substrates such as DMSO TMAO are also used by *Shewanella* to be electron acceptors (Xiong et al., 2016). Due to the easy growth and high EET ability, *Shewanella* was considered the model bacteria of electron transfer.

1.3 Extracellular electron transfer pathway

Although a wide variety of bacteria have EET capabilities, however, two EET pathways only were used by bacteria. Directly EET pathway: the electron was transferred to the electron acceptor directly via contact with extracellular solid electron acceptor by cell outer membrane protein or nanowires (Malvankar & Lovley, 2012; Pirbadian et al., 2014; Reguera et al., 2005; Shi et al., 2009). Indirectly EET pathway: some bacteria lack electron transfer functional proteins so it cannot conduct anaerobic respiration by directly EET, but, the more flexible redox molecular can be used for them to transfer electrons to extracellular. Some chemicals secreted by bacteria itself or environmental existence can act as the electron shuttle to transfer electrons from the cellular metabolism to the outside of the cell (Liu et al., 2010). In some bacteria, the two methods can transform into each other to enhance the anaerobic respiration together. (Figure 1-2)

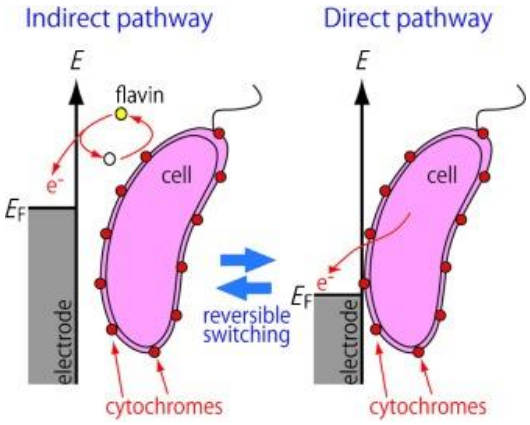

Figure 1-2 Schematic illustrations depicting the switching of the EET pathway (Liu et al., 2010)

1.3.1 Direct extracellular electron transfer

For the electrogenic bacteria, redox protein and structure protein constructed pathways for

exchanging the electron between the cell and outside minerals. It was reported that the direct EET occurred when the distance was less than 20Å between the outer membrane protein and electron acceptor (Shi et al., 2012). The direct EET via OMCs was studied a lot in *Shewanella oneidensis* MR-1. CymA, FccA, and MtrCAB-OmcA are involved in the direct EET, besides, small tetraheme cytochrome (STC) in the periplasm also plays a vital role in this process. Hydroquinone in the inner membrane can be oxidized by the tetraheme cytochrome C quinone oxidase (CymA), then, electrons will be transferred to the soluble c-cytochromes fumarate reductase (FccA) and STC. Due to the flexibility of STC and FccA, electrons can be transferred to the fixed MtrCAB-OmcA complex. During this process, the lack of any component will severely impair the EET functions. MtrC and OmcA mutations show a low EET ability, besides, the strain which lacks CymA shows an 80% decrease in the export electrons (Michal et al., 2014). However, the strain which miss the FccA showed no effect on the EET ability, but, the double mutations of FccA and STC lost the ability for growth under the Fe^{3+} as an electron acceptor (Alves et al., 2015). The electron transfer pathway in the *Shewanella oneidensis* MR-1 should be QH_2→CymA→STC or FccA→MtrCAB-OmcA (Figure 1-3).

For some gram-negative bacteria, electrons also can be directly transferred to the extracellular electron acceptor by the membrane protein like the flavoproteins (Light et al., 2019).

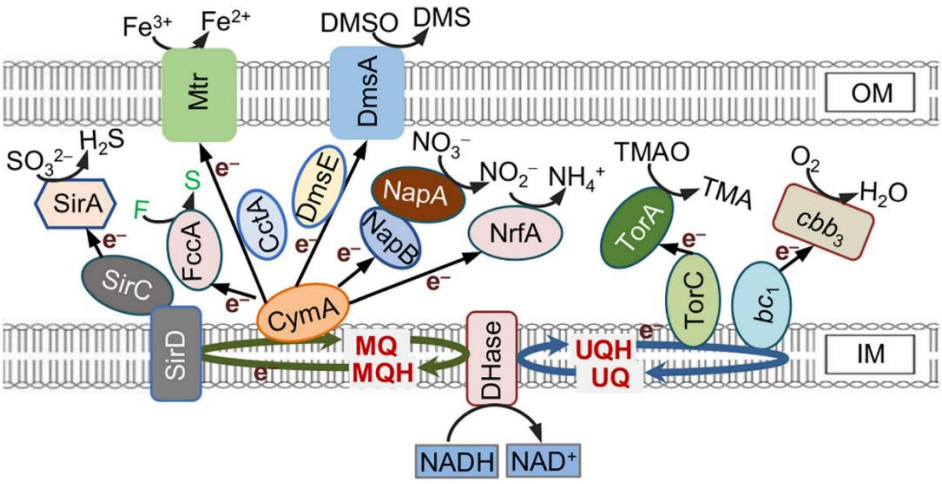

Figure 1-3 Direct extracellular electron transfer (EET) pathways in *Shewanella oneidensis* MR-1 (Sun et al., 2021).

Nanowire for electron transfer is a very important pathway. A nanowire is a type of

conductive filament around the electrogenic bacteria. Nanowires were first discovered on *Geobacter* species, which can transfer electrons to the electrode and metal surface by several times longer than itself. After further analyzing the composition of nanowires in *Geobacter*, it was found that the nanowire was constructed by the OmcS protein which relies on the PilA. Heme is tightly arranged inside the nanowires, forming a channel for electron transfer (Lovley & Walker, 2019).

Shewanella is also able to produce nanowires, which show different behavior with *Geobacter* (Figure 1-4). It's nanowires as extensions of the outer membrane and periplasm that include the multiheme cytochromes responsible for EET, rather than pilin-based structures as previously thought. Under the oxygen limitation environment, nanowires will grow to transfer electrons, which provided a chance for bacteria to respirate over a long distance. The outer membrane extension type nanowire transfer electron with the electron hopping in the outer membrane protein MtrC and OmcA. During the electron transfer process, nanowires touch the extracellular electron acceptor, then, the electron was transported to the outside by the lateral EET along MtrC/OmcA (Leung et al., 2013; Pirbadian et al., 2014).

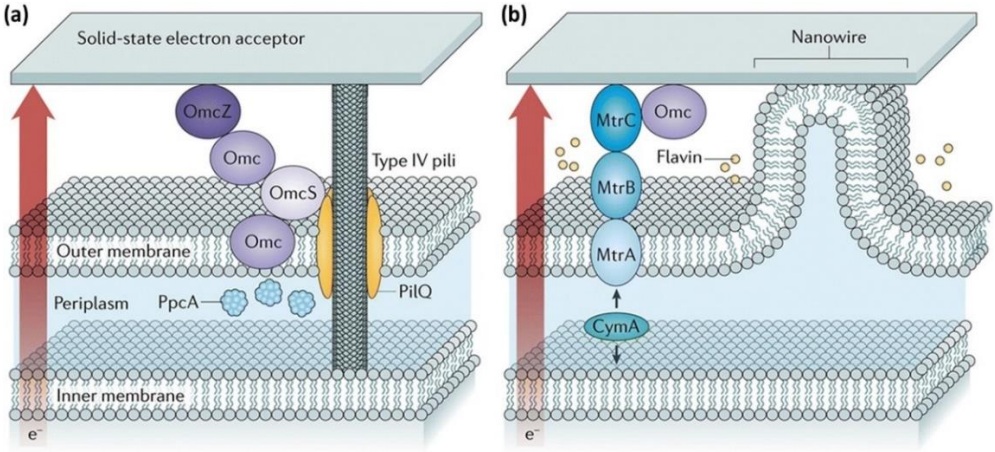

Figure 1-4 Proposed EET mechanisms in *Geobacter* spp. and *Shewanella* spp (Zou et al., 2018)

1.3.2 Indirect extracellular electron transfer

Redox mediators are involved in indirect EET, which is an important mechanism for extracellular electron transfer. Mediators can accept electrons from cellular metabolism and transfer electrons to extracellular electron acceptors, which can be secreted by bacteria or

existence in the natural environment (Liu et al., 2018). When the insoluble electron acceptor was the only electron acceptor, like an electrode, the indirect EET shows a vital role in the bacteria's anaerobic respiration. Loyed et al. first identify the Flavin Mononucleotide (FMN) and Riboflavin (RF) as the electron shuttle, which enhanced the cell growth and Fe^{3+} reduction. D.R. Bond found that RF participated in extracellular electron transfer by electrode detection. However, the current production decreased by 70% after removing RF from the electrolyte (Marsili et al., 2008). Flavin was considered to transfer electrons by a 2-electron reaction, which brings two electrons and two protons (Okamoto et al., 2013; Okamoto, Kalathil, et al., 2014). Mediators like quinone, phenazines, and flavin show high efficiency on the EET (Newman & Kolter, 2000; Wang et al., 2010).

Shewanella synthesis intracellular flavin before exporting to the extracellular by the FAD exporter (which is encoded by gene *bfe*), however, the deletion of gene *bfe* caused a 75% decrease of current production, proving the importance of flavin in the extracellular electron (Kotloski & Gralnick, 2013). Endogenous flavin only is 2 μM which limited the extracellular electron transfer rate. The current production was hugely increased by the overexpressed flavin gene (Yang et al., 2015).

However, the low concentration of flavin showed a sharp increase in the current production, which is higher than the stoichiometric ratio by the shuttling mechanisms. Okamoto et al. found that flavin can enhance the current production by the 1-electron reaction via binding with outer membrane cytochromes. FMN and RF can be a cofactor for the MtrC and OmcA, respectively, which enhances the current production more than 10 times within 10 μM (Okamoto et al., 2013; Okamoto, Kalathil, et al., 2014). Besides, *Geobacter* also showed the same result as *Shewanella* (Okamoto, Nakamura, et al., 2014). For some electrogenic microbes, multiple pathways of extracellular delivery complement each other to enhance the capacity of EET, which is a smart strategy for the microbe's survival under nutrition shortage and an oxygen-limited environment.

1.4 Extracellular electron transfer bridge C-type cytochromes

Cytochromes are important proteins in the electron transfer chain for cellular respiration, which function from the heme inside of the protein (Ow et al., 2008). The transition between

Fe^{2+} and Fe^{3+} provides an environment for redox reactions. In the eukaryote cell, cytochromes are expressed on the mitochondrion membrane to participate in the electron transfer, where it can accept the electron from NADH dehydrogenase and transfer the electron to the next respiration complex. In the prokaryote, cytochrome C expresses both the inner membrane and outer membrane, which allow electron transfer from the inside to the outside along the cytochrome C due to the different redox potential of different locations of heme. During the electron transfer process, a series of heme align to a conduit for electron transfer. As for the electrochemical active microorganisms, the most common electron transfer group is cytochrome C, even some bacteria nanowires and pili are constituted by cytochrome C (Deng et al., 2018) .

Here, six cytochromes in *Shewanella oneidensis* MR-1 which are studied in this paper will be introduced.

CymA is a tetraheme cytochrome C quinone oxidase that is the smallest example of a quinol dehydrogenase in nature. It is located on the inner membrane and plays a central role in the anaerobic respiration in *Shewanella* (Myers & Myers, 2000). Electrons from the organic matter metabolism were transferred to the quinone pool, and the inner membrane protein CymA acted as the electron transfer station to transfer electrons to the periplasmic protein, then, electrons can be transferred outside of the cell. *E-coli* can obtain EET ability by expressing CymA on the inner membrane and MtrCAB on the outer membrane (Jensen et al., 2010). The mutant strain which lacks CymA shows the EET ability was seriously impaired.

Shewanella oneidensis MR-1 outer membrane is considered insulation, which prevents the leakage of electrons from the periplasm. To reduce the extracellular substrate, the electron should across the outer membrane to arrive at the electron acceptor by conductive wire or electron shuttle. To address this issue, *Shewanella oneidensis* MR-1 express MtrCAB (Figure 1-5) which across the outer membrane to transfer electrons from the periplasm. MtrCAB complex consists of three proteins MtrA, MtrB and MtrC. MtrB is a beta-barrel protein, which includes 26 antiparallel beta strands, across the outer membrane to form a channel. MtrB provides a transmembrane sheath for the MtrA and an anchor position for MtrC. MtrA contains 10 hemes inside the protein that forms an 80Å electron transport line to across the outer

membrane. The heme (A1) of the periplasmic part can accept electrons from the inside, and heme A10 connects the outside cytochromes MtrC. MtrC is one of the terminals of the electron chain in *Shewanella oneidensis* MR-1, which can directly contact the solid electron acceptor surface to transfer electrons, it has been proved that even lacking MtrC, soluble Fe^{3+} still can be reduced but the insoluble iron oxides, which demonstrated the importance of MtrC on the contact insoluble substrate (Figure 1-5) (Edwards et al., 2020).

One of the homologous proteins of MtrC is OmcA, expressed near the MtrC, 10 hemes was encapsulated inside of protein to construct an electron pathway. It has a similar function to MtrC and these two outer membrane cytochromes show a complementary role, while one of them lacking, another will undertake the electron transfer function. The extracellular electron transfer function can be impaired only if these two cytochromes were deleted rather than one of them. MtrC/OmcA are located on the cell surface in a flexible manner, which diffuses on the cell surface to transfer electrons, proven by the single particle tracking (Chong et al., 2022).

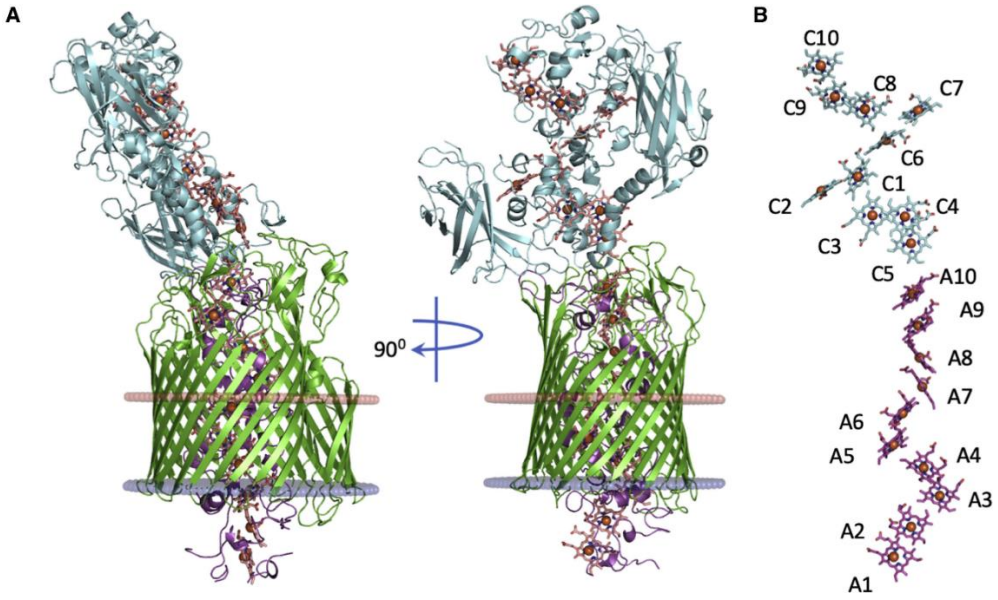

Figure 1-5 The X-Ray crystal structure of the Mtr complex (Edwards et al., 2020)

Under the anaerobic condition, fumarate as an electron acceptor is a widespread way for bacteria, unlike the extracellular solid electron acceptors, fumarate can enter the periplasm by diffusion, which is convenient for bacteria to utilize fumarate for respiration. The fumarate reductase (FccA) in MR-1 is a tetraheme cytochrome C with a larger C-terminal FAD-binding domain, unlike other fumarate reductases, FccA is a periplasmic protein, it can directly get

electrons from the inner membrane. Fumarate can be reduced to succinate by FccA unidirectionally in *Shewanella oneidensis* MR-1. Four heme arrangement is close, where contact each other by Van der Waals, electrons along the heme center cross FAD arrive at fumarate. Finally, fumarate was reduced to succinate. In some extracellular electron uptake processes, fumarate usually can be as electron acceptor to produce cathodic current (Schuetz et al., 2009).

Dimethyl sulfoxide (DMSO) is widely spread in many aquatic environments such as deep oceanic water, which provided a possibility for bacteria to anaerobic respiratory (Xiong et al., 2017). *Shewanella* species can use multiple electron acceptors, and DMSO is one of them. It was reported that DMSO reductases are similar complex to MtrCAB. During the DMSO reduced process, the electron was transferred from the inner membrane CymA to a soluble part of DMSO reductases DmsE (predicted tetraheme cytochromes), then, the electron was transported to the DMSO reductase complex DsmABF. DmsF is a beta-barrel protein that across the outer membrane of bacteria to form a channel that connects the periplasm and extracellular. Meanwhile, the outer membrane protein DmsAB were anchored on the DmsF, which constructed an electron pathway from the inner membrane to the outside to reduce DMSO. DMSO was reduced to dimethyl sulfide (DMS) (Figure 1-6). In addition, in some *Shewanella* species, DMSO reductases expression was controlled by the temperature and press which enhanced the survival ability of bacteria under adverse conditions (Gralnick et al., 2006).

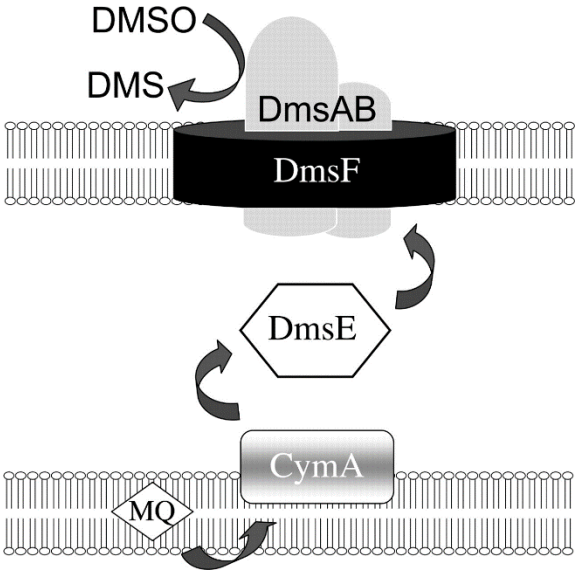

Figure 1-6 Model for DMSO respiration in S. *oneidensis* (Gralnick et al., 2006).

1.5 Biotechnology based on extracellular electron transfer

1.5.1 Microbial fuel cell (MFC)

Due to the high demand for energy and the shortage of fossil fuels, the development of renewable and sustainable energy sources is necessary. The microbial fuel cell is a device that generates electricity by converting chemical energy stored in organic matter as shown in Figure 1-7 (Rabaey & Verstraete, 2005), a double chamber MFC. The double chamber MFC is divided into two chambers by a proton exchange membrane. As for *Geobacter* MFC, bacteria form biofilm in an anode with an anaerobic condition (Kim & Lee, 2010). Electrons could be transferred to the anode by EAB from organic matters, the reaction of the anode is as follows

$$CH_3COO^- + 4H_2O \rightarrow 2HCO_3^- + 9H^+ + 8e^- \quad (1)$$

the proton across a semipermeable membrane to be reduced H2O at the cathode

$$O_2 + 4H^+ + 4e^- \rightarrow 2H_2O \quad (2)$$

The anode and cathode are connected by external wires and resistors to form a complete loop. As far, the power density of MFC is still very low, so that it is impossible to replace fuel cells. Considering the low power density, many strategies were explored to enhance efficiency. Mesoporous materials were used to modify electrodes to enhance biofilm formation (Wang et al., 2013), and redox mediators also can be used to increase MFC output (Chen et al., 2021) (Najafpour et al., 2011). Recently, silver nanoparticles can be applied to improve power density in MFC (Cao et al., 2021).

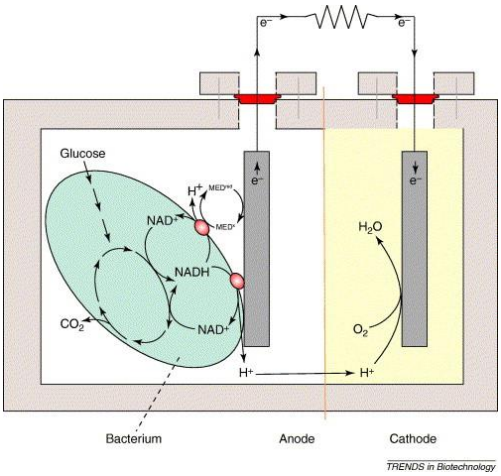

Figure 1-7 Schematic diagram of a typical two-chamber microbial fuel cell (Fleming,

2010)

1.5.2 Bioremediation based on extracellular electron transfer

Environmental pollution has become an urgent problem for human beings, especially, since toxic metal pollution can impair ecology seriously (Ali et al., 2022). The traditional way for treating pollution is not only low efficiency but also high investment. However, microbial degradation and remediation of pollutants are friendly for the environment at low cost (Rabenstein et al., 2009). Due to the strong redox ability of EAB, it can be considered a good method to reduce heavy metals such as the soluble U (VI) and Cr (IV) can be reduced to insoluble U (IV) and Cr (III) (Shi et al., 2016). For some organic pollution like benzene, toluene, ethylbenzene, and xylenes, EAB can reduce toxic compounds to less or non-toxic compounds (Chen et al., 2021; Liu et al., 2019; You et al., 2020). Bioelectrochemical system (BES) which is based on the EAB is a promising technology for pollution remediation. Hydrocarbon-polluted soils and sediments can be degraded by BES, it is fast than pollution natural attenuation (Espinoza-Tofalos et al., 2020). Besides, it was used to refractory pesticides (Cao et al., 2015). In short, bioremediation is a potential way to solve environment pollution with many benefits.

1.5.3 Biosensor based on extracellular electron transfer

Electrochemical sensors usually use potentiometric amperometric or conductometric signals to detect some substrate changes (Baranwal et al., 2022). Typical biosensors of BES are based on the MFC because of its diverse applications, which are mainly used in detecting environmental toxicity and bioactive substances (Zhou et al., 2017). BES biosensors are the most popular for detecting biological oxygen demand (BOD) (Yamashita et al., 2016). EAB bacteria are immobilized on the fiber between the electrode and porous membrane, the dissolved oxygen was reduced at the cathode across the membrane, resulting in the decrease of current as shown in Figure 1-8. Besides, the BES-based biosensor can be used for detecting pH and salinity, temperature, and so on (Brochu et al., 2020; Tremouli et al., 2017). Recently, oral pathogens can be detected by the BES biosensors, in this kind of system, special substrates and mediators were added into this system to enhance the EET ability of the pathogens, which can

be observed to increase current production (Naradasu et al., 2020).

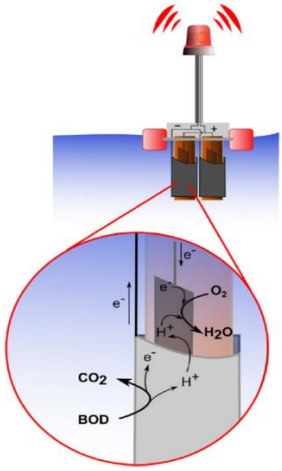

Figure 1-8 Schematic diagram of microbial fuel cells for sensing BOD (Sonawane et al., 2020)

1.5.4 Microbial electrochemical synthesis

As the demand for foil fuel, alternative renewable energy sources are widely attracting attention. Besides, carbon dioxide control and emission reduction have become an important issue that needs to be solved urgently around the world (Sathiendrakumar, 2003). If carbon dioxide can be reduced to carbon organic compounds, it will be a good way to kill two birds with one stone. Microbial electrochemical synthesis cleverly converts carbon dioxide into organic matter, such as methane, acetic acid, butyric acid (Schlager et al., 2017). In this system, EAB transfers electrons from the cathode to reduce the carbon dioxide to organic matter, meanwhile, the organic pollution can be degraded by EAB in the anode reactor, which composes a highly effective electrochemical bioreactor (Li et al., 2022; Su & Ajo-Franklin, 2019).

1.6 Limitations for extracellular electron transfer

1.6.1 The limitation of extracellular electron transfer by outer membrane cytochromes

Since the outer membrane protein is key for extracellular electron transfer, it has been proven that overexpressing the outer membrane cytochromes MtrCAB can enhance the current

production, which means the outer membrane is a limitation for the electron transfer (Vellingiri et al., 2019). Cell membrane composition can be changed by the pre-culture at 4 ℃, the electron which across MtrC increases 18 times than pre-culture at 30 ℃ (Long & Okamoto, 2021). Those results demonstrated that outer membrane protein limits the EET rate. Electron transfer pathway insides of MtrC along the heme 10 →heme 9 →heme 8 →heme 6 →heme7, finally the electron can be accepted by the extracellular electron acceptors.

For outer membrane cytochromes, MtrCAB crystal structure reveals heme interactions within the protein. Electron transfer to exogenous electron acceptors by offering a large surface area with multiple surface-exposed hemes. Spectroscopic and simulation studies have found that electrons can pass between adjacent heme prosthetic groups within the MtrCAB complex at nanosecond rates and suggested that these rapid transfers are facilitated by cysteine linkages positioned between those tetrapyrroles (Campbell et al., 2022). In MtrA, heme 10 is thought to mediate interprotein electron transfer to heme 5 of MtrC. Electron transfer between these hemes, which have an edge–edge distance of 8 Å, is thought to be rate limiting for EET through the MtrCAB complex. While these studies have revealed a complex network of molecular interactions within the Mtr complex, including protein–cofactor and protein-protein interactions, It cannot yet anticipate how changes to the primary structure of MtrCAB affect EET (Campbell et al., 2022).

Our previous reports also proved the conformation of MtrC can be changed with the different hematite nanoparticles, which are measured by the in situ circular dichroism (CD) spectroscopy. And also, it demonstrates the arrangement of heme can be important to the EET, the closer arrangement of the hemes will result in an increased rate of electron transfer (Tokunou et al., 2018; Tokunou & Okamoto, 2019). The conformation of the OMCs changes can affect the EET rate, which provided insight into the best condition for the bacteria to transfer electrons.

To increase EET rate, redox molecular was used to be electron shuttle. Redox mediator is a smart strategy for enhancing the EET rate by binding with cytochromes. It is reported that the flavin binding site is near heme 7 in the MtrC and OmcA which was evaluated by computer simulation (Babanova et al., 2017; Breuer, Rosso, & Blumberger, 2015). Heme 7 exposes the

surface of the protein and it was considered a terminal heme in the MtrC. Flavin can be a bridge between the heme 7 and the extracellular electron acceptor which shortens the distance for electron transport. The flavin binding with OMCs can be a 1-electron reaction by forming the hydroquinone rather than 2-electron reaction, in this way, the electron transfer rate can be increased more than 10 times. This evidence shows that outer membrane is a limitation for extracellular electron transfer.

1.6.2 Proton transfer limits extracellular electron transfer

EET pathways and dynamics have been extensively studied in the past decades, but the proton transfer kinetics during the EET had been poorly studied. Proton transfer to the periplasm is accompanied by electron transfer, then, electron transfer to the extracellular electron acceptors, proton should be transferred to the outside for keeping the charge balance. A proton motive force (PMF) was considered the main way to consume electrons in the periplasm, however, the mutant strain Δ*ATPase* (A proton transporter) showed a comparable current production with the wild type, which demonstrated proton was not used to form the PMF to produce ATP, and also the ATP in the *Shewanella oneidensis* MR-1 was thought to comes from substrate level phosphorylation. The previous study in our laboratory demonstrated that proton transfer limits electron transfer. The kinetic studies by isotope labeling reveal protons as a limiting factor for extracellular electron transfer (Okamoto et al., 2017).

Coincidentally, the artificial liposomes with MtrCAB complex showed a high rate of electron transfer with the help of Valinomycin (a cation carrier to transfer the cation according to concentration diffusion). Besides, the mutant strain Δ*OmpW* (a cation transporter in the outer membrane) shows the 40% of current production decreased (Bretschger et al., 2007). Those results clearly demonstrated that proton transfer is a limitation for the EET process. The more evidence and function of proton transfer in the EET process still need to be explored (Okamoto et al., 2016).

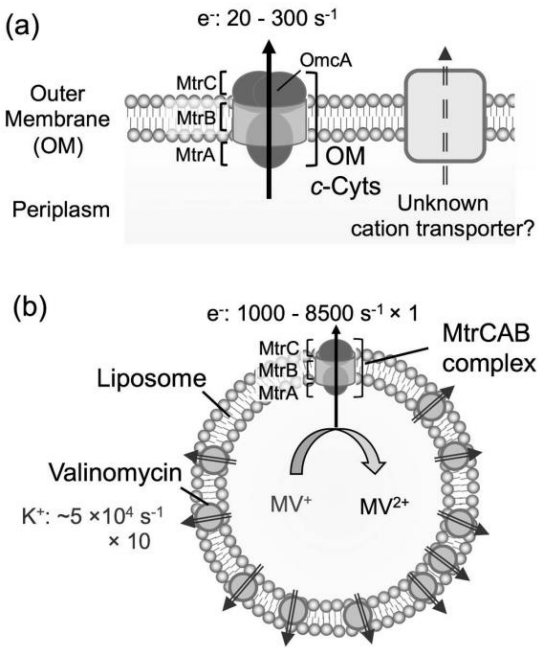

Figure 1-9 Schematic illustration of electron and proton flow across (a) the outer membrane (OM) of *S. oneidensis* MR-1 and (b) the lipid membrane in a liposome system (Okamoto et al., 2016).

1.6.3 C-type cytochromes redox state for extracellular electron transfer

Redox protein serval as a conductive pathway for electron transfer, so the redox state of redox protein is vital for extracellular electron transfer. For the outer membrane protein MtrC or OmcA, the heme redox state, and some redox sites are important for sustaining the electron transfer function.

There is a highly conserved CX_8C disulfide according to the crystal of MtrC, when it was replaced by AX_8A, cell growth was severely compromised under aerobic conditions rather than the anaerobic condition, which may be caused by the generation of reactive oxygen species. Besides, in the purified protein, the formation of a disulfide bond impaired the flavin binding with MtrC, which demonstrated that the oxidative of MtrC cannot form the semiquinone to transfer electrons (Edwards et al., 2015). The heme center is a conduit for the extracellular electron transfer in the cytochromes. Differences in redox state for heme may cause changes of EET ability. A homolog of MtrC crystal reveals that hemes show different redox potential under different redox states. Electron transfer pathway from heme 9 to heme 3 under oxidized state,

but electron from heme 9 to heme 7 or heme 9 to heme 2 under the reduced state, and also, heme 7 and heme 2 exposed outsides but the heme 3 was buried inside of protein (Watanabe et al., 2017) (Figure 1-10).

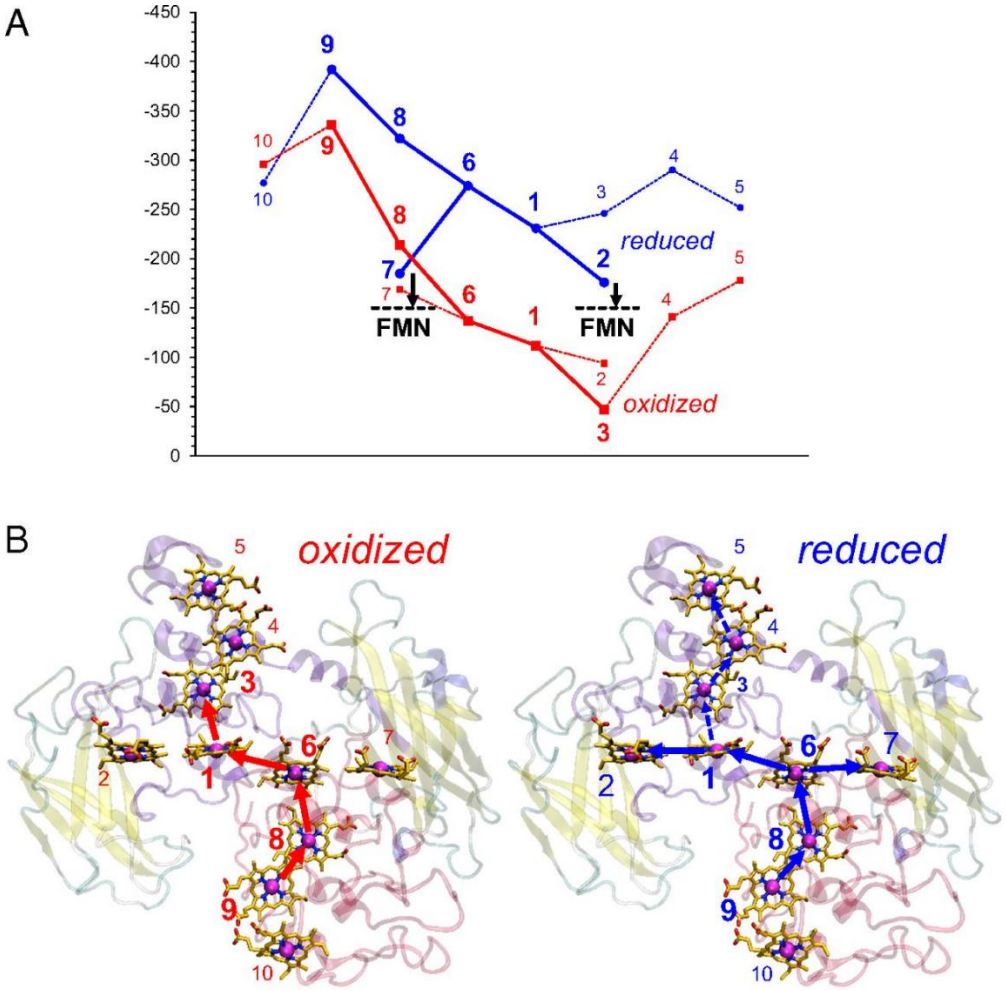

Figure 1-10 redox potential profiles of oxidized (red) and reduced (blue) MtrF (Watanabe et al., 2017)

1.6.4 Other limitations for extracellular electron transfer

EAB is more likely to form the biofilm when it adheres to the electrode surface, which can increase the EET rate. Bacteria secrete extracellular polymeric substances (EPS) contains for the bacterial community survival, meanwhile, some mediators can be secreted to the EPS, besides, quorum sensing should be accrued in the biofilm, which means biofilm formation is important to enhance the EET rate. Additionally, the EET rate can be limited by cellular metabolism, extracellular electron acceptor, and so on (Renslow et al., 2013).

1.7 New technologies for exploring extracellular electron transfer

1.7.1 High throughput electrochemical system

Electrochemical measurements have been studied for decades to investigate EET mechanisms in microorganisms. The three-electrode electrochemical reactor is a traditional bioelectrochemical system (BES), consisting of a working electrode (WE), a counter electrode (CE), and a reference electrode (RF). However, traditional BES is only one condition of a reactor, and it is impossible to use it to study EET under many different conditions. As the high throughput system (HT) develops, the HT system was used to rapidly study the microbial biofuel cells (MFC). Cell polarizability can be an indicator of extracellular electron transfer due to the correlation between cell polarizability and outer membrane cytochromes, therefore, high throughput microfluidic dielectrophoresis was used to screen the EET species (Wang et al., 2019). It still doesn't have a direct way to screen EET bacteria, and it cannot monitor the EET ability of bacteria on time. To better characterize the EET capability of bacteria, the 96-well electrode system was developed, this high throughput system can be used to screen EET microbe for the microbial fuel cells, it showed good performance on the sensitive and bacteria numbers (Tahernia et al., 2020). However, it is not an independent three-electrode system, it cannot change the potential of each well. The ideal high throughput should be an independent three-electrode system for each well, for that we can use the different conditions to investigate EET. In this study, an ideal high throughput system was developed with highly reproducible to study the most suitable mediator's concentration and electrode potential for the bacteria, besides, the whole mutant library of *Shewanella oneidensis* MR-1 was screened for exploring the genes which limit EET.

1.7.2 Whole-cell heme redox state measurement

Due to the difference between the protein under physiological conditions and the purification conditions, so develop the whole-cell measurement to measure the protein conformation is important and necessary to explore the real changes of the protein. For decades, the conformation of outer membrane cytochromes was studied by the NMR or small-angle x-

ray scattering using purified protein. Our previous study developed a whole-cell outer membrane cytochromes measurement to overcome the current obstacle. Circular dichroism (CD) spectroscopy has been studied for the inter-heme conformation and interactions with purified peptides and proteins. The ten hemes in the MtrC will provide a large amplitude in CD signal according to their exciton coupling between π conjugated systems, which is inversely proportional to the cube of the distance. According to this, the whole-cell OMCs conformation measurement was developed, which can be used to monitor the redox state of OMCs and the packing of inside hemes.

1.8 Objectives and outline of the present thesis

Extracellular electron transfer is a type of respiration under oxygen limitation for anaerobic microorganisms to produce energy. Electrons from organic metabolism were transported to the extracellular electron acceptor with the help of membrane proteins across the insulated membrane. The technology based on EET was wildly applied in many fields, such as microbial fuel cells, the treatment of heavy metals in sewage, biosensor, and microbial electrochemical synthesis. Additional redox mediators can enhance more than 10 times EET efficiency, flavin which is secreted by the bacteria itself can boost the current production by binding with outer membrane cytochromes. However, in the real application of EET-based technology, for example, in the MFC, the working environment has fluctuations in potential and solution balance, leading to ambiguity in the interaction and robustness between flavins and bacteria.

In this study, our purpose is to clarify the factors affecting the performance of flavin on microbial current production in order to stabilize and maximize MFC power output and EET technology performance in the model bacteria *Shewanella onidensis* MR-1.

Electrode potential and redox additive are the limitations of the EET rate, herein, a high-throughput platform with low deviation was constructed to apply two-dimensional Bayesian estimation for electrode potential and redox-active additive concentration to optimize microbial current production (I_c). A 96-channel potentiostat represents <10% SD for maximum I_c. 576 time- I_c profiles were obtained in 120 different electrolytes and potentiostatic conditions with

two model electrogenic bacteria, *Shewanella* and *Geobacter*. Acquisition functions showed the highest performance per concentration for riboflavin over a wide potential range in *Shewanella oneidensis* MR-1. The underlying mechanism was validated by electrochemical analysis with mutant strains lacking outer-membrane redox enzymes. Our results revealed the binding mechanism of flavin with OMCs under the negative electrode potential. (Chapter 2)

Flavin cofactor was proven to be vital for the EET enhancement. However, the effect of flavins vastly decreases upon the dissociation from OMCs to be soluble electron shuttle. Therefore, identifying a critical factor to stabilize the bound flavin cofactor is essential. Herein, the reduced heme centers in OMCs promote riboflavin binding to OMCs by modulating the intracellular electron pathways in *Shewanella oneidensis* MR-1. UV-vis and circular dichroism spectroscopy in situ shows showed that fumarate or dimethyl sulfoxide (DMSO) oxidizes heme centers in OMCs even at low concentration concentrations (< 1 mM fumarate or 5 mM DMSO) with lactate as an electron donor. Differential pulse voltammetry detected the more soluble flavins and the less bound semiquinone in the presence of fumarate or DMSO in the wild type. However, mutant strains lacking a reductase for fumarate or DMSO recovered the effect of riboflavin. These results strongly suggest that the reduced heme centers promote riboflavin to bind OMCs, and alternative electron acceptors suppress power generation in MFC even more than the stoichiometric ratio. (Chapter 3)

Flavin was considered to transfer electrons by the bring the two electrons and two protons, besides, proton transfer is a limitation on EET process that has been proved, and more evidences should be explored. Herein, different pH and deuterium water were used to check the proton effect on the EET. The result showed I_c is a positive relation with pH gradients, besides, after flavin adding, the proton limitation was recused, which suggests the proton limits extracellular electron transfer. As the proton gradient is important for membrane potential, herein, the role of membrane potential in the EET process was proved under cell hyperpolarization conditions, flavin shows stronger binding affinity than the depolarization conditions. Besides, EET rate was increased by activating the proton transporter via light. Those results demonstrated proton transfer and membrane potential are limitation for EET. (Chapter 4)

An efficient approach to discovering the gene which limits the EET process is whole

genome screening, however, the current electrochemical reactor has low throughput. For solving this, in the present study, a high-throughput electrochemical system was developed. The mutant library of *Shewanella oneidensis* MR-1 was directly screened by a high-throughput 3-electrode electrochemical assay. Anomaly detection was used to identify the critical protein for EET on the carbon working electrode. The high throughput system combined with an anomaly detection algorithm presents 25 genes from over 1000 that showed low I_c. To further confirm our results, the traditional 3-electrode electrochemical system was used, and results showed 15 mutants in 25 produced lower I_c than the wild type. Narrowing down essential genes by approach facilitates discovering unknown genes for foundations and maturing EET on a carbon electrode in *Shewanella oneidensis* MR-1. (Chapter 5)

In the present study, a high throughput system with high reliability was used to optimize flavin concentration to improve the efficiency of EET, besides, semiquinone formation can be affected by the heme redox state and membrane potential. Finally, the high throughput system was used to screen genes that limit the EET rate. Prospects were given in chapter 6.

Reference

Ali, M. M., Islam, M. S., Islam, A., Bhuyan, M. S., Ahmed, A. S. S., Rahman, M. Z., & Rahman, M. M. (2022). Toxic metal pollution and ecological risk assessment in water and sediment at ship breaking sites in the Bay of Bengal Coast, Bangladesh. *Marine Pollution Bulletin*, *175*, 113274. https://doi.org/10.1016/j.marpolbul.2021.113274

Alves, M. N., Neto, S. E., Alves, A. S., Fonseca, B. M., Carrêlo, A., Pacheco, I., Paquete, C. M., Soares, C. M., & Louro, R. O. (2015). Characterization of the periplasmic redox network that sustains the versatile anaerobic metabolism of Shewanella oneidensis MR-1. *Front Microbiol*, *6*, 665. https://doi.org/10.3389/fmicb.2015.00665

Babanova, S., Matanovic, I., Cornejo, J., Bretschger, O., Nealson, K., & Atanassov, P. (2017). Outer membrane cytochromes/flavin interactions in Shewanella spp.—A molecular perspective. *Biointerphases*, *12*(2), 021004. https://doi.org/10.1116/1.4984007

Baranwal, J., Barse, B., Gatto, G., Broncova, G., & Kumar, A. (2022). Electrochemical Sensors and Their Applications: A Review. *Chemosensors*, *10*(9), 363. https://www.mdpi.com/2227-9040/10/9/363

Bennett, G. N., & San, K. Y. (2017). Strategies for manipulation of oxygen utilization by the electron transfer chain in microbes for metabolic engineering purposes. *J Ind Microbiol Biotechnol*, *44*(4-5), 647-658. https://doi.org/10.1007/s10295-016-1851-6

Bretschger, O., Obraztsova, A., Sturm, C. A., Chang, I. S., Gorby, Y. A., Reed, S. B., Culley, D. E., Reardon, C. L., Barua, S., Romine, M. F., Zhou, J., Beliaev, A. S., Bouhenni, R., Saffarini, D., Mansfeld, F., Kim, B.-H., Fredrickson, J. K., & Nealson, K. H. (2007). Current Production and Metal Oxide Reduction by Shewanella oneidensis MR-1 Wild Type and Mutants. *Applied and Environmental Microbiology*, *73*(21), 7003-7012. https://doi.org/doi:10.1128/AEM.01087-07

Breuer, M., Rosso, Kevin M., & Blumberger, J. (2015). Flavin Binding to the Deca-heme Cytochrome MtrC: Insights from Computational Molecular Simulation. *Biophysical Journal*, *109*(12), 2614-2624. https://doi.org/https://doi.org/10.1016/j.bpj.2015.10.038

Breuer, M., Rosso, K. M., Blumberger, J., & Butt, J. N. (2015). Multi-haem cytochromes in Shewanella oneidensis MR-1: structures, functions and opportunities. *Journal of*

The Royal Society Interface, *12*(102), 20141117. https://doi.org/doi:10.1098/rsif.2014.1117

Brochu, N., Gong, L., Greener, J., & Miled, A. (2020). *Ultra-low power pH sensor powered by microbial fuel cells* (Vol. 11235). SPIE. https://doi.org/10.1117/12.2547233

Campbell, I. J., Atkinson, J. T., Carpenter, M. D., Myerscough, D., Su, L., Ajo-Franklin, C. M., & Silberg, J. J. (2022). Determinants of Multiheme Cytochrome Extracellular Electron Transfer Uncovered by Systematic Peptide Insertion. *Biochemistry*, *61*(13), 1337-1350. https://doi.org/10.1021/acs.biochem.2c00148

Cao, B., Zhao, Z., Peng, L., Shiu, H.-Y., Ding, M., Song, F., Guan, X., Lee, C. K., Huang, J., Zhu, D., Fu, X., Wong, G. C. L., Liu, C., Nealson, K., Weiss, P. S., Duan, X., & Huang, Y. (2021). Silver nanoparticles boost charge-extraction efficiency in Shewanella microbial fuel cells. *Science*, *373*(6561), 1336-1340. https://doi.org/doi:10.1126/science.abf3427

Cao, X., Song, H.-l., Yu, C.-y., & Li, X.-n. (2015). Simultaneous degradation of toxic refractory organic pesticide and bioelectricity generation using a soil microbial fuel cell. *Bioresource Technology*, *189*, 87-93. https://doi.org/https://doi.org/10.1016/j.biortech.2015.03.148

Chen, H., Yu, Y., Yu, Y., Ye, J., Zhang, S., & Chen, J. (2021). Exogenous electron transfer mediator enhancing gaseous toluene degradation in a microbial fuel cell: Performance and electron transfer mechanism. *Chemosphere*, *282*, 131028. https://doi.org/https://doi.org/10.1016/j.chemosphere.2021.131028

Chong, G. W., Pirbadian, S., Zhao, Y., Zacharoff, L. A., Pinaud, F., & El-Naggar, M. Y. (2022). Single molecule tracking of bacterial cell surface cytochromes reveals dynamics that impact long-distance electron transport. *Proceedings of the National Academy of Sciences*, *119*(19), e2119964119. https://doi.org/doi:10.1073/pnas.2119964119

Deng, X., Dohmae, N., Nealson, K. H., Hashimoto, K., & Okamoto, A. (2018). Multi-heme cytochromes provide a pathway for survival in energy-limited environments. *Science Advances*, *4*(2), eaao5682. https://doi.org/doi:10.1126/sciadv.aao5682

Dilling, W., & Cypionka, H. (1990). Aerobic respiration in sulfate-reducing bacteria. *FEMS Microbiology Letters*, *71*(1-2), 123-127. https://doi.org/10.1111/j.1574-

6968.1990.tb03809.x

Edwards, M. J., White, G. F., Butt, J. N., Richardson, D. J., & Clarke, T. A. (2020). The Crystal Structure of a Biological Insulated Transmembrane Molecular Wire. *Cell*, *181*(3), 665-673.e610. https://doi.org/https://doi.org/10.1016/j.cell.2020.03.032

Edwards, M. J., White, G. F., Norman, M., Tome-Fernandez, A., Ainsworth, E., Shi, L., Fredrickson, J. K., Zachara, J. M., Butt, J. N., Richardson, D. J., & Clarke, T. A. (2015). Redox Linked Flavin Sites in Extracellular Decaheme Proteins Involved in Microbe-Mineral Electron Transfer. *Scientific Reports*, *5*(1), 11677. https://doi.org/10.1038/srep11677

Espinoza-Tofalos, A., Alviz-Gazitua, P., Franzetti, A., & Seeger, M. (2020). Bio-electrochemical Remediation of Petroleum Hydrocarbons. In P. Kumar & C. Kuppam (Eds.), *Bioelectrochemical Systems: Vol.2 Current and Emerging Applications* (pp. 269-285). Springer Singapore. https://doi.org/10.1007/978-981-15-6868-8_12

Fernie, A. R., Carrari, F., & Sweetlove, L. J. (2004). Respiratory metabolism: glycolysis, the TCA cycle and mitochondrial electron transport. *Current Opinion in Plant Biology*, *7*(3), 254-261. https://doi.org/10.1016/j.pbi.2004.03.007

Fleming, J. T. (2010). Electronic interfacing with living cells. *Advances in Biochemical Engineering/Biotechnology*, *117*, 155-178. https://doi.org/10.1007/10_2009_5

Fontanesi, F. Mitochondria: Structure and Role in Respiration. In *eLS* (pp. 1-13). https://doi.org/https://doi.org/10.1002/9780470015902.a0001380.pub2

Gao, K., & Lu, Y. (2021). Putative Extracellular Electron Transfer in Methanogenic Archaea [Review]. *Frontiers in Microbiology*, *12*. https://doi.org/10.3389/fmicb.2021.611739

Ge, Y., Zhu, J., Ye, X., & Yang, Y. (2017). Spoilage potential characterization of Shewanella and Pseudomonas isolated from spoiled large yellow croaker (Pseudosciaena crocea). *Letters in Applied Microbiology*, *64*(1), 86-93. https://doi.org/10.1111/lam.12687

Gong, Z., Yu, H., Zhang, J., Li, F., & Song, H. (2020). Microbial electro-fermentation for synthesis of chemicals and biofuels driven by bi-directional extracellular electron transfer. *Synthetic and Systems Biotechnology*, *5*(4), 304-313. https://doi.org/https://doi.org/10.1016/j.synbio.2020.08.004

Gralnick, J. A., Vali, H., Lies, D. P., & Newman, D. K. (2006). Extracellular respiration of dimethyl sulfoxide by Shewanella oneidensis strain MR-1. *Proceedings of the National Academy of Sciences*, *103*(12), 4669-4674. https://doi.org/doi:10.1073/pnas.0505959103

Gregory, K. B., Bond, D. R., & Lovley, D. R. (2004). Graphite electrodes as electron donors for anaerobic respiration. *Environmental Microbiology*, *6*(6), 596-604. https://doi.org/10.1111/j.1462-2920.2004.00593.x

Hau, H. H., & Gralnick, J. A. (2007). Ecology and biotechnology of the genus Shewanella. *Annual Review of Microbiology*, *61*, 237-258. https://doi.org/10.1146/annurev.micro.61.080706.093257

Hedderich, R., Klimmek, O., Kröger, A., Dirmeier, R., Keller, M., & Stetter, K. O. (1998). Anaerobic respiration with elemental sulfur and with disulfides. *FEMS Microbiology Reviews*, *22*(5), 353-381. https://doi.org/10.1111/j.1574-6976.1998.tb00376.x

How Can Faecalibacterium prausnitzii Employ Riboflavin for Extracellular Electron Transfer? (2012). *Antioxidants & Redox Signaling*, *17*(10), 1433-1440. https://doi.org/10.1089/ars.2012.4701

Huang, J., Cai, X. L., Peng, J. R., Fan, Y. Y., & Xiao, X. (2022). Extracellular pollutant degradation feedback regulates intracellular electron transfer process of exoelectrogens: Strategy and mechanism. *Science of the Total Environment*, *853*, 158630. https://doi.org/10.1016/j.scitotenv.2022.158630

Ihara, S., Wakai, S., Maehara, T., & Okamoto, A. (2022). Electrochemical Enrichment and Isolation of Electrogenic Bacteria from 0.22 µm Filtrate. *Microorganisms*, *10*(10), 2051. https://www.mdpi.com/2076-2607/10/10/2051

Ishii, S., Suzuki, S., Yamanaka, Y., Wu, A., Nealson, K. H., & Bretschger, O. (2017). Population dynamics of electrogenic microbial communities in microbial fuel cells started with three different inoculum sources. *Bioelectrochemistry*, *117*, 74-82. https://doi.org/10.1016/j.bioelechem.2017.06.003

Jensen, H. M., Albers, A. E., Malley, K. R., Londer, Y. Y., Cohen, B. E., Helms, B. A., Weigele, P., Groves, J. T., & Ajo-Franklin, C. M. (2010). Engineering of a synthetic electron conduit

in living cells. *Proceedings of the National Academy of Sciences*, *107*(45), 19213-19218. https://doi.org/doi:10.1073/pnas.1009645107

Jiang, Y., Shi, M., & Shi, L. (2019). Molecular underpinnings for microbial extracellular electron transfer during biogeochemical cycling of earth elements. *Science China Life Sciences*, *62*(10), 1275-1286. https://doi.org/10.1007/s11427-018-9464-3

Keogh, D., Lam, L. N., Doyle, L. E., Matysik, A., Pavagadhi, S., Umashankar, S., Low, P. M., Dale, J. L., Song, Y., Ng, S. P., Boothroyd, C. B., Dunny, G. M., Swarup, S., Williams, R. B. H., Marsili, E., & Kline, K. A. (2018). Extracellular Electron Transfer Powers Enterococcus faecalis Biofilm Metabolism. *mBio*, *9*(2), e00626-00617. https://doi.org/doi:10.1128/mBio.00626-17

Kim, M.-S., & Lee, Y.-j. (2010). Optimization of culture conditions and electricity generation using Geobacter sulfurreducens in a dual-chambered microbial fuel-cell. *International Journal of Hydrogen Energy*, *35*(23), 13028-13034. https://doi.org/https://doi.org/10.1016/j.ijhydene.2010.04.061

Kjeldsen, K. U., Schreiber, L., Thorup, C. A., Boesen, T., Bjerg, J. T., Yang, T., Dueholm, M. S., Larsen, S., Risgaard-Petersen, N., Nierychlo, M., Schmid, M., Bøggild, A., van de Vossenberg, J., Geelhoed, J. S., Meysman, F. J. R., Wagner, M., Nielsen, P. H., Nielsen, L. P., & Schramm, A. (2019). On the evolution and physiology of cable bacteria. *Proceedings of the National Academy of Sciences*, *116*(38), 19116-19125. https://doi.org/doi:10.1073/pnas.1903514116

Kotloski, N. J., & Gralnick, J. A. (2013). Flavin electron shuttles dominate extracellular electron transfer by Shewanella oneidensis. *mBio*, *4*(1). https://doi.org/10.1128/mBio.00553-12

Leung, K. M., Wanger, G., El-Naggar, M. Y., Gorby, Y., Southam, G., Lau, W. M., & Yang, J. (2013). Shewanella oneidensis MR-1 Bacterial Nanowires Exhibit p-Type, Tunable Electronic Behavior. *Nano Letters*, *13*(6), 2407-2411. https://doi.org/10.1021/nl400237p

Li, J., Wen, Z., Xu, Q., Chen, K., Zhang, T., Wu, J., & Ci, S. (2022). N-doped carbon networks as bifunctional electrocatalyst toward integrated electrochemical devices for Zn-air batteries driving microbial CO2 electrolysis cell. *Journal of CO2 Utilization*, *62*, 102068.

https://doi.org/https://doi.org/10.1016/j.jcou.2022.102068

Light, S. H., Méheust, R., Ferrell, J. L., Cho, J., Deng, D., Agostoni, M., Iavarone, A. T., Banfield, J. F., D'Orazio, S. E. F., & Portnoy, D. A. (2019). Extracellular electron transfer powers flavinylated extracellular reductases in Gram-positive bacteria. *Proceedings of the National Academy of Sciences*, *116*(52), 26892-26899. https://doi.org/doi:10.1073/pnas.1915678116

Light, S. H., Su, L., Rivera-Lugo, R., Cornejo, J. A., Louie, A., Iavarone, A. T., Ajo-Franklin, C. M., & Portnoy, D. A. (2018). A flavin-based extracellular electron transfer mechanism in diverse Gram-positive bacteria. *Nature*, *562*(7725), 140-144. https://doi.org/10.1038/s41586-018-0498-z

Liu, H., Matsuda, S., Kato, S., Hashimoto, K., & Nakanishi, S. (2010). Redox-Responsive Switching in Bacterial Respiratory Pathways Involving Extracellular Electron Transfer. *ChemSusChem*, *3*(11), 1253-1256. https://doi.org/https://doi.org/10.1002/cssc.201000213

Liu, S., Liu, H., Wang, Z., Cui, Y., Chen, R., Peng, Z., Yuan, S., & Shi, L. (2019). Benzene promotes microbial Fe(III) reduction and flavins secretion. *Geochimica et Cosmochimica Acta*, *264*, 92-104. https://doi.org/https://doi.org/10.1016/j.gca.2019.08.013

Liu, X., Shi, L., & Gu, J. D. (2018). Microbial electrocatalysis: Redox mediators responsible for extracellular electron transfer. *Biotechnology Advances*, *36*(7), 1815-1827. https://doi.org/10.1016/j.biotechadv.2018.07.001

Long, X., & Okamoto, A. (2021). Outer membrane compositions enhance the rate of extracellular electron transport via cell-surface MtrC protein in Shewanella oneidensis MR-1. *Bioresource Technology*, *320*, 124290. https://doi.org/https://doi.org/10.1016/j.biortech.2020.124290

Lovley, D. R., & Coates, J. D. (2000). Novel forms of anaerobic respiration of environmental relevance. *Current Opinion in Microbiology*, *3*(3), 252-256. https://doi.org/https://doi.org/10.1016/S1369-5274(00)00085-0

Lovley, D. R., Fraga, J. L., Coates, J. D., & Blunt-Harris, E. L. (1999). Humics as an electron donor for anaerobic respiration. *Environmental Microbiology*, *1*(1), 89-98. https://doi.org/10.1046/j.1462-2920.1999.00009.x

Lovley, D. R., & Holmes, D. E. (2022). Electromicrobiology: the ecophysiology of phylogenetically diverse electroactive microorganisms. *Nature Reviews Microbiology*, *20*(1), 5-19. https://doi.org/10.1038/s41579-021-00597-6

Lovley, D. R., Stolz, J. F., Nord, G. L., & Phillips, E. J. (1987). Anaerobic production of magnetite by a dissimilatory iron-reducing microorganism. *Nature*, *330*(6145), 252-254.

Lovley, D. R., & Walker, D. J. F. (2019). Geobacter Protein Nanowires [Review]. *Frontiers in Microbiology*, *10*. https://doi.org/10.3389/fmicb.2019.02078

Malvankar, N. S., & Lovley, D. R. (2012). Microbial Nanowires: A New Paradigm for Biological Electron Transfer and Bioelectronics. *ChemSusChem*, *5*(6), 1039-1046. https://doi.org/https://doi.org/10.1002/cssc.201100733

Marsili, E., Baron, D. B., Shikhare, I. D., Coursolle, D., Gralnick, J. A., & Bond, D. R. (2008). Shewanella secretes flavins that mediate extracellular electron transfer. *Proceedings of the National Academy of Sciences*, *105*(10), 3968-3973. https://doi.org/doi:10.1073/pnas.0710525105

Michal, S., Alex, S., Shmuel, R., Emanuel, E., & Rivka, C. (2014). Anode Biofilm. In W. Chin-Tsan (Ed.), *Technology and Application of Microbial Fuel Cells* (pp. Ch. 4). IntechOpen. https://doi.org/10.5772/58432

Myers, C. R., & Nealson, K. H. (1988). Bacterial manganese reduction and growth with manganese oxide as the sole electron acceptor. *Science*, *240*(4857), 1319-1321. https://doi.org/10.1126/science.240.4857.1319

Myers, J. M., & Myers, C. R. (2000). Role of the tetraheme cytochrome CymA in anaerobic electron transport in cells of Shewanella putrefaciens MR-1 with normal levels of menaquinone. *Journal of Bacteriology*, *182*(1), 67-75. https://doi.org/10.1128/jb.182.1.67-75.2000

Najafpour, G., Rahimnejad, M., & Ghoreshi, A. (2011). The Enhancement of a Microbial Fuel Cell for Electrical Output Using Mediators and Oxidizing Agents. *Energy Sources, Part A: Recovery, Utilization, and Environmental Effects*, *33*(24), 2239-2248. https://doi.org/10.1080/15567036.2010.518223

Naradasu, D., Guionet, A., Miran, W., & Okamoto, A. (2020). Microbial current production

from Streptococcus mutans correlates with biofilm metabolic activity. *Biosensors and Bioelectronics*, *162*, 112236. https://doi.org/https://doi.org/10.1016/j.bios.2020.112236

Nealson, K. H., & Saffarini, D. (1994). Iron and manganese in anaerobic respiration: environmental significance, physiology, and regulation. *Annual Review of Microbiology*, *48*, 311-343. https://doi.org/10.1146/annurev.mi.48.100194.001523

Newman, D. K., & Kolter, R. (2000). A role for excreted quinones in extracellular electron transfer. *Nature*, *405*(6782), 94-97. https://doi.org/10.1038/35011098

Okamoto, A., Hashimoto, K., Nealson, K. H., & Nakamura, R. (2013). Rate enhancement of bacterial extracellular electron transport involves bound flavin semiquinones. *Proceedings of the National Academy of Sciences*, *110*(19), 7856-7861. https://doi.org/doi:10.1073/pnas.1220823110

Okamoto, A., Kalathil, S., Deng, X., Hashimoto, K., Nakamura, R., & Nealson, K. H. (2014). Cell-secreted Flavins Bound to Membrane Cytochromes Dictate Electron Transfer Reactions to Surfaces with Diverse Charge and pH. *Scientific Reports*, *4*(1), 5628. https://doi.org/10.1038/srep05628

Okamoto, A., Nakamura, R., Nealson, K. H., & Hashimoto, K. (2014). Bound Flavin Model Suggests Similar Electron-Transfer Mechanisms in Shewanella and Geobacter. *ChemElectroChem*, *1*(11), 1808-1812. https://doi.org/https://doi.org/10.1002/celc.201402151

Okamoto, A., Tokunou, Y., Kalathil, S., & Hashimoto, K. (2017). Proton Transport in the Outer-Membrane Flavocytochrome Complex Limits the Rate of Extracellular Electron Transport. *Angewandte Chemie International Edition*, *56*(31), 9082-9086. https://doi.org/https://doi.org/10.1002/anie.201704241

Okamoto, A., Tokunou, Y., & Saito, J. (2016). Cation-limited kinetic model for microbial extracellular electron transport via an outer membrane cytochrome C complex. *Biophys Physicobiol*, *13*, 71-76. https://doi.org/10.2142/biophysico.13.0_71

Ow, Y.-L. P., Green, D. R., Hao, Z., & Mak, T. W. (2008). Cytochrome c: functions beyond respiration. *Nature Reviews Molecular Cell Biology*, *9*(7), 532-542. https://doi.org/10.1038/nrm2434

Pankratova, G., Hederstedt, L., & Gorton, L. (2019). Extracellular electron transfer features of Gram-positive bacteria. *Analytica Chimica Acta*, *1076*, 32-47. https://doi.org/https://doi.org/10.1016/j.aca.2019.05.007

Pedersen, M. B., Gaudu, P., Lechardeur, D., Petit, M. A., & Gruss, A. (2012). Aerobic respiration metabolism in lactic acid bacteria and uses in biotechnology. *Annual Review of Food Science and Technology*, *3*, 37-58. https://doi.org/10.1146/annurev-food-022811-101255

Pirbadian, S., Barchinger, S. E., Leung, K. M., Byun, H. S., Jangir, Y., Bouhenni, R. A., Reed, S. B., Romine, M. F., Saffarini, D. A., Shi, L., Gorby, Y. A., Golbeck, J. H., & El-Naggar, M. Y. (2014). Shewanella oneidensis MR-1 nanowires are outer membrane and periplasmic extensions of the extracellular electron transport components. *Proceedings of the National Academy of Sciences*, *111*(35), 12883-12888. https://doi.org/doi:10.1073/pnas.1410551111

Potter, M. C. (1911). Electrical effects accompanying the decomposition of organic compounds. *Proceedings of the royal society of London. Series b, containing papers of a biological character*, *84*(571), 260-276.

Rabaey, K., & Verstraete, W. (2005). Microbial fuel cells: novel biotechnology for energy generation. *Trends in Biotechnology*, *23*(6), 291-298. https://doi.org/https://doi.org/10.1016/j.tibtech.2005.04.008

Rabenstein, A., Koch, T., Remesch, M., Brinksmeier, E., & Kuever, J. (2009). Microbial degradation of water miscible metal working fluids. *International Biodeterioration & Biodegradation*, *63*(8), 1023-1029. https://doi.org/https://doi.org/10.1016/j.ibiod.2009.07.005

Raymond, P., Al-Ani, A., & Pradet, A. (1985). ATP Production by Respiration and Fermentation, and Energy Charge during Aerobiosis and Anaerobiosis in Twelve Fatty and Starchy Germinating Seeds. *Plant Physiology*, *79*(3), 879-884. https://doi.org/10.1104/pp.79.3.879

Reguera, G., McCarthy, K. D., Mehta, T., Nicoll, J. S., Tuominen, M. T., & Lovley, D. R. (2005). Extracellular electron transfer via microbial nanowires. *Nature*, *435*(7045), 1098-1101.

https://doi.org/10.1038/nature03661

Renslow, R., Babauta, J., Kuprat, A., Schenk, J., Ivory, C., Fredrickson, J., & Beyenal, H. (2013). Modeling biofilms with dual extracellular electron transfer mechanisms. *Physical Chemistry Chemical Physics*, *15*(44), 19262-19283. https://doi.org/10.1039/c3cp53759e

Rosenbaum, M., Aulenta, F., Villano, M., & Angenent, L. T. (2011). Cathodes as electron donors for microbial metabolism: which extracellular electron transfer mechanisms are involved? *Bioresource Technology*, *102*(1), 324-333. https://doi.org/10.1016/j.biortech.2010.07.008

Sacco, N. J., Bonetto, M. C., & Cortón, E. (2017). Isolation and Characterization of a Novel Electrogenic Bacterium, Dietzia sp. RNV-4. *PloS One*, *12*(2), e0169955. https://doi.org/10.1371/journal.pone.0169955

Sarma, H., Bhattacharyya, P. N., Jadhav, D. A., Pawar, P., Thakare, M., Pandit, S., Mathuriya, A. S., & Prasad, R. (2021). Fungal-mediated electrochemical system: Prospects, applications and challenges. *Current Research in Microbial Sciences*, *2*, 100041. https://doi.org/https://doi.org/10.1016/j.crmicr.2021.100041

Sathiendrakumar, R. (2003). Greenhouse emission reduction and sustainable development. *International Journal of Social Economics*, *30*(12), 1233-1248. https://doi.org/10.1108/03068290310500643

Schäpper, D., Alam, M. N. H. Z., Szita, N., Eliasson Lantz, A., & Gernaey, K. V. (2009). Application of microbioreactors in fermentation process development: a review. *Analytical and Bioanalytical Chemistry*, *395*(3), 679-695. https://doi.org/10.1007/s00216-009-2955-x

Schlager, S., Fuchsbauer, A., Haberbauer, M., Neugebauer, H., & Sariciftci, N. S. (2017). Carbon dioxide conversion to synthetic fuels using biocatalytic electrodes. *Journal of Materials Chemistry A*, *5*(6), 2429-2443.

Schuetz, B., Schicklberger, M., Kuermann, J., Spormann, A. M., & Gescher, J. (2009). Periplasmic electron transfer via the c-type cytochromes MtrA and FccA of Shewanella oneidensis MR-1. *Appl Environ Microbiol*, *75*(24), 7789-7796. https://doi.org/10.1128/aem.01834-09

Shi, L., Dong, H., Reguera, G., Beyenal, H., Lu, A., Liu, J., Yu, H.-Q., & Fredrickson, J. K. (2016). Extracellular electron transfer mechanisms between microorganisms and minerals. *Nature Reviews Microbiology*, *14*(10), 651-662. https://doi.org/10.1038/nrmicro.2016.93

Shi, L., Richardson, D. J., Wang, Z., Kerisit, S. N., Rosso, K. M., Zachara, J. M., & Fredrickson, J. K. (2009). The roles of outer membrane cytochromes of Shewanella and Geobacter in extracellular electron transfer. *Environmental Microbiology Reports*, *1*(4), 220-227. https://doi.org/https://doi.org/10.1111/j.1758-2229.2009.00035.x

Shi, L., Rosso, K., Clarke, T., Richardson, D., Zachara, J., & Fredrickson, J. (2012). Molecular Underpinnings of Fe(III) Oxide Reduction by Shewanella Oneidensis MR-1 [Review]. *Frontiers in Microbiology*, *3*. https://doi.org/10.3389/fmicb.2012.00050

Simonte, F., Sturm, G., Gescher, J., & Sturm-Richter, K. (2017). Extracellular electron transfer and biosensors. *Bioelectrosynthesis*, 15-38.

Sonawane, J. M., Ezugwu, C. I., & Ghosh, P. C. (2020). Microbial Fuel Cell-Based Biological Oxygen Demand Sensors for Monitoring Wastewater: State-of-the-Art and Practical Applications. *ACS Sensors*, *5*(8), 2297-2316. https://doi.org/10.1021/acssensors.0c01299

Su, L., & Ajo-Franklin, C. M. (2019). Reaching full potential: bioelectrochemical systems for storing renewable energy in chemical bonds. *Current Opinion in Biotechnology*, *57*, 66-72. https://doi.org/https://doi.org/10.1016/j.copbio.2019.01.018

Sun, W., Lin, Z., Yu, Q., Cheng, S., & Gao, H. (2021). Promoting Extracellular Electron Transfer of Shewanella oneidensis MR-1 by Optimizing the Periplasmic Cytochrome c Network [Original Research]. *Frontiers in Microbiology*, *12*. https://doi.org/10.3389/fmicb.2021.727709

Tahernia, M., Mohammadifar, M., Gao, Y., Panmanee, W., Hassett, D. J., & Choi, S. (2020). A 96-well high-throughput, rapid-screening platform of extracellular electron transfer in microbial fuel cells. *Biosensors and Bioelectronics*, *162*, 112259. https://doi.org/https://doi.org/10.1016/j.bios.2020.112259

Tanaka, K., Yokoe, S., Igarashi, K., Takashino, M., Ishikawa, M., Hori, K., Nakanishi, S., & Kato, S. (2018). Extracellular Electron Transfer via Outer Membrane Cytochromes in a Methanotrophic Bacterium Methylococcus capsulatus (Bath). *Front Microbiol*, *9*, 2905.

https://doi.org/10.3389/fmicb.2018.02905

Tokunou, Y., Chinotaikul, P., Hattori, S., Clarke, T. A., Shi, L., Hashimoto, K., Ishii, K., & Okamoto, A. (2018). Whole-cell circular dichroism difference spectroscopy reveals an in vivo-specific deca-heme conformation in bacterial surface cytochromes. *Chem Commun (Camb)*, *54*(99), 13933-13936. https://doi.org/10.1039/c8cc06309e

Tokunou, Y., & Okamoto, A. (2019). Geometrical Changes in the Hemes of Bacterial Surface c-Type Cytochromes Reveal Flexibility in Their Binding Affinity with Minerals. *Langmuir*, *35*(23), 7529-7537. https://doi.org/10.1021/acs.langmuir.8b02977

Tremouli, A., Martinos, M., & Lyberatos, G. (2017). The Effects of Salinity, pH and Temperature on the Performance of a Microbial Fuel Cell. *Waste and Biomass Valorization*, *8*(6), 2037-2043. https://doi.org/10.1007/s12649-016-9712-0

Ueki, T. (2021). Cytochromes in Extracellular Electron Transfer in Geobacter. *Appl Environ Microbiol*, *87*(10). https://doi.org/10.1128/aem.03109-20

Vellingiri, A., Song, Y. E., Munussami, G., Kim, C., Park, C., Jeon, B.-H., Lee, S.-G., & Kim, J. R. (2019). Overexpression of c-type cytochrome, CymA in Shewanella oneidensis MR-1 for enhanced bioelectricity generation and cell growth in a microbial fuel cell. *Journal of Chemical Technology & Biotechnology*, *94*(7), 2115-2122. https://doi.org/https://doi.org/10.1002/jctb.5813

Wang, Q., Jones, A. D., 3rd, Gralnick, J. A., Lin, L., & Buie, C. R. (2019). Microfluidic dielectrophoresis illuminates the relationship between microbial cell envelope polarizability and electrochemical activity. *Sci Adv*, *5*(1), eaat5664. https://doi.org/10.1126/sciadv.aat5664

Wang, Y., Kern, S. E., & Newman, D. K. (2010). Endogenous Phenazine Antibiotics Promote Anaerobic Survival of Pseudomonas aeruginosa via Extracellular Electron Transfer. *Journal of Bacteriology*, *192*(1), 365-369. https://doi.org/doi:10.1128/JB.01188-09

Wang, Y., Li, B., Zeng, L., Cui, D., Xiang, X., & Li, W. (2013). Polyaniline/mesoporous tungsten trioxide composite as anode electrocatalyst for high-performance microbial fuel cells. *Biosensors and Bioelectronics*, *41*, 582-588.

https://doi.org/https://doi.org/10.1016/j.bios.2012.09.054

Watanabe, H. C., Yamashita, Y., & Ishikita, H. (2017). Electron transfer pathways in a multiheme cytochrome MtrF. *Proceedings of the National Academy of Sciences*, *114*(11), 2916-2921. https://doi.org/doi:10.1073/pnas.1617615114

Xie, Q., Lu, Y., Tang, L., Zeng, G., Yang, Z., Fan, C., Wang, J., & Atashgahi, S. (2021). The mechanism and application of bidirectional extracellular electron transport in the field of energy and environment. *Critical Reviews in Environmental Science and Technology*, *51*(17), 1924-1969. https://doi.org/10.1080/10643389.2020.1773728

Xiong, L., Jian, H., & Xiao, X. (2017). Deep-Sea Bacterium Shewanella piezotolerans WP3 Has Two Dimethyl Sulfoxide Reductases in Distinct Subcellular Locations. *Applied and Environmental Microbiology*, *83*(18), e01262-01217. https://doi.org/doi:10.1128/AEM.01262-17

Xiong, L., Jian, H., Zhang, Y., & Xiao, X. (2016). The Two Sets of DMSO Respiratory Systems of Shewanella piezotolerans WP3 Are Involved in Deep Sea Environmental Adaptation. *Front Microbiol*, *7*, 1418. https://doi.org/10.3389/fmicb.2016.01418

Yamashita, T., Ookawa, N., Ishida, M., Kanamori, H., Sasaki, H., Katayose, Y., & Yokoyama, H. (2016). A novel open-type biosensor for the in-situ monitoring of biochemical oxygen demand in an aerobic environment. *Scientific Reports*, *6*(1), 38552. https://doi.org/10.1038/srep38552

Yang, Y., Ding, Y., Hu, Y., Cao, B., Rice, S. A., Kjelleberg, S., & Song, H. (2015). Enhancing Bidirectional Electron Transfer of Shewanella oneidensis by a Synthetic Flavin Pathway. *ACS Synthetic Biology*, *4*(7), 815-823. https://doi.org/10.1021/sb500331x

You, J., Deng, Y., Chen, H., Ye, J., Zhang, S., & Zhao, J. (2020). Enhancement of gaseous o-xylene degradation in a microbial fuel cell by adding Shewanella oneidensis MR-1. *Chemosphere*, *252*, 126571. https://doi.org/https://doi.org/10.1016/j.chemosphere.2020.126571

Youn, H.-D., Kim, K.-J., Maeng, J.-S., Han, Y.-H., Jeong, I.-B., Jeong, G., Kang, S.-O., & Hah, Y. C. (1995). Single electron transfer by an extracellular laccase from the white-rot fungus Pleurotus ostreatus. *Microbiology*, *141*(2), 393-398.

https://doi.org/https://doi.org/10.1099/13500872-141-2-393

Yu, K., Huang, Z., Xiao, Y., & Wang, D. (2022). Shewanella infection in humans: Epidemiology, clinical features and pathogenicity. *Virulence*, *13*(1), 1515-1532. https://doi.org/10.1080/21505594.2022.2117831

Yuan, Q., Wang, S., Wang, X., & Li, N. (2021). Biosynthesis of vivianite from microbial extracellular electron transfer and environmental application. *Science of The Total Environment*, *762*, 143076. https://doi.org/https://doi.org/10.1016/j.scitotenv.2020.143076

Zhou, T., Han, H., Liu, P., Xiong, J., Tian, F., & Li, X. (2017). Microbial Fuels Cell-Based Biosensor for Toxicity Detection: A Review. *Sensors*, *17*(10), 2230. https://www.mdpi.com/1424-8220/17/10/2230

Zou, L., Qiao, Y., & Li, C. M. (2018). Boosting Microbial Electrocatalytic Kinetics for High Power Density: Insights into Synthetic Biology and Advanced Nanoscience. *Electrochemical Energy Reviews*, *1*(4), 567-598. https://doi.org/10.1007/s41918-018-0020-1

Chapter 2 Multivariate landscapes constructed by Bayesian Estimation over five hundred microbial electrochemical time profiles

2.1 Introduction

Electroactive bacteria that perform extracellular electron transfer (EET) to/from electrodes show great potential for applications in the fields of energy and environmental sustainability, including power generation from wastewater, bioremediation, chemical production, and amperometric biosensors. (Logan et al., 2019; Shi et al., 2016) With the increasing demand for commercialization (Ziara et al., 2018), various strategies are being adopted to improve and optimize the performance of bioelectrochemical systems (BESs), including reactor configurations and varying operating conditions, electrode material development, and additives based on fundamental EET mechanisms (Chen et al., 2019; Gadkari et al., 2020; Jiang et al., 2010; Liang et al., 2011; Logan, 2010; Watson et al., 2011). However, understanding the complexity of BESs, which includes elucidation of interaction between different impactful parameters (Figure 2-1A) and controlling of microbial electrochemical catalysis, remains a challenge. Data science shows potential for capturing the landscape of such complex systems from limited databases. However, the effective use of data science to BESs has been a challenge, as it requires a massive dataset with defined parameters and high reproducibility, referred to as a “high-quality database”. The less controlled experimental aspects while obtaining large data from manual experiments often cause serious reproducibility concerns, which restrict the consensual knowledge gain. Hence, high-quality database is the core area for applying data science to experimental studies. (Ahmadi et al., 2021; An et al., 2021; Du et al., 2021; Zhong et al., 2020) However, although significant development has been achieved in high-throughput BESs, there are no reports on a system that can achieve enough reproducibility while simultaneously controlling the following three parameters for each reactor: potential, electrolyte, and microorganism, which are critical for BES performance. (Call & Logan, 2011; Molderez et al., 2021; Molderez et al., 2019; Szydlowski et al., 2021; Tahernia et al., 2020; Vergani et al., 2012) Furthermore, appropriate data processing algorithms for dealing with a large volume of current time profile data have not been established yet. (Molderez et al., 2021) Therefore, even in the most recent studies using data science for the number of supervised data

is very limited, at nine. (de Ramón-Fernández et al., 2020; Lesnik & Liu, 2017; Tsompanas et al., 2019) The foundation for applying data science to BESs still requires two innovations: a high-quality data collection system and an analysis platform for massive time-current profile data.

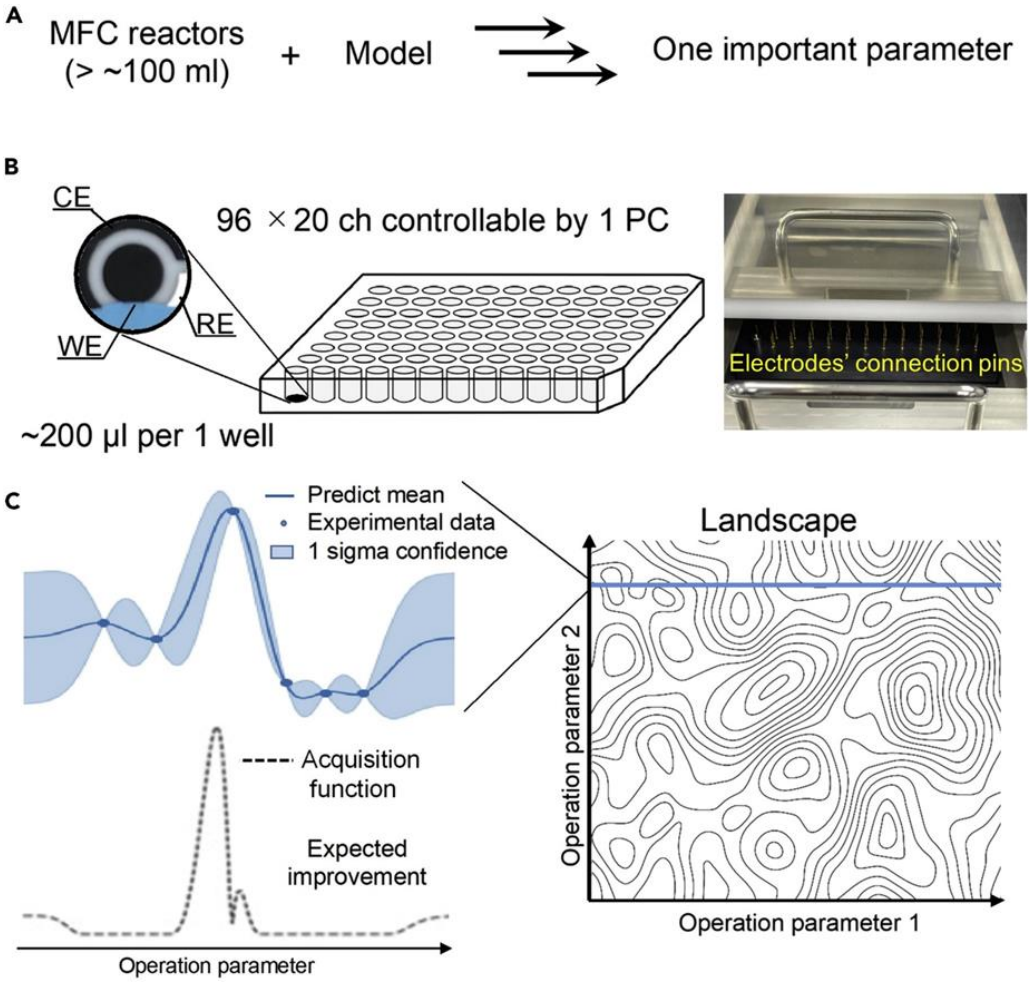

Figure 2-1 Approaches for reaction optimization.

(A) Mechanistic studies enable systematic identification of important parameters. (B) Developed high-throughput electrochemical system that operates single-potential amperometry in 96-well plate with printed working electrode (WE), counter electrode (CE) and reference electrode (RE). WE and CE are carbon, and RE is Ag/AgCl electrode. (C) Graphic outline of Bayesian optimization for two parameters. 1-D example depicting a Gaussian process surrogate model fitted to data collected from objective and the corresponding expected utility surface,

which is maximized to select the optimum condition. The solid line and the shaded area represent the mean of prediction and one-sigma confidence interval, respectively.

In this study, we developed a high-throughput potentiostat system with 96 well plates with silk-screen-printed electrodes, and which was applied to landscape the redox mediator concentration and electrode potential constructed from 576 time-profiles of microbial current production (Figure 2-1B and C). One of the most important controllable factors for BES performance is the type and concentration of the redox mediator. (Zhang et al., 2019) External redox mediators play a vital role in enhancing the electron transfer between bacteria and the electrode. (Kumar et al., 2017; Martinez & Alvarez, 2018) The performance of mediators may be considerably different depending on their redox potential, diffusion constant of shuttling electron mediators, and ability to bind with bacterial membrane enzymes. (Okamoto, Saito, et al., 2014) Furthermore, the electrode potential can modify global gene regulation and metabolic pathways in electrogenic bacteria. Therefore, microbial current production may be beyond our physicochemical understanding of the EET mechanism, which is suitable for application in data science. We used *Shewanella oneidensis* MR-1 to compare the impact of variables, different mediators [riboflavin (RF), flavin mononucleotide (FMN), 2-hydroxy-1,4-naphthoquinone (HNQ), anthraquinone-1,5-disulfonate (AQDS)], the concentration of mediators (1–100 μM), and poised potentials (+200 to −300 mV vs. Ag/AgCl). In addition, the potential and riboflavin concentration dependency were examined using *Geobacter sulfurreducens* PCA. Flavins are known to strongly enhance current generation in *S. oneidensis* MR-1 and *G. sulfurreducens* PCA, model EET bacteria, as a bound cofactor by forming an intermediate semi-reduced state. (A. Okamoto et al., 2013; Okamoto, Nakamura, et al., 2014) In contrast, HNQ and AQDS indirectly shuttle electrons between bacteria and the electrode. The basis for combining data science and microbial electrochemistry can provide a series of methods, not only as a solid basis for optimizing and enhancing BES performance but also for identifying critical parameters for biotic and abiotic complex systems.

2.2 Materials and Methods

2.2.1 *Shewanella oneidensis* MR-1 and *Geobacter sulfurreducens* PCA cultivation

S. *oneidensis* MR-1 was cultured in 10 mL of LB medium at 30 °C for 20 h under aerobic conditions, by picking a single colony from the LB solid medium plate. The bacteria were washed twice with defined medium (DM) with a composition of 2.5 g of $NaHCO_3$, 0.08 g of $CaCl_2$, 1 g of NH_4Cl, 0.2 g of $MgCl_2$, 10 g of NaCl, 7.2 g of HEPES, and 0.5 g of yeast extract in 1 L of ultrapure water. The cells were centrifuged at 7200 × g for 5 min, and the supernatant was removed. Cell pellets obtained after centrifugation were resuspended in 10 mL DML (DM medium with 10 mM lactate). To remove reductive energy, cells were pre-cultured in DML for 4 h under anaerobic conditions and then washed with DM medium. Finally, the cell OD was adjusted to 0.5, using DML as the final concentration in the screen-printed electrochemical cells.

G. *sulfurreducens* PCA freeze stock was used for inoculation of the culture in anaerobic PSN medium (Okamoto, Saito, et al., 2014) supplied with 20 mM acetate and 80 mM fumarate. Cells were allowed to grow in an anaerobic chamber at 30 °C for 3-4 days. Finally, the suspended cells were centrifuged (10 min at 5000 × g) and washed with the PSN medium for electrochemical measurements.

2.2.2 Experimental

Screen-printed electrochemical array formed by 96 three-electrode electrochemical cells (DRP×11L (U100), Metrohm, DropSens, Japan) were utilized for this study. The electrochemical array was fixed at the bottom of a standard microtiter ELISA plate with 96 wells. Plastic substrate (L7.4 cm x W11 cm x H0.5 mm) was used as the base for screen printing the three electrodes. The screen-printed carbon (surface area: 7.07 mm^2 for each well) was used as the working electrode (WE). Also, for each cell, screen printed carbon and Ag/AgCl were used as the auxiliary (counter electrode (CE)) and reference electrode (RE), respectively. The backside of the plates was printed with gold plated contact paths where 96 × 3 contacts were present corresponding to independent WE, CE, and RE printed for each well. Each well had the standard volume capacity of around 300-400 µL and working volume of 200 µL was used. After the anolyte addition, all plates were sealed with sterile aluminum seals. Since

multichannel 96 well systems were used where effective volume of each cell was very less (~200 µL), it was ensured that no turbulence effect the operation by adding medium, bacterial cells, and mediators at the beginning of experiments. Nevertheless, to probe the mechanism, control cells were included in the experiments where no exogeneous small molecule mediators were added and hence rational analysis for elucidation of mechanism can be ensured.

In scheme of current time profile experiments, first, single potential amperometry measurements with our custom potentiostat using 96 well plates were compared with a commercial potentiostat (VMP3; Biologic Science Instruments, Seyssinet-Pariset, France) using screen-printed electrodes with the same electrode material and working volume as 96 well plates. For the multivariable impact study, five 96 well electrochemical plates were selected for S. *oneidensis* MR1 and one plate for G. *sulfurreducens* PCA. For *S. oneidensis* MR1, the first plate was checked by poising a single potential (vs. Ag/AgCl) for two rows each, that is, the first two rows were poised at +200 mV, followed by two rows at −100, −200, and −300 mV without the addition of any external mediator. Four plates were tested by poising a single potential per plate with varying mediator concentrations. DM (pH 7.8) containing lactate as the sole electron donor and DM containing each redox molecule was de-aerated by bubbling with nitrogen for 30 min. An electrolyte (200 µL) was then added to each electrochemical cell containing 10 mM lactate, the desired concentrations of flavin analogs and quinones (1 – 100 µM), and MR1 cell suspensions with OD_{600nm} = 0.5. PLATEMASTER® P220 (Gilson, USA) was used for pipetting volumes of 2−220 µL for high-throughput manual pipetting of 96-wells. For G. *sulfurreducens* PCA, single plate was used to study 24 conditions. This includes four poised potential conditions (+200 −100, −200, and −300 mV) and six RF mediator concentrations (0, 100, 250, 500, 1000, and 5000 nM). All the experiments were performed in a COY anaerobic chamber. The temperature was maintained at 30 °C during the measurements.

2. 3. Results and Discussion

2.3.1 Optimal experimental condition of electrode plate

To look for the best material for working electrode, there candidates, gold and carbon and platinum were used to be working electrode. The result showed as Figure 2-2A, carbon

electrode shows the higher current production, However, gold and platinum electrode showed very low current production, which may be the toxic of metal for the bacteria, but the carbon is more fit to form the biofilm for the bacteria. To further explore the electron donor concentrations effect on the EET, here, different concentration lactate was used. The results showed, there is big difference from 10 mM to 100 mM, which suggests the electron donor is already sufficient at the 10 mM. (Figure 2-2B)

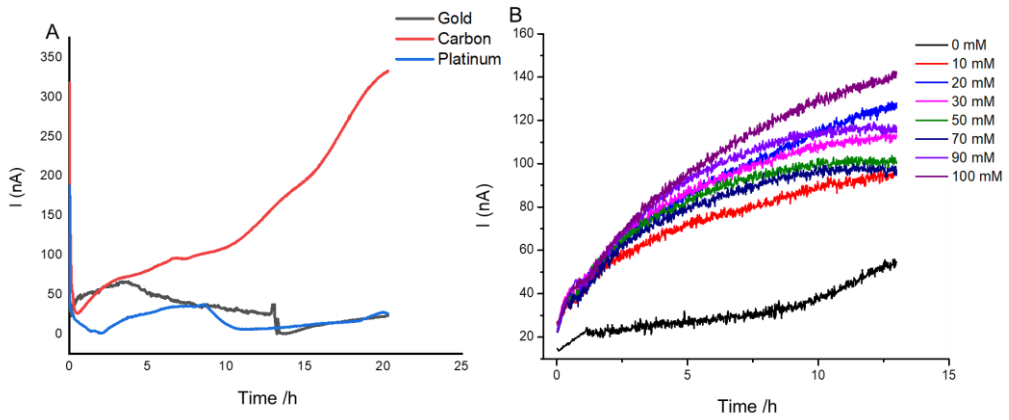

Figure 2-2 Best condition of electrode plate material and lactate concentrations.

(A) current production of *S. oneidensis* MR1 under different working electrode. (B) Current production of *S. oneidensis* MR1 with different lactate concentrations.

2.3.2 The stability of high throughput system

To evaluate the variation in the electrochemical signal from each well in a high-throughput system, the same sample conditions were measured in a 96 well three-electrode screen-printed electrochemical plate with our custom-made potentiostat. *S. oneidensis* MR-1 cells were filled into all the wells at an OD of 0.5 in an electrolyte of 200 μL, and the electrode potential was then poised at +200 mV (vs. Ag/AgCl) in the anaerobic chamber at 30 °C. A total of 95 out of 96 wells showed stable current generation without any significant noise (Figure 2-3A), indicating that manufacturing the custom potentiostat did not noticeably limit the number of effective channels. Each well showed almost identical time-current (I-T) profiles, where the current production started with a steep rise and then gradually saturated. Given that scarce current was produced in the absence of lactate as the sole electron donor (Figure 2-3A), the

current production (I_c) in each well was attributable to the EET process associated with metabolic lactate oxidation. Furthermore, the current production value and I-T profile were almost identical to those of the well-established commercially available potentiostat (VMP3; Biologic) (Figure 2-4A and B), suggesting that potentiostatic conditions were achieved using our custom-made potentiostat. At the end of the current measurement, the WE surface was covered by MR-1 cells (Figure2-3B), similar to conventional BES reactors. (Patil et al., 2013; Zhao et al., 2015) These results demonstrated that 96 well plates with Ag/AgCl printed RE were stable during measurement, and I-T profiles for each well reflected the microbial activity on the bioanode.

To quantify the variation in the data, we analyzed each time profile for the maximum current production, slope, and curvature. No baseline correction was applied, as *S. oneidensis* MR-1 cells were mixed in the electrolyte prior to addition to the electrochemical plate. Max I_c, slope, and curvature had standard deviations of approximately 8.4, 11.6, and 18.4%, respectively, whereas mean absolute percentage errors for each case were 6.7, 8.8, and 13.8%, respectively (Figure 2-3C and D). While the maximum I_c has the lowest deviation percentage from the mean, the other two also lie within the standard deviation, which is comparable with previous high-throughput systems, with and without electrodes.(Matsui et al., 2018; Riba et al., 2016) Thus, based on the data variation, our system demonstrated high reproducibility through all wells in the 96 well plate.

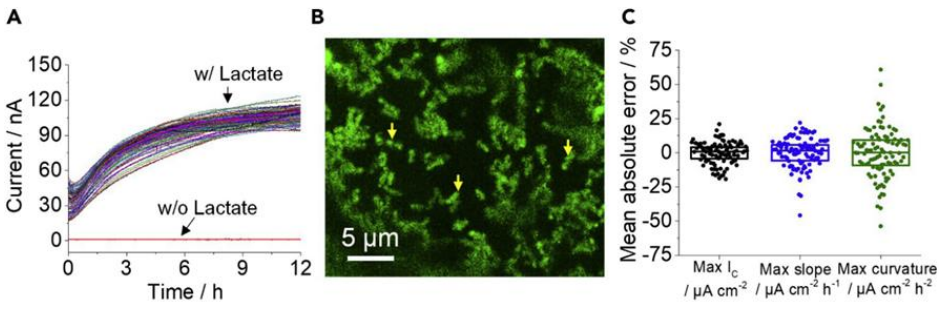

D

	Maximum Current (μA/cm^2)	Maximum Slope [μA/(cm^2·h)]	Maximum Curvature [μA/(cm^2·h^2)]
Mean	1.654	0.291	0.087
Standard deviation	0.138	0.034	0.016
Standard deviation (%)	8.35	11.58	18.42
Mean absolute error (%)	6.66	8.84	13.85

Figure 2-3 Low deviation current profiles in 96 well screen-printed electrochemical plate

(A) Catalytic current profiles of microbial lactate oxidation by *S. oneidensis* MR-1 in 96 well screen-printed electrochemical plate poised at +200 mV (vs. Ag/AgCl). (B) *S. oneidensis* MR-1 attached on the electrode surface observed by fluorescence microscopy. The arrows indicate the bacterial cells. Scale bar is 5 μm. (C and D) Statistical parameters for maximum current production, slope, and curvature. Box and whiskers in Figure 2-3C represent mean ± SD and range (10-90%)

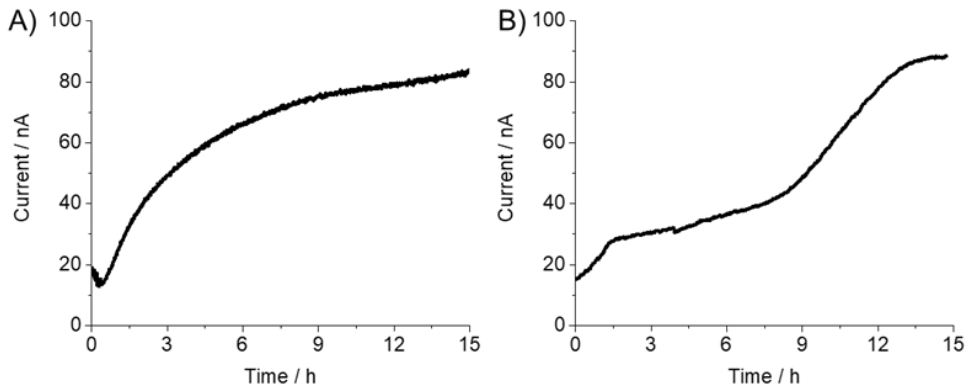

Figure 2-4 Catalytic current profiles of microbial lactate oxidation by *S. oneidensis* MR-1

(A) current measured with our custom made potentiostat and (B) current measured with commercially available potentiostat (VMP3; Biologic) at +200 mV (vs. Ag/AgCl).

2.3.3 The performance of high throughput system on mediators

Next, we compared the data for some key variables (poised potential, mediator type, and concentration on I_c) with 120 different electrolytes and potentiostatic conditions in standalone screen-printed 576 wells (Figure 2-5), using six 96 well electrochemical plates, with at least n = 4 (n is the number of wells used for one condition) (Figure 2-6, and Figure 2-7A and 2-6D). In all cases, I_c increased immediately upon poising the electrode potential. In the absence of redox mediators, maximum I_c decreased at a more negative electrode potential, suggesting that the biological effect of increasing I_c at negative potentials did not occur in our system (Figure 2-6 and Figure 2-7B).(Hirose et al., 2018) For *S. oneidensis* MR1, an increase in current production with an increase in mediator concentration was observed for all redox mediators at each electrode potential (Figure 2-6). For the positively poised electrode at +200 mV, flavins and HNQ showed relatively large currents at low (1–10 μM) and high concentrations (100 μM),

respectively This is consistent with the difference between the bound cofactor and electron shuttling mechanism reported previously. (Akihiro Okamoto et al., 2013) AQDS showed the least current enhancement among the four redox mediators. A more negative electrode potential (−100 to −300 mV) resulted in a lower I_c for all tested mediators and concentrations. Meanwhile, the impact of the decrease was substantial in the case of HNQ, as shown in Figure 2-6, a reduction in current by seven times was observed when the poised potential was decreased gradually from +200 mV to −300 mV. However, the I_c decrease was only observed from −200 to −300 mV in riboflavin and FMN, suggesting that bound cofactors and redox shuttles have different potential dependencies on the current production performance.

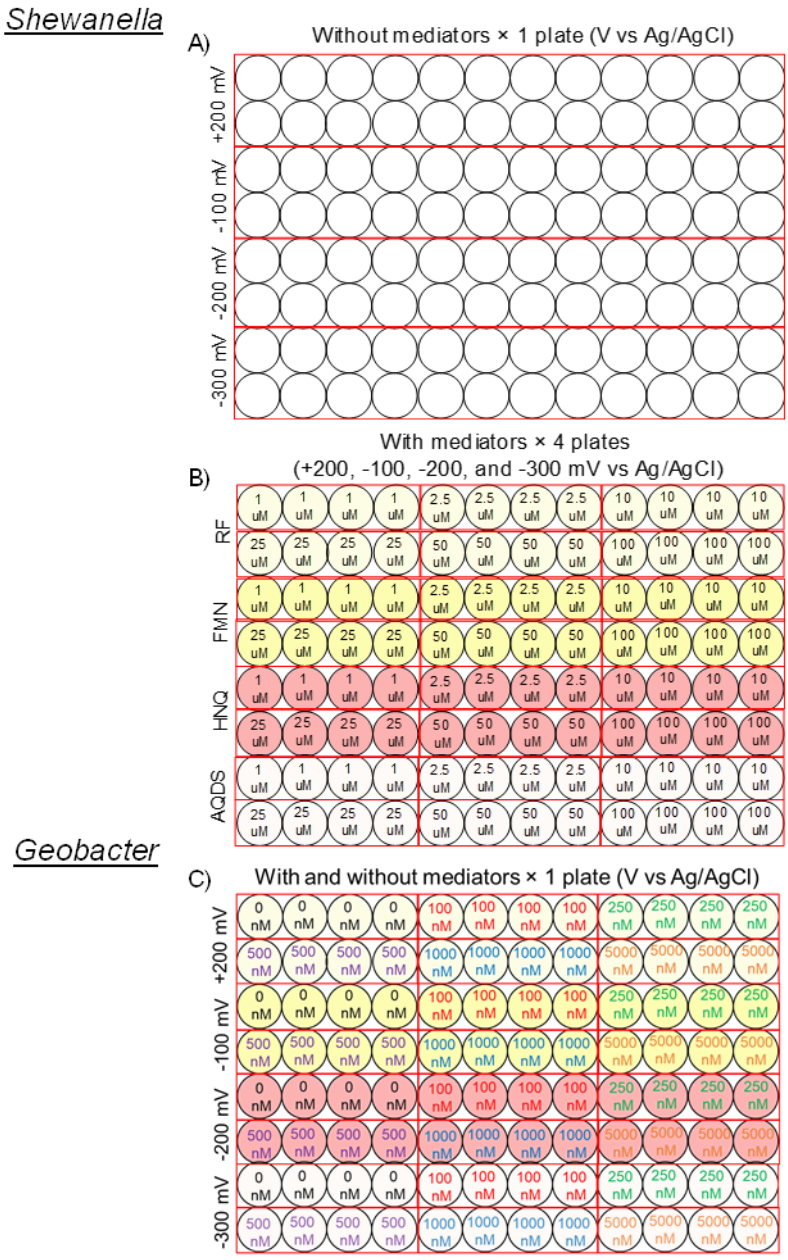

Figure 2-5 Experimental plan for obtaining high quality data from more than five hundred microbial electrochemical time profiles

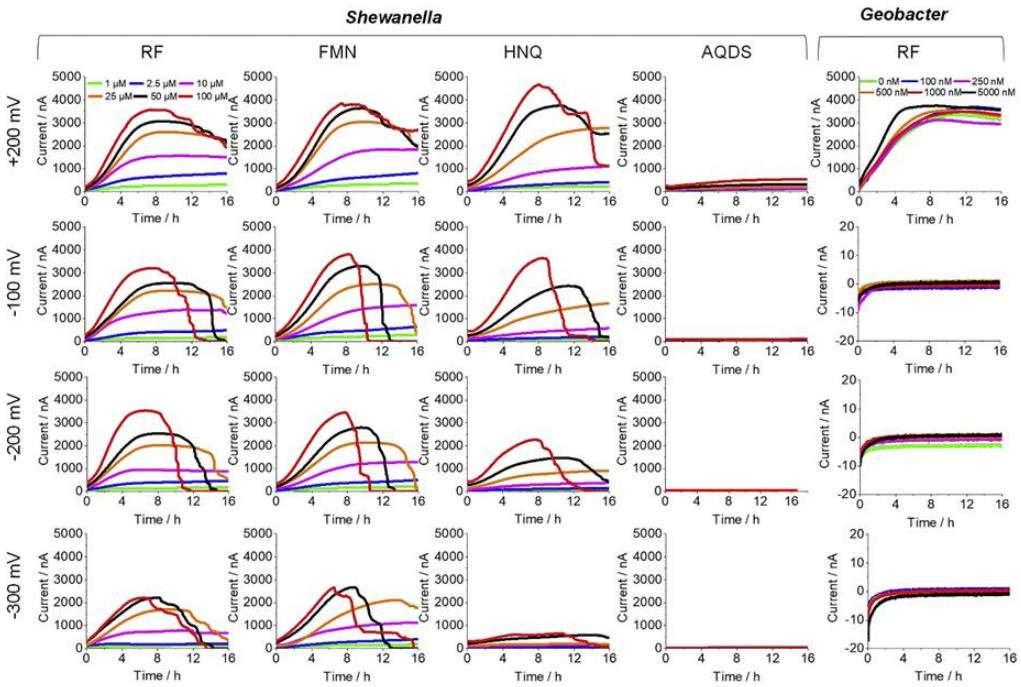

Figure 2-6 Impact of redox mediators and electrode potential on current production. Time-current profiles in the presence of redox mediators at different electrode potential and concentration in *S. oneidensis* MR-1 and *G. sulfurreducens* PCA.

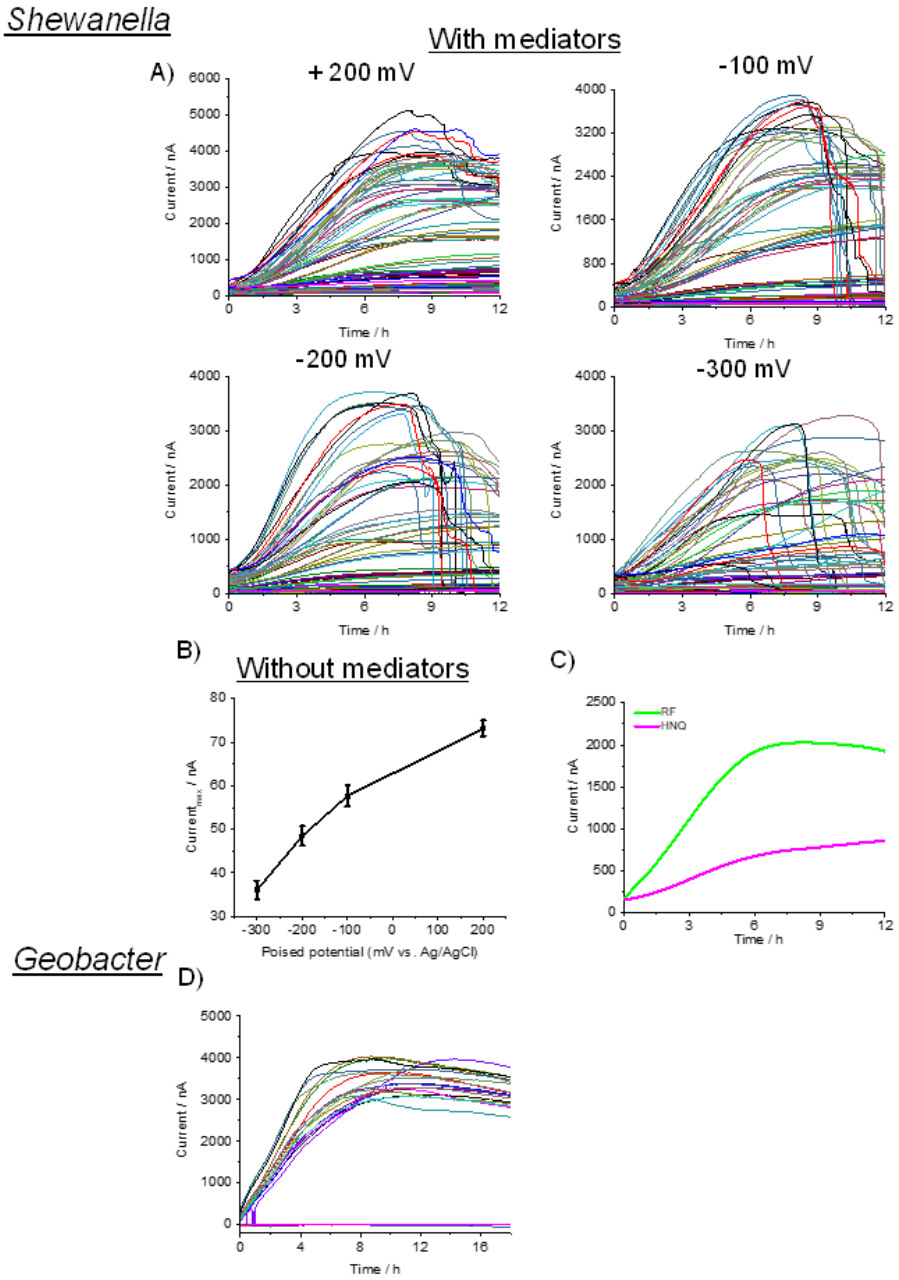

Figure 2-7 Time-current profiles under different conditions for *S. oneidensis* MR-1 and *G. sulfurreducens* PCA

(A) Time-current profiles in the presence of redox mediators at different electrode potential and concentration in *S. oneidensis* MR-1. (B) Maximum current production by *S. oneidensis* MR-1 without mediator addition at different electrode potential. Each data point is average of max current from 24 wells. (C) A single time-current profile for RF and HNQ at poised potential of +200 mV (vs. Ag/AgCl) indicating maximum current was achieved before

12 hours for RF case. (D) Time-current profiles in the presence of redox mediators at different electrode potential and concentration in *G. sulfurreducens* PCA.

For *S. oneidensis* MR1, A) one plate was checked by poising a single potential (vs. Ag/AgCl) for two rows each ranging from +200 mV to −300 mV without the addition of any external mediator. B) Four plates were tested by poising a single potential per plate with varying mediator (RF, FMN, HNQ, AQDS) concentrations. For *G. sulfurreducens* PCA, C) Single plate was used to study twenty-four conditions with varying potential (+200 −100, −200, and −300 mV) and RF concentrations (0, 100, 250, 500, 1000, and 5000 nM).

To analyze such differences in potential dependency among these redox mediators in detail, we estimated the enhancement factor and its efficiency against the concentration of redox mediators (Figure 4). In some cases, I_c did not reach its peak during the electrochemical assay (Figure 2-7 C). Therefore, we evaluated the performance in terms of the current enhancement factor using the maximum slope achieved in each case. The current enhancement factor was calculated using the following relation:

$$\mathrm{EF}\ (\alpha) = \frac{\mathrm{Smax} - \mathrm{Smax,ref}}{\mathrm{Smax,ref}} \qquad (1)$$

where EF is the current enhancement factor, S_{max} is the maximum slope for each tested case with different mediators and poised potentials, and $S_{max,ref}$ is the maximum slope of the reference cells without mediators at different poised potentials. The EF was then normalized to the added mediator's concentration to present the efficiency of each mediator molecule to enhance EET using the relation:

$$\text{Additives performance} = \frac{\mathrm{EF}}{\mathrm{C}} \qquad (2)$$

where C is the concentration of mediators for each tested case. To plot additive performance against electron potential or mediator concentration, we conducted Bayesian estimation. Bayesian statistics were employed to explore the most efficient conditions, which were determined by the balance between additive addition and current enhancement. The basic idea

of optimizing a function $f(x)$ is to determine x that maximizes $f(x)$. In Bayesian optimization, a regression model based on a Gaussian process (GP) is built for $f(x)$ from a dataset of observed x and $f(x)$. In this study, x is a 2-D vector composed of the poised voltage and the concentration of the mediator, and $f(x)$ is the additive performance. In this study, a scikit-learn library (i.e., sklearn Gaussian process regressor) was used to build a GP model and a combination of three types of kernels (i.e., radial basis function, constant, and white kernels) was employed as the GP kernel. From the mean and standard deviation of the GP posterior predictive at x ($\mu(x)$ and $\sigma(x)$, respectively), the most probable x that might give the maximum value is estimated on the basis of an acquisition function. We used expected improvement (EI) as the acquisition function, which is defined as the following formula:

$$\mathrm{EI}(x) = \begin{cases} (\mu(x) - f(x)_{\max} - \xi)\Phi(Z) + \sigma(x)\phi(Z), & \sigma(x) > 0 \\ 0, & \sigma(x) = 0 \end{cases} \quad (3)$$

where

$$Z = \frac{\mu(x) - f(x)_{\max} - \xi}{\sigma(x)} \quad (4)$$

Here, $\Phi(Z)$ and $\phi(Z)$ are the cumulative distribution function and the probability density function of Z, respectively. The parameter ξ was introduced to tune the degree of trade-off between exploration and exploitation. In this study, ξ was set at 0.01 of the standard deviation of a dataset.

The EF profiles showed that, at lower mediator concentrations, RF and FMN exhibited higher current enhancement than HNQ and AQDS (Figure 2-8). For flavins, the EFs did not significantly vary with electrode potential at all concentrations (Figure 2-8A). High EF was observed with HNQ and AQDS, specifically when both concentration and potential were both high and positive (Figure 2-8B). These results demonstrate that the EFs show the overall transition in the I-T profile under different conditions, as shown in Figure 2-7. The GP models and corresponding EIs are depicted for additive performance as 2D-heatmaps, as shown in Figure 2-8C, with the optimized conditions for each mediator marked in these panels. The GP models effectively integrate the data into a two-dimensional landscape, and the estimated condition for the peak performance is consistent with raw data, except for the highest

performance of HNQ at 1 μM concentration, which may be associated with the amplification of error from the low current range. As shown in Figure 2-8C, a low (<10 μM) concentration of RF was estimated for additive peak performance, and the peak potential ranged from +200 mV to -100 mV. In contrast, the peak performance was localized at positive potentials from +150 mV to 0 mV and at HNQ concentrations greater than 50 μM. FMN and AQDS showed similar tendencies to RF and HNQ, respectively (Figure 2-8C).

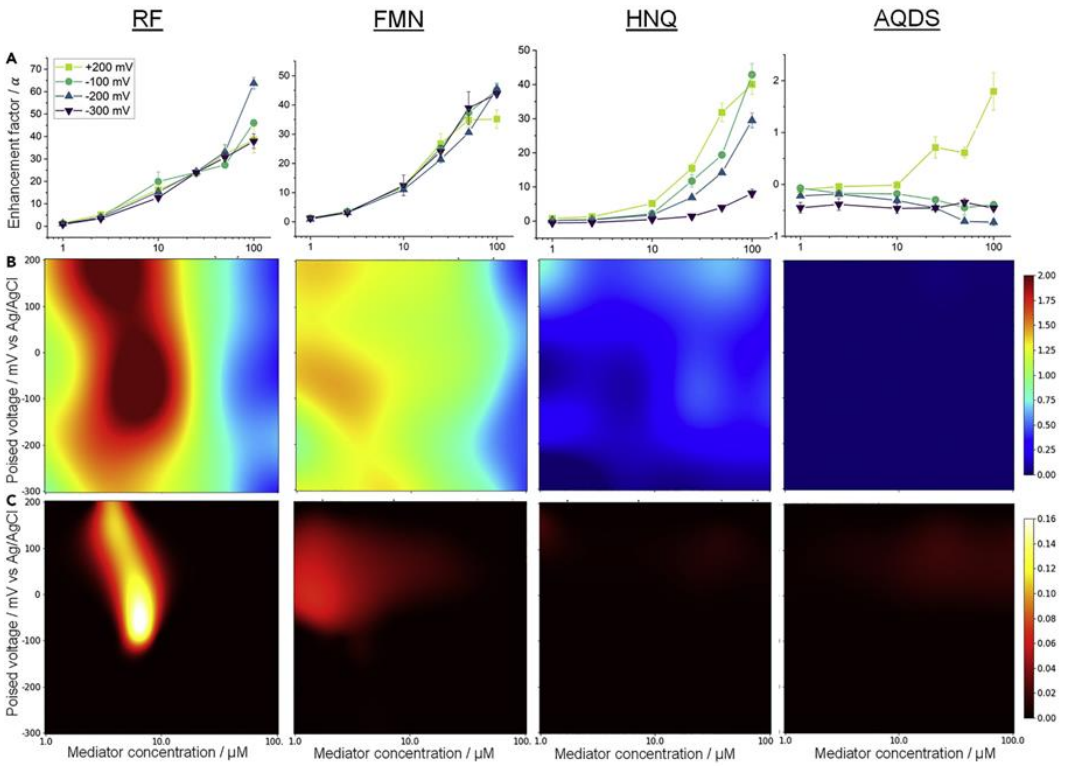

Figure 2-8 Additive's performance dependency on concentration and electrode potential for redox mediators.

(A) Current enhancement for RF, FMN, HNQ, and AQDS additive concentration and poised electrode potentials where enhancement factor was calculated using maximum slope against base current without any additives. B) Gaussian process regression model for the RF, FMN, HNQ, and AQDS additive performance against additive concentration and poised electrode potentials. C) Heatmaps for the expected improvements in RF, FMN, HNQ, and AQDS additive performance against additive concentration and poised electrode potentials.

The potential dependency of EI at peak performance concentration for each mediator showed that the EI functions of RF and FMN had one large peak and a shoulder, while those

of HNQ and AQDS had one peak (Figure 2-9), suggesting that the two redox reactions are involved in current production in the presence of flavins. Given that the redox potentials of bound RF and FMN, HNQ, and AQDS are closely located (Shi et al., 2012; Wu et al., 2014), the peak and the shoulder at around -100 mV are most likely assignable to their redox reaction with the electrode surface. Meanwhile, the main peak of flavins observed at -200 to -150 mV may also be attributable to the bound flavin cofactors in the outer membrane cytochrome (OMCs). Bound flavin cofactors in OMCs mediate the single-electron redox reaction to form a semiquinone state (Sq); therefore, there are two types of redox reactions, oxidized (Ox) / Sq and Sq / hydroquinone (Hq). While the Sq/Hq coupling redox reaction was reported to mediate electron uptake from the electrode surface (Okamoto, Hashimoto, et al., 2014), the Sq/Hq reaction may mediate anodic current production at a negative electrode potential, more so than the Ox/Sq coupling reaction in MR-1.

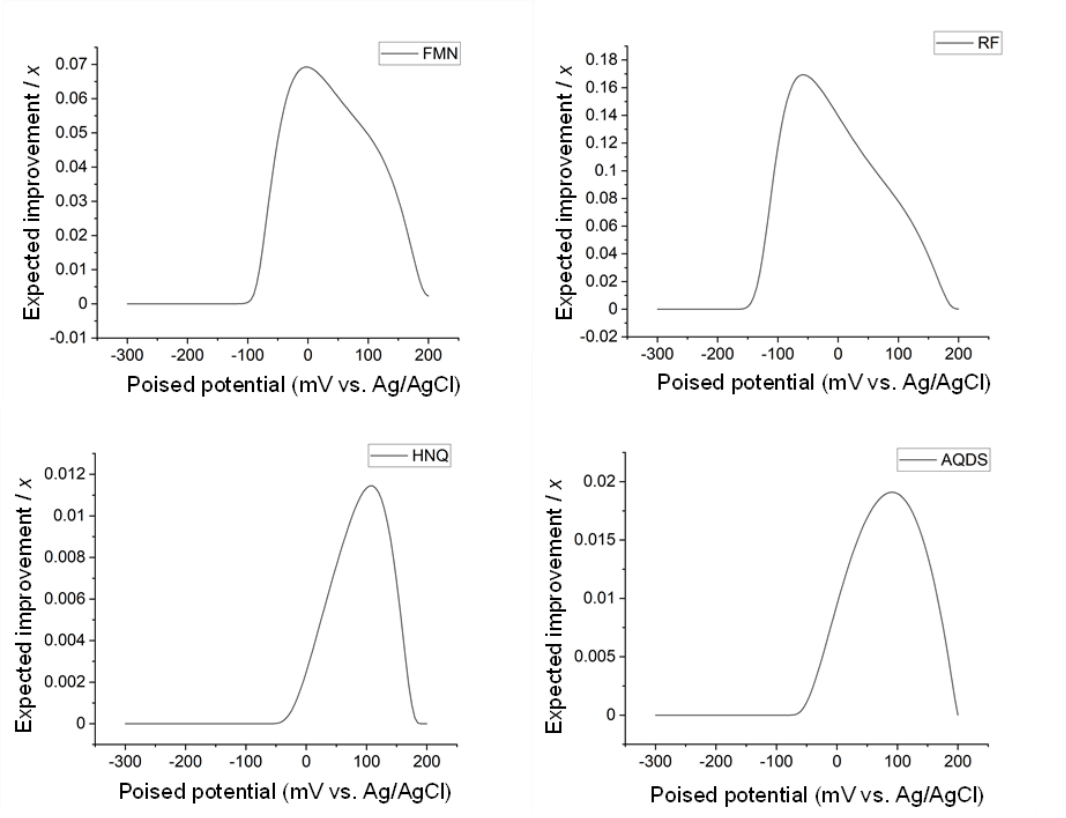

Figure 2-9 Cross section data of expected improvement (EI)

Expected improvement for each mediator (RF, FMN, HNQ, and AQDS) in the potential direction at the point where the EI of each mediator takes its maximum value.

To examine the origin of I_c enhancement at the negative electrode potential in the presence of flavins, we electrochemically analyzed the presence of Sq/Hq redox coupling using differential pulse voltammetry (DPV) during potential poising at -200 mV at various RF concentrations (Figure 2-10 and 2-9). We observed peaks at -460 and -30 mV vs. Ag/AgCl, and the peak current increased with increasing RF concentration (Figure 2-10A). Plots of I_c and the peak currents at -460 mV showed a linear correlation passing through the original point (Figure 2-10B), suggesting that both peaks are assignable to RF and the redox signal at -460 mV attributable to RF mediates I_c under -200 mV incubation condition. Accordingly, the linear voltammetry measurement showed the onset potential of LSV started from around -0.6 V, consistent with the onset of the RF peak at -460 mV (Figure 2-10C). When an excessive amount of RF was added to detect the DPV signal of the free form, an additional peak at -430 mV was detected. The half-peak width ($E_{w1/2}$) for the signals at -460 and -30 mV was approximately 130 mV, and $E_{w1/2}$ for -430 mV peak was approximately 50 mV, which is consistent with the one- and two-electron flavin redox processes, suggesting that -460, -430, and -30 mV are Sq/Hq, Ox/Hq, and Ox/Sq redox reactions, respectively. This assignment is in accordance with the relative location potential for each redox couple, that is, the two-electron Ox/Hq peak is between the two redox peaks for the single-electron redox reaction, and the observation that -460 and -30 mV peak currents both increased with the added flavin concentration. Given that the Sq/Hq redox couple was stabilized in OMCs under cathodic electrode conditions in MR-1 (Okamoto, Hashimoto, et al., 2014), we used a mutant strain lacking OMCs (*Δomc-all*). The impact of gene deletion resulted in slight I_c enhancement with increasing RF concentration. A clear decrease in the LSV and DPV signals was attributable to electron flow mediated by Sq/Hq (Figure 2-10 C and D). These results further demonstrate that the Sq/Hq redox couple is the main mechanism for I_c enhancement under negative electrode poising conditions.

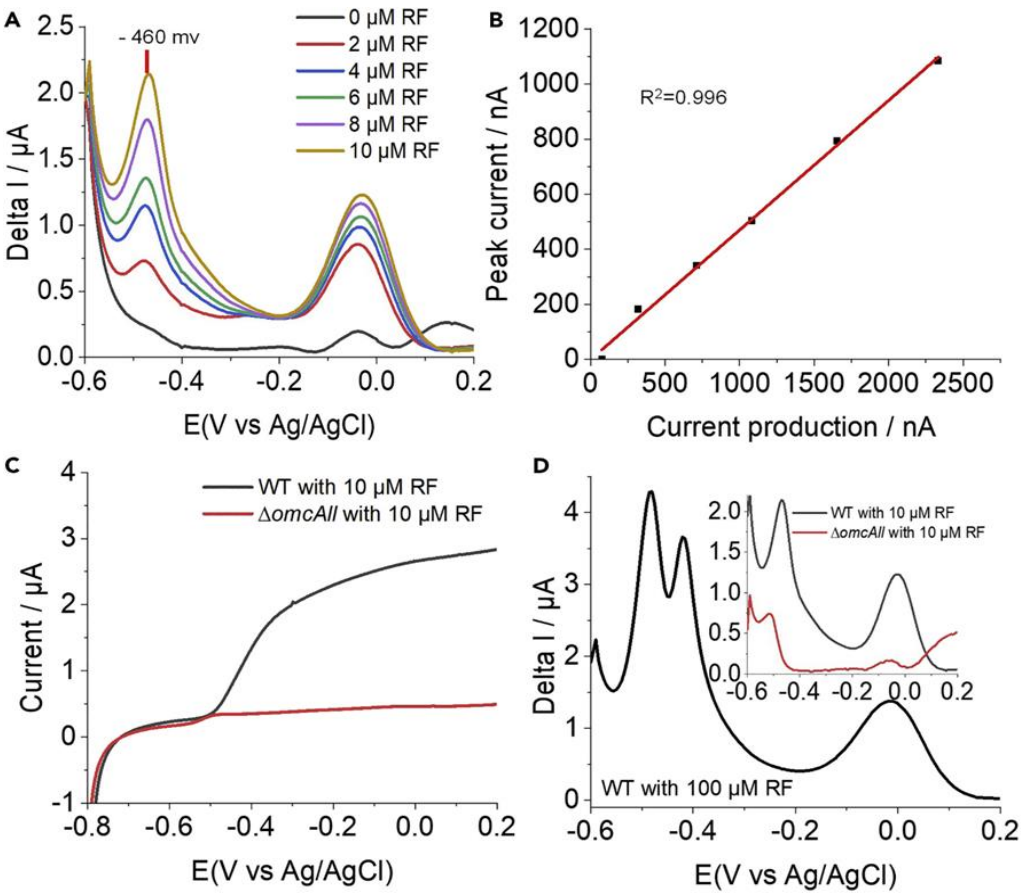

Figure 2-10 Contribution of the EET pathway associated with RF as a bound cofactor with OMCs formation in microbial current generation.

(A) DP voltammograms for WT measured at different RF concentration an hour after RF addition (B) Plots of peak current at -460 from each DP voltammogram The squares of the correlation coefficients were estimated by the addition of the point of origin to the obtained data. (C) Linear Sweep Voltammetry for WT and *Δomc-all* at 10 μM RF. (D) DP voltammogram for WT at excess addition of RF after incubation at −200 mV (vs. Ag/AgCl). Inset: DP voltammogram for WT at excess addition of RF after incubation at −200 mV (vs. Ag/AgCl).

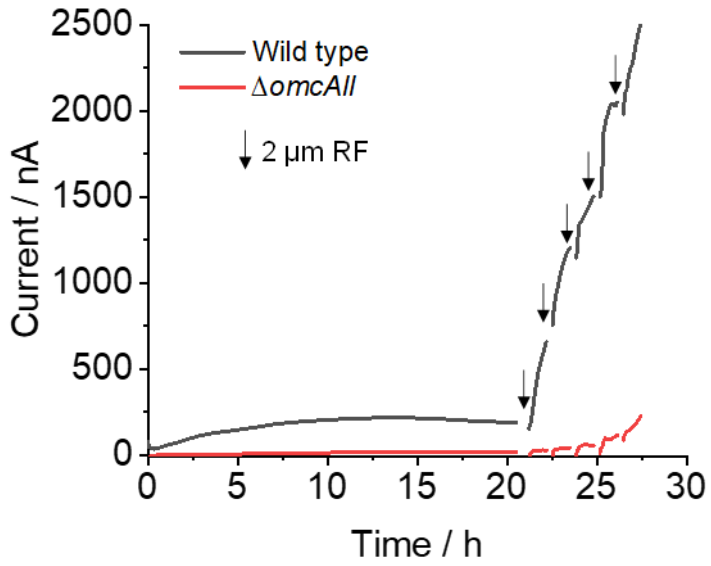

Figure 2-11 Impact of mutant strain *Δomc-all* on microbial current production with RF

Time profiles of microbial current production (I_c) at an electrode potential of -200 mV (vs. Ag/AgCl) at increasing RF concentration for MR-1 wild type (WT) and mutant strain lacking genes encoding OMCs (*Δomc*-all).

In contrast, such tolerance for the negative electrode potential was not observed in *G. sulfurreducens*, which is also capable of using riboflavin as a redox cofactor in c-type cytochromes (Okamoto, Saito, et al., 2014). Current production was measured under the same conditions as *S. oneidensis* MR-1, except for the electrolyte medium and concentration range of riboflavin, because the dissociation constant of riboflavin for binding OMCs was 100 times lower than that in *S. oneidensis* MR-1.(Jiang & Kappler, 2008; Tokunou et al., 2016) The effect of RF addition was not significant, most likely because the riboflavin secreted or contained in the medium was sufficiently higher than the Kd value. Meanwhile, I_c was considerably suppressed at more negative electrode potential than -0.1 V (Figure 2-6). Given that preculture conditions are uniform and not physiological, the EET mechanism most likely caused an immediate I_c decrease. Assuming that the low current production at a negative potential is caused by the dissociation of riboflavin from OMCs, the interaction of OMCs with the negatively poised electrode may change the binding affinity of RF to OMCs. These results suggest that while the current production capability of *G. sulfurreducens* is higher than that of

S. oneidensis MR-1 under positively poised conditions, *S. oneidensis* MR-1 is advantageous for sustainability under conditions of anodic potential fluctuation with varying wastewater conditions. In real wastewater treatment systems, the redox potential substantially changes depending on the wastewater oxidation-reduction reactions. (Li & Bishop, 2004) For instance, the redox potential of wastewater increases in the presence of strong oxidizing agents such as hydrogen peroxide, or decreases in the presence of strong reducing agents such as sodium bisulfite. (Higgins, 2008) The biological oxidation-reduction reactions such as nitrification, denitrification, biological phosphorus removal, and the removal of biological oxygen demand (carbon- and hydrogen-containing compounds) also dictate the redox potential conditions. Most of these processes occur in the range of -300 mV to +200 mV, varying from anaerobic to aerobic systems. (Goncharuk et al., 2010; Higgins, 2008) In this aspect, the tolerance to negative electrode potential in MR-1 is important, as among the bacteria that power BESs, *S. oneidensis* MR-1 species are widely studied for bioremediation and environmental energy recovery, owing to their robust growth in both aerobic and anaerobic environments within a wide range of redox potentials. (Lovley, 2006; Verma et al., 2021) However, the potential range advantage of *S. oneidensis* MR-1 has not been highlighted. This study, which captured the landscape of varying electrode potentials, not only identified the optimum additive conditions against the range of potentials but also help elucidating mechanism in EET. This model will help real wastewater systems to control the addition of current enhancement agents in varying redox potentials for the maximum performance of BESs.

2.4 Conclusion

We demonstrated the utility of applying data science to complex bacteria and electrode interactions by successfully developing a high-throughput and low-deviation electrochemical platform that could generate a database with quality reaching a level to effectively utilize data science. Two-dimensional landscapes of electrode potential and additive concentration generated from Bayesian estimation were mostly consistent with the bound and diffusible mechanisms in redox mediators, verifying that quality of database is sufficient to apply data

science analysis. Furthermore, the uninvestigated region of electrode potential and mediator concentration showed electron transfer mechanism via a bound flavin cofactor with a negatively poised electrode surface, further validating the data base quality and provide the first example of a electron transfer mechanism found by data science, highlighting the importance of the data science approach for fundamental understanding of BES. By further combining with the other data science model, our Bayesian estimation model may enable complex BES models to improve the performance of practical systems. (Shahriari et al., 2016) Owing to the flexibility of the electrolyte, potential poising, and electrode material, the present system can be extended to many other applications in electromicrobiology—in not only microbial fuel cells but also microbial electrosynthesis to develop carbon-neutral systems or metabolic activity sensor technologies for antibiotic drug discovery. (Miran et al., 2021; Naradasu et al., 2020)

Reference

Ahmadi, M., Ziatdinov, M., Zhou, Y., Lass, E. A., & Kalinin, S. V. (2021). Machine learning for high-throughput experimental exploration of metal halide perovskites. *Joule*, *5*(11), 2797-2822. https://doi.org/https://doi.org/10.1016/j.joule.2021.10.001

An, N. G., Kim, J. Y., & Vak, D. (2021). Machine learning-assisted development of organic photovoltaics via high-throughput in situ formulation [10.1039/D1EE00641J]. *Energy & Environmental Science*, *14*(6), 3438-3446. https://doi.org/10.1039/D1EE00641J

Call, D. F., & Logan, B. E. (2011). A method for high throughput bioelectrochemical research based on small scale microbial electrolysis cells. *Biosens Bioelectron*, *26*(11), 4526-4531. https://doi.org/10.1016/j.bios.2011.05.014

Chen, S., Patil, S. A., Brown, R. K., & Schröder, U. (2019). Strategies for optimizing the power output of microbial fuel cells: Transitioning from fundamental studies to practical implementation. *Applied Energy*, *233-234*, 15-28. https://doi.org/https://doi.org/10.1016/j.apenergy.2018.10.015

de Ramón-Fernández, A., Salar-García, M. J., Ruiz Fernández, D., Greenman, J., & Ieropoulos, I. A. (2020). Evaluation of artificial neural network algorithms for predicting the effect of the urine flow rate on the power performance of microbial fuel cells. *Energy*, *213*, 118806. https://doi.org/https://doi.org/10.1016/j.energy.2020.118806

Du, X., Lüer, L., Heumueller, T., Wagner, J., Berger, C., Osterrieder, T., Wortmann, J., Langner, S., Vongsaysy, U., Bertrand, M., Li, N., Stubhan, T., Hauch, J., & Brabec, C. J. (2021). Elucidating the Full Potential of OPV Materials Utilizing a High-Throughput Robot-Based Platform and Machine Learning. *Joule*, *5*(2), 495-506. https://doi.org/10.1016/j.joule.2020.12.013

Gadkari, S., Fontmorin, J.-M., Yu, E., & Sadhukhan, J. (2020). Influence of temperature and other system parameters on microbial fuel cell performance: Numerical and experimental investigation. *Chemical Engineering Journal*, *388*, 124176. https://doi.org/https://doi.org/10.1016/j.cej.2020.124176

Goncharuk, V., Bagrii, V., Mel'nik, L., Chebotareva, R., & Bashtan, S. (2010). The use of redox potential in water treatment processes. *J. Water Chem. Technol.*, *32*, 1-9. https://doi.org/10.3103/S1063455X10010017

Higgins, P. (2008). ORP Management in wastewater as an indicator of process efficiency. *YSI, Yellow Springs, OH http://www. ysi. com/media/pdfs/A567-ORP-Management-in-Wastewater-as-an-Indicator-of-Process-Efficiency. pdf (accessed on 15.08. 13)*.

Hirose, A., Kasai, T., Aoki, M., Umemura, T., Watanabe, K., & Kouzuma, A. (2018). Electrochemically active bacteria sense electrode potentials for regulating catabolic pathways. *Nature Communications*, *9*(1), 1083. https://doi.org/10.1038/s41467-018-03416-4

Jiang, D., Li, X., Raymond, D., Mooradain, J., & Li, B. (2010). Power recovery with multi-anode/cathode microbial fuel cells suitable for future large-scale applications. *International Journal of Hydrogen Energy*, *35*(16), 8683-8689. https://doi.org/https://doi.org/10.1016/j.ijhydene.2010.04.136

Jiang, J., & Kappler, A. (2008). Kinetics of Microbial and Chemical Reduction of Humic Substances: Implications for Electron Shuttling. *Environmental Science & Technology*, *42*(10), 3563-3569. https://doi.org/10.1021/es7023803

Kumar, A., Hsu, L. H.-H., Kavanagh, P., Barrière, F., Lens, P. N. L., Lapinsonnière, L., Lienhard V, J. H., Schröder, U., Jiang, X., & Leech, D. (2017). The ins and outs of microorganism–electrode electron transfer reactions. *Nature Reviews Chemistry*, *1*(3), 0024. https://doi.org/10.1038/s41570-017-0024

Lesnik, K. L., & Liu, H. (2017). Predicting Microbial Fuel Cell Biofilm Communities and Bioreactor Performance using Artificial Neural Networks. *Environmental Science & Technology*, *51*(18), 10881-10892. https://doi.org/10.1021/acs.est.7b01413

Li, B., & Bishop, P. L. (2004). Oxidation-reduction potential changes in aeration tanks and microprofiles of activated sludge floc in medium- and low-strength wastewaters. *Water Environment Research*, *76*(5), 394-403. https://doi.org/10.2175/106143004x151662

Liang, P., Wang, H., Xia, X., Huang, X., Mo, Y., Cao, X., & Fan, M. (2011). Carbon nanotube powders as electrode modifier to enhance the activity of anodic biofilm in microbial fuel

cells. *Biosensors and Bioelectronics*, *26*(6), 3000-3004. https://doi.org/https://doi.org/10.1016/j.bios.2010.12.002

Logan, B. E. (2010). Scaling up microbial fuel cells and other bioelectrochemical systems. *Appl Microbiol Biotechnol*, *85*(6), 1665-1671. https://doi.org/10.1007/s00253-009-2378-9

Logan, B. E., Rossi, R., Ragab, A. a., & Saikaly, P. E. (2019). Electroactive microorganisms in bioelectrochemical systems. *Nature Reviews Microbiology*, *17*(5), 307-319. https://doi.org/10.1038/s41579-019-0173-x

Lovley, D. R. (2006). Bug juice: harvesting electricity with microorganisms. *Nature Reviews Microbiology*, *4*(7), 497-508. https://doi.org/10.1038/nrmicro1442

Martinez, C. M., & Alvarez, L. H. (2018). Application of redox mediators in bioelectrochemical systems. *Biotechnol Adv*, *36*(5), 1412-1423. https://doi.org/https://doi.org/10.1016/j.biotechadv.2018.05.005

Matsui, T. S., Wu, H., & Deguchi, S. (2018). Deformable 96-well cell culture plate compatible with high-throughput screening platforms. *PLOS ONE*, *13*(9), e0203448. https://doi.org/10.1371/journal.pone.0203448

Miran, W., Naradasu, D., & Okamoto, A. (2021). Pathogens electrogenicity as a tool for in-situ metabolic activity monitoring and drug assessment in biofilms. *iScience*, *24*(2), 102068. https://doi.org/10.1016/j.isci.2021.102068

Molderez, T. R., Prévoteau, A., Ceyssens, F., Verhelst, M., & Rabaey, K. (2021). A chip-based 128-channel potentiostat for high-throughput studies of bioelectrochemical systems: Optimal electrode potentials for anodic biofilms. *Biosensors and Bioelectronics*, *174*, 112813. https://doi.org/https://doi.org/10.1016/j.bios.2020.112813

Molderez, T. R., Zhang, X., Rabaey, K., & Verhelst, M. (2019). A Current-Driven Six-Channel Potentiostat for Rapid Performance Characterization of Microbial Electrolysis Cells. *IEEE Transactions on Instrumentation and Measurement*, *68*(12), 4694-4702. https://doi.org/10.1109/TIM.2019.2898049

Naradasu, D., Guionet, A., Miran, W., & Okamoto, A. (2020). Microbial current production from Streptococcus mutans correlates with biofilm metabolic activity. *Biosensors and Bioelectronics*, *162*, 112236. https://doi.org/https://doi.org/10.1016/j.bios.2020.112236

Okamoto, A., Hashimoto, K., & Nealson, K. H. (2014). Flavin Redox Bifurcation as a Mechanism for Controlling the Direction of Electron Flow during Extracellular Electron Transfer. *Angewandte Chemie International Edition*, *53*(41), 10988-10991. https://doi.org/https://doi.org/10.1002/anie.201407004

Okamoto, A., Hashimoto, K., Nealson, K. H., & Nakamura, R. (2013). Rate enhancement of bacterial extracellular electron transport involves bound flavin semiquinones. *Proceedings of the National Academy of Sciences of the United States of America*, *110*(19), 7856-7861. https://doi.org/10.1073/pnas.1220823110

Okamoto, A., Hashimoto, K., Nealson, K. H., & Nakamura, R. (2013). Rate enhancement of bacterial extracellular electron transport involves bound flavin semiquinones. *Proceedings of the National Academy of Sciences*, *110*(19), 7856. https://doi.org/10.1073/pnas.1220823110

Okamoto, A., Nakamura, R., Nealson, K. H., & Hashimoto, K. (2014). Bound Flavin Model Suggests Similar Electron-Transfer Mechanisms in Shewanella and Geobacter. *ChemElectroChem*, *1*(11), 1808-1812. https://doi.org/https://doi.org/10.1002/celc.201402151

Okamoto, A., Saito, K., Inoue, K., Nealson, K. H., Hashimoto, K., & Nakamura, R. (2014). Uptake of self-secreted flavins as bound cofactors for extracellular electron transfer in Geobacter species [10.1039/C3EE43674H]. *Energy & Environmental Science*, *7*(4), 1357-1361. https://doi.org/10.1039/C3EE43674H

Patil, S. A., Górecki, K., Hägerhäll, C., & Gorton, L. (2013). Cisplatin-induced elongation of Shewanella oneidensis MR-1 cells improves microbe–electrode interactions for use in microbial fuel cells [10.1039/C3EE41974F]. *Energy & Environmental Science*, *6*(9), 2626-2630. https://doi.org/10.1039/C3EE41974F

Riba, J., Gleichmann, T., Zimmermann, S., Zengerle, R., & Koltay, P. (2016). Label-free isolation and deposition of single bacterial cells from heterogeneous samples for clonal culturing. *Scientific Reports*, *6*(1), 32837. https://doi.org/10.1038/srep32837

Shahriari, B., Swersky, K., Wang, Z., Adams, R. P., & Freitas, N. d. (2016). Taking the Human Out of the Loop: A Review of Bayesian Optimization. *Proceedings of the IEEE*, *104*(1), 148-175. https://doi.org/10.1109/JPROC.2015.2494218

Shi, L., Dong, H., Reguera, G., Beyenal, H., Lu, A., Liu, J., Yu, H.-Q., & Fredrickson, J. K. (2016). Extracellular electron transfer mechanisms between microorganisms and minerals. *Nature Reviews Microbiology*, *14*(10), 651-662. https://doi.org/10.1038/nrmicro.2016.93

Shi, Z., Zachara, J. M., Shi, L., Wang, Z., Moore, D. A., Kennedy, D. W., & Fredrickson, J. K. (2012). Redox Reactions of Reduced Flavin Mononucleotide (FMN), Riboflavin (RBF), and Anthraquinone-2,6-disulfonate (AQDS) with Ferrihydrite and Lepidocrocite. *Environmental Science & Technology*, *46*(21), 11644-11652. https://doi.org/10.1021/es301544b

Szydlowski, L., Ehlich, J., Goryanin, I., & Pasternak, G. (2021). High-throughput 96-well bioelectrochemical platform for screening of electroactive microbial consortia. *Chemical Engineering Journal*, 131692. https://doi.org/https://doi.org/10.1016/j.cej.2021.131692

Tahernia, M., Mohammadifar, M., Gao, Y., Panmanee, W., Hassett, D. J., & Choi, S. (2020). A 96-well high-throughput, rapid-screening platform of extracellular electron transfer in microbial fuel cells. *Biosensors and Bioelectronics*, *162*, 112259. https://doi.org/https://doi.org/10.1016/j.bios.2020.112259

Tokunou, Y., Hashimoto, K., & Okamoto, A. (2016). Acceleration of Extracellular Electron Transfer by Alternative Redox-Active Molecules to Riboflavin for Outer-Membrane Cytochrome c of Shewanella oneidensis MR-1. *The Journal of Physical Chemistry C*, *120*(29), 16168-16173. https://doi.org/10.1021/acs.jpcc.6b00349

Tsompanas, M.-A., You, J., Wallis, L., Greenman, J., & Ieropoulos, I. (2019). Artificial neural network simulating microbial fuel cells with different membrane materials and electrode configurations. *Journal of Power Sources*, *436*, 226832. https://doi.org/https://doi.org/10.1016/j.jpowsour.2019.226832

Vergani, M., Carminati, M., Ferrari, G., Landini, E., Caviglia, C., Heiskanen, A., Comminges, C., Zor, K., Sabourin, D., Dufva, M., Dimaki, M., Raiteri, R., Wollenberger, U., Emneus, J., & Sampietro, M. (2012). Multichannel Bipotentiostat Integrated With a Microfluidic

Platform for Electrochemical Real-Time Monitoring of Cell Cultures. *IEEE Transactions on Biomedical Circuits and Systems*, *6*(5), 498-507. https://doi.org/10.1109/TBCAS.2012.2187783

Verma, J., Kumar, D., Singh, N., Katti, S. S., & Shah, Y. T. (2021). Electricigens and microbial fuel cells for bioremediation and bioenergy production: a review. *Environmental Chemistry Letters*, *19*(3), 2091-2126. https://doi.org/10.1007/s10311-021-01199-7

Watson, V. J., Saito, T., Hickner, M. A., & Logan, B. E. (2011). Polymer coatings as separator layers for microbial fuel cell cathodes. *Journal of Power Sources*, *196*(6), 3009-3014. https://doi.org/https://doi.org/10.1016/j.jpowsour.2010.11.105

Wu, Y., Liu, T., Li, X., & Li, F. (2014). Exogenous Electron Shuttle-Mediated Extracellular Electron Transfer of Shewanella putrefaciens 200: Electrochemical Parameters and Thermodynamics. *Environmental Science & Technology*, *48*(16), 9306-9314. https://doi.org/10.1021/es5017312

Zhang, X., Li, X., Zhao, X., & Li, Y. (2019). Factors affecting the efficiency of a bioelectrochemical system: a review [10.1039/C9RA03605A]. *RSC Advances*, *9*(34), 19748-19761. https://doi.org/10.1039/C9RA03605A

Zhao, C.-e., Wu, J., Kjelleberg, S., Loo, J. S. C., & Zhang, Q. (2015). Employing a Flexible and Low-Cost Polypyrrole Nanotube Membrane as an Anode to Enhance Current Generation in Microbial Fuel Cells. *Small*, *11*(28), 3440-3443. https://doi.org/https://doi.org/10.1002/smll.201403328

Zhong, M., Tran, K., Min, Y., Wang, C., Wang, Z., Dinh, C.-T., De Luna, P., Yu, Z., Rasouli, A. S., Brodersen, P., Sun, S., Voznyy, O., Tan, C.-S., Askerka, M., Che, F., Liu, M., Seifitokaldani, A., Pang, Y., Lo, S.-C., Ip, A., Ulissi, Z., & Sargent, E. H. (2020). Accelerated discovery of CO2 electrocatalysts using active machine learning. *Nature*, *581*(7807), 178-183. https://doi.org/10.1038/s41586-020-2242-8

Ziara, R. M. M., Dvorak, B. I., & Subbiah, J. (2018). Chapter 7 - Sustainable Waste-to-Energy Technologies: Bioelectrochemical Systems. In T. A. Trabold & C. W. Babbitt (Eds.), *Sustainable Food Waste-To-energy Systems* (pp. 111-140). Academic Press. https://doi.org/https://doi.org/10.1016/B978-0-12-811157-4.00007-3

Chapter 3 Enhancement of microbial current production by riboflavin requires the reduced heme centers in outer membrane cytochromes in *Shewanella*

3.1 Introduction

Certain microorganisms transfer metabolically generated electrons to extracellular solids, such as iron and manganese, to terminate anaerobic respiration (Lovley & Phillips, 1988; Myers & Nealson, 1988). The extracellular electron transfer (EET) mechanism has been studied to improve the efficiency of bioremediation and bioenergy production and the understanding of the cycling of biogeochemical minerals (Lloyd & Lovley, 2001; Logan & Rabaey, 2012; Shi et al., 2016). One of the primary mechanisms for EET is associated with multi-heme protein *c*-type cytochrome complexes across the outer membrane. The outer membrane cytochromes (OMCs) have been identified in various electrogenic bacteria and investigated most well in *Shewanella oneidensis* MR-1 and *Geobacter sulfurreducens* PCA (Deng et al., 2018; Shi et al., 2016; Tanaka et al., 2018). Meanwhile, given the power efficiency of microbial fuel cell (MFC) and the degradation of pollutants currently were limited by EET (Huang et al., 2022; Schröder, 2007), the mechanism for enhancing and maintaining the rate of EET via OMCs needs to be investigated.

Self-secreted riboflavin (RF) and flavin mononucleotide enhance the EET rate via OMCs at a few μM levels, comparable with ~100 μM redox mediators that shuttles between microbe and electrode via diffusion-limited kinetics (Okamoto et al., 2013; A. Okamoto et al., 2014; Akihiro Okamoto, Koichiro Saito, et al., 2014; Tokunou et al., 2019; Xu et al., 2016). Various redox mediators have been used in *S. oneidensis* MR-1 to enhance the rate of EET via OMCs. These molecules directly mediate electron transfer to the electrode surface as a non-covalent cofactor in OMCs (Okamoto et al., 2013; A. Okamoto et al., 2014; Akihiro Okamoto, Koichiro Saito, et al., 2014; Tokunou et al., 2019). Given the bound cofactor mechanism has been demonstrated in *S. oneidensi*s MR-1 and *G. sulfurreducen* PCA (Okamoto et al., 2013; A. Okamoto et al., 2014; Akihiro Okamoto, Ryuhei Nakamura, et al., 2014; Akihiro Okamoto, Koichiro Saito, et al., 2014; Tokunou et al., 2019; Xu et al., 2016), the contribution of the bound cofactor mechanism with cell-secreted flavins should be critical for the power efficiency in

mediator-less MFC. Accordingly, the deletion of gene *bef* a gene essential for flavin biosynthesis can decrease the current production by 75% in *S. oneidensis* MR-1 (Kotloski & Gralnick, 2013). However, the effect of flavins largely decreases upon the dissociation of the bound cofactor from OMCs to be a soluble electron shuttle (Okamoto et al., 2013; A. Okamoto et al., 2014; Akihiro Okamoto, Koichiro Saito, et al., 2014; Tokunou et al., 2019; Xu et al., 2016). Therefore, identifying a critical factor to stabilize the bound flavin cofactor is critical for the power efficiency and stability of mediator-less MFCs.

While the binding mechanism between flavin and OMCs has been investigated, essential factors have been debated. The presence of lactate as an electron donor was vital for *S. oneidensis* MR-1 to form the bound flavin semiquinone with OMCs (Okamoto et al., 2013). In silico estimation using the crystal structure of a homologous protein with MtrC, a component of OMCs, suggested the reduced state of heme stabilizes the flavin binding to OMCs (Breuer et al., 2015; Hong & Pachter, 2016; Watanabe et al., 2017). These studies suggested that electron input forms reduced heme centers to stabilize the bound flavin in the OMCs of *S. oneidensis* MR-1. Meanwhile, a crystal of MtrC revealed that the CX_8C disulfide motif is a strictly conserved and oxidized heme centers stabilized the formation of bound flavin in purified MtrC after the cleavage of the disulfide bond (Edwards et al., 2015). Therefore, the contribution of the reduced heme center for MFCs performance remains under debate due to the lack of methodology to monitor and control the heme redox state of OMCs in the intact cell.

Recently, we developed whole-cell circular dichroism (CD) spectroscopy to monitor the inter heme interaction in MtrC (Tokunou et al., 2018; Tokunou & Okamoto, 2019). Because the exciton coupling effect among ten heme centers is very strong, the molar CD coefficient ($\Delta\varepsilon$) is 100-fold higher than the other mono-heme cytochrome in *S. oneidensis* MR-1 (Tokunou et al., 2018). The major CD signal from *S. oneidensis* MR-1 is assigned with MtrC by using a mutant strain lacking the gene (Tokunou et al., 2018). Therefore, CD spectroscopy enables monitoring of the oxidation state of the heme redox center, specifically in OMCs of an intact cell. In the present study, we examined the effect of the heme oxidation state in OMCs on the formation of bound flavin in situ during the current production of *S. oneidensis* MR-1. The bound flavin cofactor in OMCs has been identified as a semiquinone state, which mediated a

one-electron redox reaction. In contrast, the free RF mediates the two-electron redox reaction (Okamoto et al., 2013; A. Okamoto et al., 2014). Given both semiquinone and free-flavin peaks were identified by differential pulse voltammetry (DPV) in the previous work (Okamoto et al., 2013; Xu et al., 2016), the formation of bound semiquinone can be monitored by a feasible electrochemical method on a glass working electrode which was sprayed by Tin-doped In_2O_3 (ITO). We first examined with UV-Vis and CD spectroscopy whether the alternative electron pathway dimethyl sulfoxide (DMSO) reductase or fumarate reductase FccA could alter the oxidation state in heme centers of OMCs (Figure 3-1). Next, the effect of alternative electron acceptors, DMSO and fumarate, was examined for the semiquinone formation during microbial current production. We used six mutant strains to control the electron flow (Figure 3-1). The present study gives the knowledge to identify factors that significantly suppress the power density in MFCs, where power generation is limited by the rate of EET from electrogenic bacteria, that have bound flavin cofactor mechanisms, such as *Shewanella* and *Geobacter*.

3.2. Materials and Method

3.2.1 Cell preparation

S. oneidensis MR-1 wild type (WT) and mutant strains Δ*cymA*, ΔPEC, Δ*dms*-all, Δ*fccA,* Δ*mtrC/omcA,* and Δ*omc*-all were cultured in Luria-Bertani (LB) medium with shaking overnight under 30 ℃, and then cells were washed with defined medium (DM; $NaHCO_3$ [2.5 g], $CaCl_2 \cdot 2H_2O$ [0.08 g], NH_4Cl [1.0 g], $MgCl_2 \cdot 6H_2O$ [0.2 g], NaCl [10 g], HEPES [7.2 g], 0.5 g yeast extract, one liter ultrapure water) for two times, 6000 rpm 10 min for each time. Cell numbers were adjusted to the appropriate concentration for the next experiment by measuring optical density at λ = 600 nm (OD_{600}). Mutant strains were constructed as previously described (Table 1).

Table 1. Mutant strains used in this study

Strain	Genes deleted	Description	Source
Wild type			(Myers & Nealson, 1988)
Δ*cymA*	SO4591	Tetraheme cytochrome *c* quinone oxidase	(Bretschger et al., 2007)
ΔPEC	SO1777, SO1782, SO1427, SO4360, SO2277	The periplasmic electron carriers: MtrA, MrtD, DmsE, SO4360, CctA (small periplasmic tetraheme cytochrome)	(Coursolle & Gralnick, 2010)
Δ*dms*-all	SO1427-SO1432	The DMSO reductase operon (dmsEFABGH)	(Rowe et al., 2018)
Δ*fccA*	SO0970	Fumarate reductase (FccA)	(Bretschger et al., 2007)
Δ*mtrC/omcA*	SO1778, SO1779	Cell-surface decaheme cytochromes	(Bretschger et al., 2007)
Δ*omc*-all	SO1778-SO1782, SO2931, SO1659	All outer membrane multiheme cytochromes and their homologs	(Bücking et al., 2010)

3.2.2 Electrochemical Measurements

Electrochemical measurement was carried out as previously described by a three-electrode system single chamber (Okamoto et al., 2013). Tin-doped In_2O_3 (ITO) sprayed glass (3.1 cm^2, and thickness 1.1 mm), Ag/AgCl (saturated KCl) and platinum wire were used as working electrode (WE) reference electrode (RF) and counter electrode (CE), respectively. Five mL DM

with 10 mM lactate (sole electron donor) (DML) as an electrolyte, and then N_2 was purged for 30 mins in a sealed reactor. We kept the reactor temperature at 30 ℃ during the electrochemical measurement. The WE was poised at the potential of +200 mV (vs. Ag/AgCl KCl saturated). During microbial current production (I_c) measurement, DPV was run using an automatic polarization system (VMP3, BioLogic Company) from the initial potential of -800 mV to +500 mV, setting the pulses height, pulses width and step height as 50 mV, 300 ms, and 5 mV, respectively. The DP voltammograms deconvolved and baseline subtracted by Qsoas (Fourmond, 2016).

3.2.3 Absorption and CD spectrometry

The UV-Vis absorption and CD spectra of cell suspension samples were measured by Shimadzu UV Probe MPC-2200 and J -1500 (JASCO), respectively. The CD spectra was measured with 200 nm/min scan rate, 0.5 nm data pitch, 1.0 nm bandwidth, and 1 second digital integration time. For decreasing the background noise from cell body scattering, integrating sphere is used at the UV-Vis and CD spectrometry. Cells with $OD_{600} = 1.3 \pm 0.02$ were purged nitrogen in a sealed cuvette for 20 min to keep heme reduced state in the DM, which contains 30 mM lactate as previously described (Long & Okamoto, 2021; Tokunou & Okamoto, 2019). Then, the different concentrations of fumarate or DMSO (oxygen removed) were added to the cuvette to measure UV-Vis absorption and CD spectrometry.

3.2.4 Scanning electron microscopy (SEM)

The supernatant was removed from the ITO electrode after electrochemical measurement from the reactor. The electrode was washed with PBS, and then 2.5% glutaraldehyde was used to chemically fix the cells. Subsequently, ethanol gradients (25%, 50%, 75%, and 100%) were used for dehydration. Further, the *t*-butanol was used to treat the cell two times before freeze-dried under a vacuum. The sample was then coated with evaporated platinum for SEM observation with the Keyence VE-9800 microscope.

3.3 Results and Discussion

3.3.1 Whole-cell CD spectroscopy to monitor the effect of soluble electron acceptors on the heme oxidation state in OMCs

We first examined whether the activation of an alternative electron transport pathway could oxidize heme redox centers in an intact cell (Figure 3-1). Given reduced and oxidized heme in *c*-type cytochromes have the Soret band at 420 and 410 nm, respectively, we examined the peak position in the presence and absence of fumarate in the whole-cell UV-Vis absorption spectroscopy. While the Soret band was observed at 419 nm in the presence of 30 mM lactate, the addition of 40 mM fumarate caused a significant shift to 413 nm (Figure 3-2A). 5 mM DMSO caused only a slight shift to 418 nm, indicating 40 mM fumarate oxidized more heme centers than 5 mM DMSO in *S. oneidensis* MR-1 (Figure 3- 2B). In contrast, fumarate and DMSO showed no effect on the mutant strain Δ*fccA* and Δ*dms*-all, respectively (Figure 3-2C and D), suggesting the activation of fumarate and DMSO reduction pathway oxidizes heme centers partially in an intact cell even in the presence of lactate.

Next, to examine the impact of fumarate addition on the heme oxidation state in OMCs, whole-cell CD spectroscopy was performed with intact cells. As previously demonstrated, CD spectrometry has a high sensitivity to MtrC, due to the strong exciton coupling among the heme centers, MtrC has 100-fold higher molar CD than mono-heme cytochrome (Tokunou et al., 2018; Tokunou & Okamoto, 2019). Consistent with the previous report, the whole-cell reduced CD peak appears at 421 nm and 412 nm (black line), and the oxidized peak position is 417 nm after adding fumarate (blue line) (Figure 3-3A). However, the mutant strain Δ*omc*-all shows no peak at 421 nm, even though the peak position did not change after adding fumarate (Figure 3-3B). The same tendency was observed for DMSO in whole-cell CD spectra of WT and Δ*omc*-all (Figure 3-3D and 3-3E). These results suggest that the peak shift observed in WT was attributed to the oxidation of OMCs.

To quantify the effect of fumarate and DMSO, we excluded other cytochromes effects to better characterize the OMCs signal by subtracting the CD spectrum of mutant strain Δ*omc*-all from that of WT for each substrate's condition. As shown in Figure 3-2E, the difference in the

CD spectrum showed a single peak at 420 nm in *S. oneidensis* MR-1 with lactate, upon the addition of fumarate, the peak shifted to 415 nm with intensity decrease in WT, but such a shift was not observed in Δ*fccA*. We also observed a quick peak shift and intensity decrease associated with fumarate concentration increase even less than 1 mM in WT but not in Δ*fccA* (Figure 3-2F, Figure 3-3A). These results strongly suggest that heme centers in OMCs are oxidized by fumarate even in the presence of lactate. Consistent with UV-Vis spectroscopy, significant but less extent of CD signal change was observed with DMSO in WT, but, even less than 5 mM of DMSO quickly decreases the peak intensity, it was not observed in Δ*dms*-all (Figure 3-2G and 3-2H). We also confirmed that fumarate and DMSO do not affect the whole-cell spectra at mutant strain Δ*fccA* and Δ*dms*-all, respectively (Figure 3-3C and 3-3F), demonstrating that the activation of these alternative electron pathways oxidizes heme centers in OMCs and even low concentration of alternative electron acceptors significantly impact the heme oxidation state in OMCs. These results confirmed that the addition of fumarate and DMSO oxidizes the heme redox center in OMCs, even in the absence of an oxidative electrode.

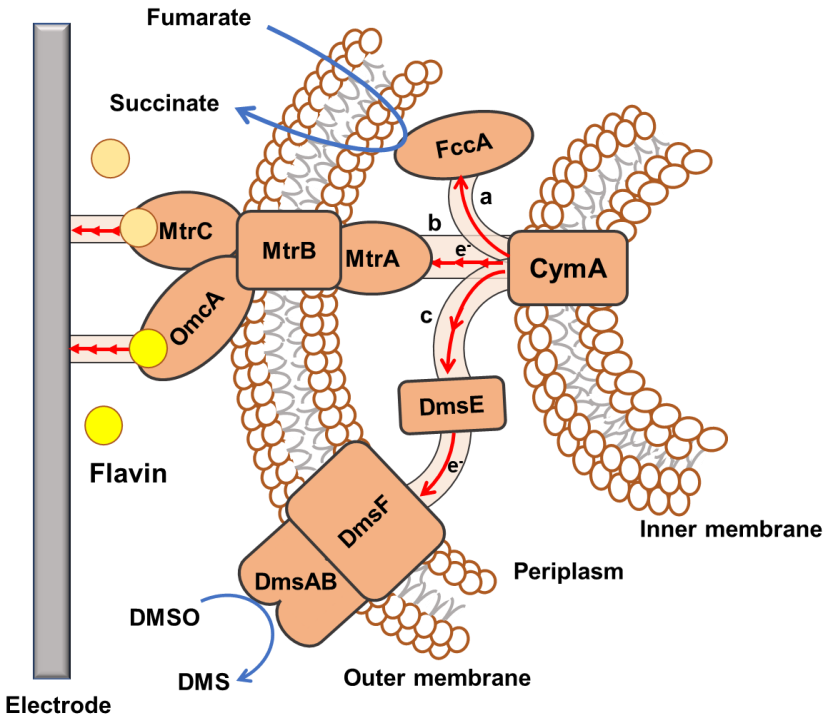

Figure 3-1 Schematic of three pathways for electron flow from the inner membrane to electron acceptors in *S. oneidensis* MR-1.

Fumarate reduction to succinate by FccA (a), extracellular transfer via MtrCAB-OmcA complex (b), and the reduction of dimethyl sulfoxide (DMSO) to dimethyl sulfide (DMS) by DmsE and DmsABF complex (c) terminate the respiratory electron transport chain from tetraheme cytochrome *c* quinone oxidase (CymA) in the inner membrane.

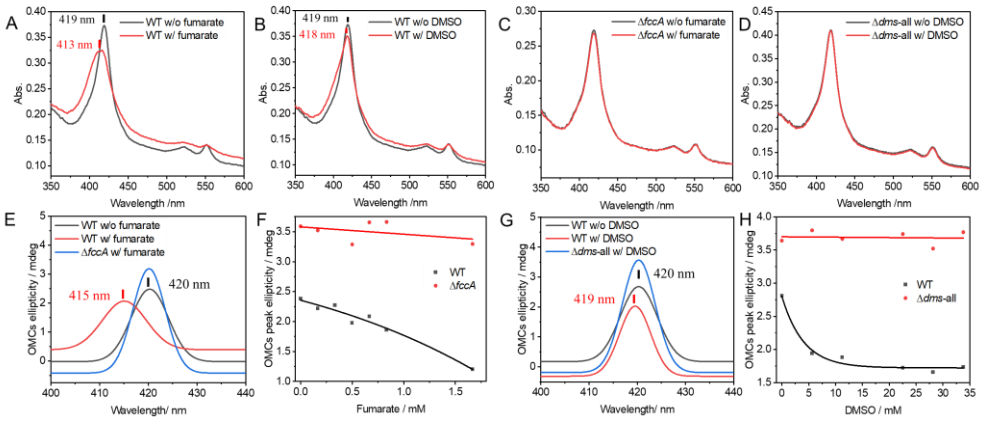

Figure 3-2 OMCs redox state measurement of wild type (WT), Δ*fccA* and Δ*dms*-all

UV-Vis spectra of OMCs in the presence/absence of fumarate (A) and dimethyl sulfoxide (DMSO) (B) in the WT. (C) UV-Vis spectra of OMCs with and without fumarate in the strain Δ*fccA*. (D) UV-Vis spectra of OMCs with and without DMSO in the strain Δ*dms*-all. (E) Difference circular dichroism (CD) spectra of WT and Δ*fccA* subtracted by Δ*omc*-all in the presence (WT, red and Δ*fccA*, blue) and absence (black) of 40 mM fumarate. (F) The CD spectra peak intensity of OMCs in the presence of different fumarate concentrations in the WT (black) and Δ*fccA* (red). (G) Difference CD spectra of WT and Δ*dms*-all subtracted by Δ*omc*-all in the presence (WT, red and Δ*dms*-all, blue) and absence (black) of DMSO. (H) CD spectra peak intensity of OMCs in the presence of different DMSO concentrations in the WT (black) and Δ*dms*-all (red). Representative data are shown from three independent experiments.

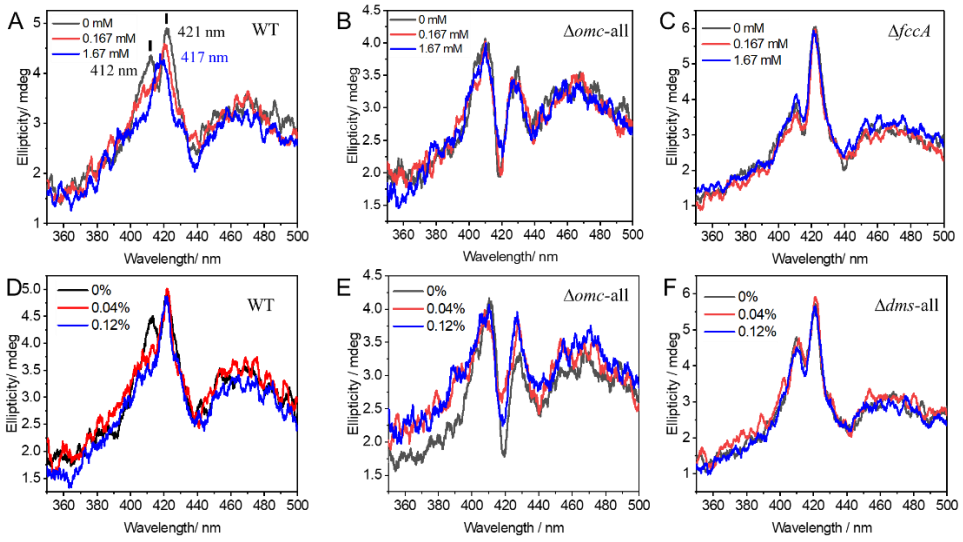

Figure 3-3 Redox state of wild type (WT) Δ*omc-all* Δ*dmsall* and Δ*fccA* in the presence of dimethyl sulfoxide (DMSO) and fumarate

Circular dichroism (CD) measurement of WT (A) Δ*omc-all* (B) and Δ*fccA* (C) in the presence of fumarate. CD measurement of WT (D) Δ*omc-all* (E) and Δ*dms-all* (F) in the presence of DMSO.

3.3.2 The effect of oxidizing heme centers in OMCs on the current enhancement by RF

Given fumarate has a stronger effect on oxidizing heme centers in OMCs than DMSO, we first examined the effect of heme oxidation on flavin binding to OMCs by using fumarate. We cultured the biofilm of *S. oneidensis* MR-1 at the poised potential of +200 mV (vs. Ag/AgCl KCl saturated). Subsequently, supernatant solution was removed carefully with the syringe, and the fresh nitrogen-purged DML containing 40 mM fumarate or 5mM DMSO was gently injected to the electrochemical rector under an anaerobic condition. The I_c from WT MR-1 was measured in the presence of 10 mM lactate at a poised potential of +200 mV (vs. Ag/AgCl KCl saturated). In the presence of 40 mM fumarate, the I_c showed three times less than that in the absence of fumarate (Figure 3-4A). This is consistent with spectroscopic data, where the activation of the fumarate reduction pathway diverted electron flux from OMCs to FccA. We next introduced RF to compare the enhancement factor of RF on the I_c. High concentration of

exogenous flavin (≥10 μM) can enhance the EET process by electron-shuttling mechanism, here, 8 μM RF was used as the cofactor for cytochromes via a one-electron redox reaction (Tokunou et al., 2019). While 8 μM RF steeply increased the I_c in the WT without fumarate, RF addition did not increase I_c in the presence of fumarate in the WT (Figure 3-4A), indicating that the presence of fumarate fully suppressed the rate enhancement effect on EET by bound RF in OMCs.

To examine whether the flavin binds to the OMCs in a semiquinone state in the presence of fumarate, the in-situ redox property of RF was examined by DPV. Oxidative peaks at -160 and -50 mV were observed as previously reported in the absence of fumarate upon deconvoluting two peaks which were assignable to the bound flavin cofactor and OMCs, respectively (Figure 3-4B). In the presence of fumarate, the peak at -160 mV was not observed, and a peak appeared only at -390 mV (Figure 3-4C), indicating that the presence of fumarate suppressed the formation of the bound flavin cofactor in OMCs. The peak of the bound flavin at -160 mV was observed in Δ*fccA* even with fumarate (Figure 3-4D), suggesting that the fumarate itself does not directly interact with flavin binding site in OMCs, but the oxidation of OMCs suppressed the bound flavin formation.

To further confirm this conclusion, we next examined the assignment of the negative redox peak at -390 mV observed in the presence of both RF and fumarate (Figure 3-4C). The peak at -390 mV was not observed in the absence of 8 μM RF (Figure 3-5). Therefore, the peak is assignable to the redox reaction of RF. Because fumarate reduction consumes two protons, proton concentration at the electrode surface should be decreased, which negatively shifts the free RF peak at -220 mV. Accordingly, the redox peak shifted to -210 mV after 12 hours (Figure 3-4C inset), when the depletion of fumarate gradually increased the I_c. To examine the assignment of the negative redox peak at -390 mV, we used the mutant strain Δ*mtrC/omcA* lacking RF binding site in OMCs but consumes lactate. The mutant strain Δ*mtrC/omcA* showed a large negative RF peak shift from -220 mV (without fumarate) (Figure 3-4E inset) to -350 mV (with fumarate) (Figure 3-4E), while no shift of peak potential was observed in the absence of bacteria (Figure 3-6A and 3-6B). The slightly negative shift (-390 mV to -350 mV) in the presence of fumarate may be caused by the lower metabolic activity of Δ*mtrC/omcA* than WT.

Therefore, these results strongly suggest that -390 mV is assignable to free RF but not bound RF. Meanwhile, the bulk pH did not change during the experiments due to buffering effect from HEPES. Therefore, these data suggest that microbial fumarate reduction increased the pH locally at the electrode surface.

In addition to the oxidative peak at -390 mV, the peak at -50 mV was not observed in Figure 3C. Because the peak was previously attributed to OMCs on the cell surface, the absence of a peak may be due to cellular detachment from the electrode surface. However, even after the addition of fumarate, the cellular attachment was confirmed by scanning electron microscopy (SEM) (Figure 3-7). Therefore, the disappearance of the OMCs signal also may be due to the pH change at the electrode surface associated with fumarate reduction.

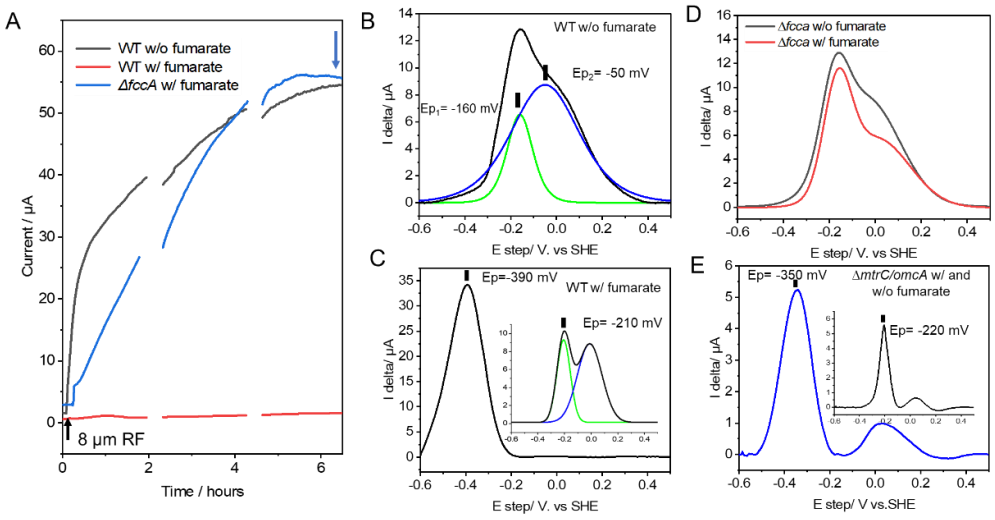

Figure 3-4 Oxidative hemes in OMCs inhibit the rate enhancement of EET by riboflavin (RF) in the presence of fumarate (1.5-column)

(A) Current production of wild type (WT) with/without fumarate, and Δ*fccA* with fumarate. Black and blue arrows present the addition of 8 μM RF and differential pulse voltammetry (DPV), respectively. Differential pulse (DP) voltammograms of WT in the absence of fumarate (B) and the presence of fumarate (C) and after adding fumarate for 12 hours (C inset). (D) DP voltammograms of mutant strain Δ*fccA* in the presence and absence of fumarate. (E) DP voltammograms for RF in the defined medium with Δ*mtrC/omcA* in the presence and absence of fumarate (inset). Representative data are shown from three independent experiments.

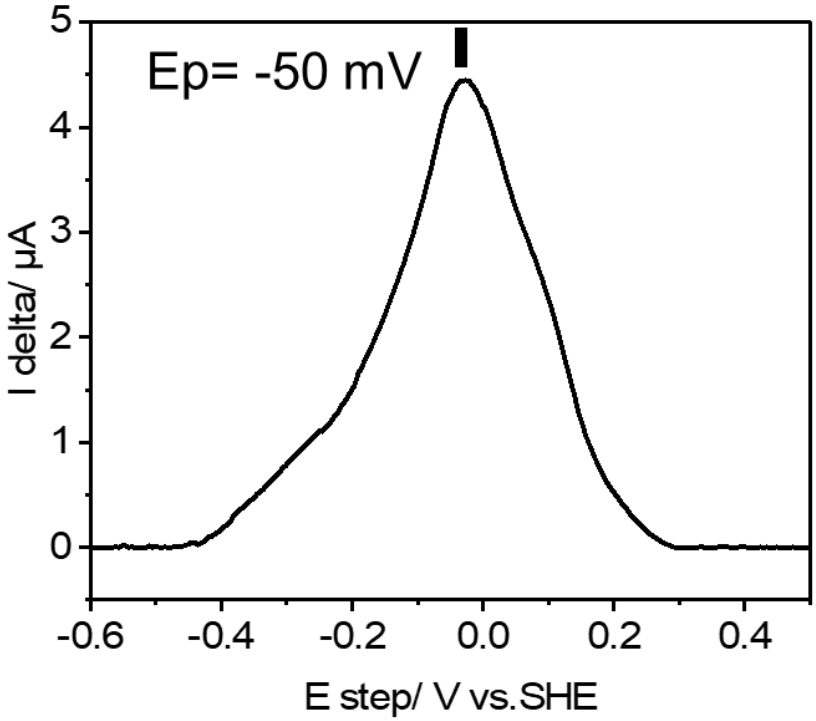

Figure 3-5 Redox property of *S. oneidensis* MR-1 biofilm

DP voltammograms for *S. oneidensis* MR-1 biofilm in the presence of fumarate without riboflavin.

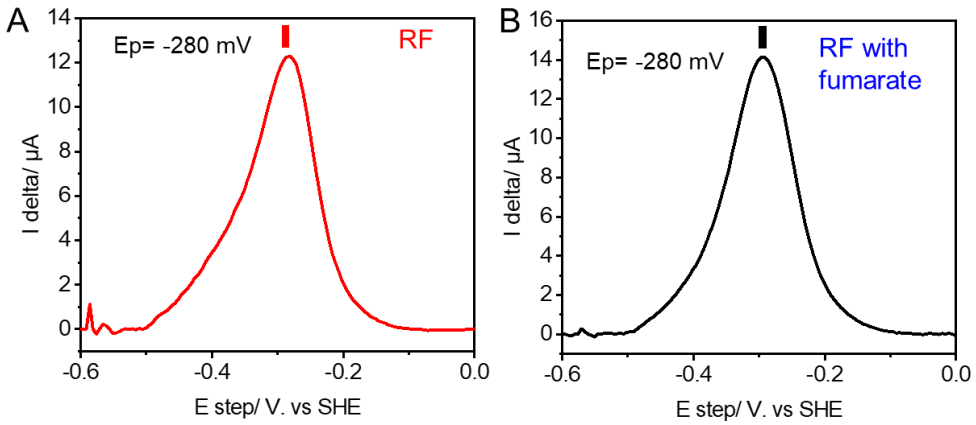

Figure 3-6 Redox property of free riboflavin.

(A) Differential pulse voltammetry (DPV) for riboflavin (RF) in the defined medium. (B) DPV for RF with fumarate in the defined medium.

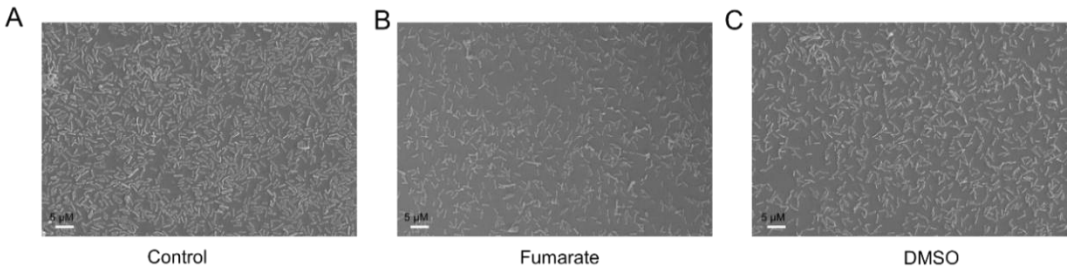

Figure 3-7 Biofilms of S. *oneidensis* MR-1 (A), and the addition of fumarate (B) and the addition of dimethyl sulfoxide (DMSO) (C).

We next confirm the significant effect of low concentration fumarate on the microbial current production. As shown in Figure 3-8A, while I_c was increased immediately after adding 8 µM RF in the absence of fumarate, even 1 and 2 mM fumarate almost completely suppressed the I_c enhancement effect of RF for hours (Figure 3-8A red and blue line). Subsequently, I_c gradually increased and reached the same level with that in the absence of fumarate, which may be caused by the depletion of fumarate. Consistent with the peak shift of flavin observed in the presence of 40 mM (Fig 3-4C), the DP voltammograms also showed a peak at -360 mV during the suppressed I_c enhancement by RF (Fig 3-8). In contrast, when I_c recovered, the peak shifted to the potential assignable to semiquinone in OMCs (Figure 3-8C). These results show that even the low concentration of fumarate significantly decrease I_c enhancement with RF by the impairing the semiquinone formation in OMCs.

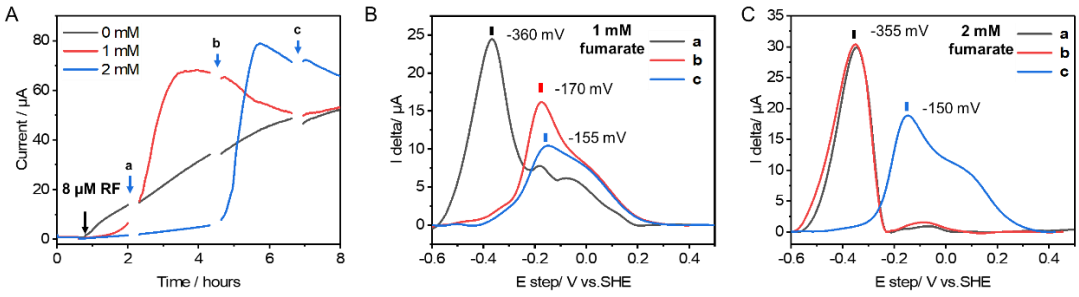

Figure 3-8 Oxidative hemes in OMCs inhibit the rate enhancement of EET by riboflavin (RF) in the presence of different concentrations of fumarate in the wild type

(A) Current production of wild type (WT) in different concentrations of fumarate. Black and blue arrows present the addition of 8 µM RF and differential pulse voltammetry (DPV), respectively. Differential pulse (DP) voltammograms of WT at points a, b and c with 1 mM

fumarate (B) and 2 mM fumarate (C). Representative data are shown from three independent experiments.

We next examined the effect of activating the DMSO reduction pathway for the formation of the bound flavin cofactor in OMCs. The presence of DMSO decreases I_c in the presence of 10 mM lactate at +200 mV (vs. Ag/AgCl KCl saturated) as observed with fumarate (Figure 3-9A). Consistent with the lower extent of heme oxidation in OMCs by DMSO than fumarate in the spectroscopic observations, I_c gradually increased upon the flavin addition within 6 hours. In the differential pulse voltammograms, three peaks were observed which had different peak positions compared with the bound flavin and OMCs in the absence of DMSO (Figure 3-9B). After 6 hours, the I_c with DMSO reached a comparable level with that without DMSO, suggesting that DMSO was consumed, and the peak position became identical with those in the absence of DMSO (Figure 3-4B), demonstrating flavin binds to OMCs without the activation of DMSO reduction pathway (Figure 3-9C). These data suggest that the activation of the DMSO reduction pathway to oxidize OMCs suppressed the bound flavin cofactor formation as with fumarate.

Three peaks at -340, -190, and 0 mV were observed in differential pulse voltammograms in the presence of DMSO during I_c measurements, and only the -340 mV peak was more negative than the free flavin peak at -220 mV in our medium condition. Given pH that on the electrode surface should increase with DMSO reduction as in the presence of fumarate, the peak at -340 mV may be assignable to the free flavin peak. To confirm the peak shift of free flavin in the presence of DMSO, we again used the mutant strain Δ*mtrC/omcA*. The RF redox potential appeared at -280 mV with mutant strain Δ*mtrC/omcA* in the presence of DMSO, which is 60 mV more negative than that of the peak position in the absence of DMSO (Figure 3-9D). The less peak shift of RF with DMSO compared with fumarate suggests that the rate of DMSO reduction is slower than fumarate reduction. Also, the lower metabolic activity of Δ*mtrC/omcA* than WT may limit the extent of the potential shift to less than that observed in WT. The peak at -190 mV may be assignable to bound RF because the impact of pH increase on the redox potential (Tokunou et al., 2019). However, the peak current decreased by more than 50% compared with that in the absence of DMSO (Figure 3-9B and 3-9C). A slight decrease in the

number of bacteria attached on the electrode does not explain the significant decrease in peak current (Figure 3-7C). We also confirmed that the presence of DMSO did not have any impact on the peak position in Δ*dms*-all (Figure 3-9E). These results strongly suggest that the oxidation of the heme center in OMCs resulted in less bound RF to OMCs and free flavin formation, supporting the conclusion from the fumarate experiments.

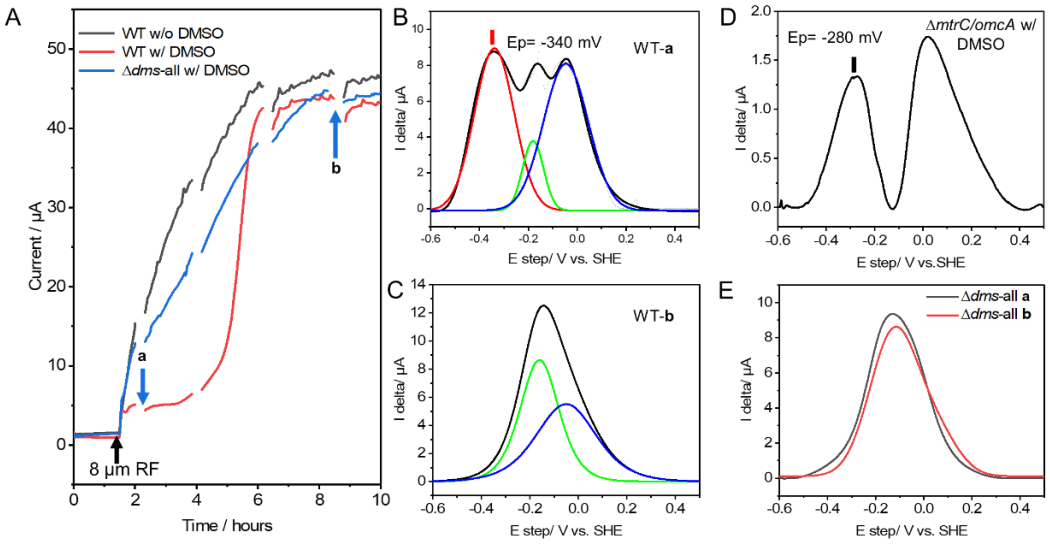

Figure 3-9 Oxidative hemes in OMCs inhibit the rate enhancement of EET by riboflavin (RF) in the presence of dimethyl sulfoxide (DMSO) (1.5-column)

(A) Current production of wild type (WT) with/without DMSO and Δ*dms*-all with DMSO. Black and blue arrows present the addition of 8 μM RF and differential pulse voltammetry (DPV), respectively. (B) and (C) DP voltammograms at the points a and b in WT with DMSO. (D) Differential pulse voltammograms for RF in the defined medium with Δ*mtrC/omcA* in the presence of DMSO. (E) DP voltammograms at the points a and b in the strain Δ*dms*-all with DMSO. Representative data are shown from three independent experiments.

3.3.3 Effect of deleting electron transport pathway to OMCs on flavocytochrome formation

To further confirm the effect of reduced hemes in OMCs on the bound flavin formation, we used mutants Δ*cymA* and ΔPEC to cut a pathway for donating respiratory electrons through MtrCAB-omcA. As reported before, I_c of Δ*cymA* and ΔPEC was significantly less than the WT strain (Figure 3-10A inset), indicating that electron flow to OMCs is suppressed in Δ*cymA* and ΔPEC (Figure 3-1). RF did not show I_c increment for Δ*cymA* and ΔPEC (Figure 3-10A, red and blue line). To examine whether the defect of I_c enhancement by RF addition effect is associated with the formation of bound RF in OMCs or not in Δ*cymA* and ΔPEC, DPV and peak deconvolution analysis were carried out in the presence of 8 μM RF among three strains. As expected, Δ*cymA* and ΔPEC did not show the oxidative peak at -160 mV of the bound flavin compared with WT, but it is at -225±5 mV which was assignable to the free flavin according to the previous results (Figure 3-10B-D). Furthermore, the peak width of -160 mV and -225±5 mV peak was 150 mV and 70 mV, indicating that RF mediated 1- and 2-electron redox reaction, respectively. These results strongly suggest that the formation of one-electron reduced semiquinone formation did not occur in Δ*cymA* and ΔPEC. In addition to peaks assignable to RF, a peak at -50 mV was observed in all three strains, attributable to the oxidation of heme centers in OMCs. Because the potential sweep was negative to positive, these heme centers were supposedly fully reduced in OMCs by electrode when DPV started. The oxidative peak area reflects the number of heme centers in each strain's OMCs. Peak current was roughly comparable at -50 mV among the three strains, suggesting that the concentration of OMCs on the electrode may not explain the disability of Δ*cymA* and ΔPEC to form bound semiquinone cofactor in OMCs. Meanwhile, the half-peak width in ΔPEC was significantly lower than WT and Δ*cymA*. Periplasmic cytochromes might contribute to the oxidative peak at -50 mV in WT and Δ*cymA* in addition to OMCs.

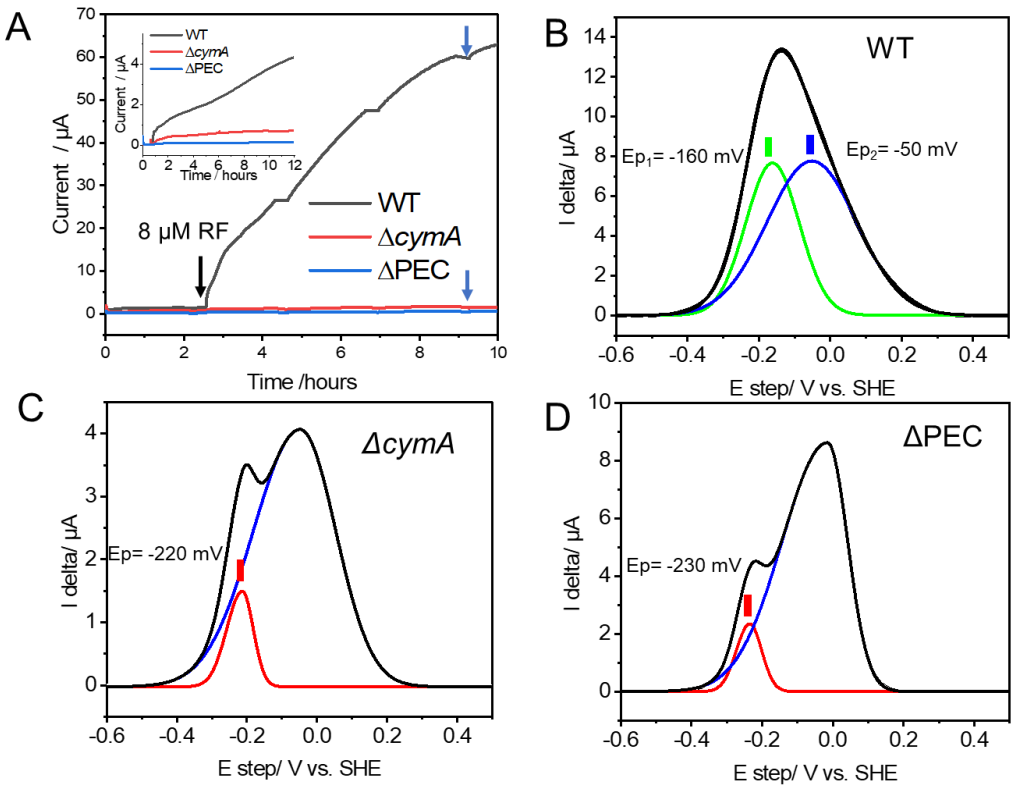

Figure 3-10 The effect of Δ*cymA* and ΔPEC on the rate enhancement effect by the bound riboflavin (RF) cofactor in OMCs (1-column)

(A) Current production of wild type (WT) and mutant strains Δ*cymA* and ΔPEC in the presence of 8 μM RF. Black and blue arrows present the addition of 8 μM RF and differential pulse voltammetry (DPV), respectively. Differential pulse voltammograms of WT (B) and Δ*cymA* (C) ΔPEC (D) in the presence of 8 μM RF. Representative data are shown from three independent experiments.

3.3.4. Discussion

While the importance of flavins for microbial current generation in mediator-less MFCs has been known for a while, how flavins can sustain their remarkable enhancement effect has been unknown. Given the binding of flavins to OMCs as a semiquinone cofactor is critical for the rate enhancement of EET, identifying a factor for controlling the binding affinity is essential. However, direct investigation of the small molecule binding to the cell-surface proteins under the current-producing conditions has been a challenge. In the present study, we combined UV-

Vis and CD spectroscopy with electrochemical analysis to study the contribution of the heme oxidation state on the flavin binding in OMCs. The oxidation state of hemes, specifically in OMCs, was monitored by the difference of CD signal where the spectrum of Δ*omc*-all was subtracted from that of WT. Alternative electron acceptors fumarate and DMSO partially oxidized the hemes in OMCs by diverting the electron pathway from OMCs (Figure 2). In whole-cell electrochemistry, the effect of RF on the enhancement of microbial current production became negligible, and differential pulse voltammetry did not detect the bound flavin cofactor in OMCs upon the oxidation of OMCs (Figure 3 4 and 5). However, the mutant strain lacking the reductase for fumarate or DMSO recovered both the current production and the bound cofactor formation. Additionally, cutting the electron flow to OMCs in Δ*cymA* and ΔPEC resulted in the scarce formation of the bound flavin (Figure 6). These results demonstrate that the reduced state of hemes is critical to stabilizing the bound flavin cofactor in OMCs. The conclusion follows the previous observation that lactate is necessary for the semiquinone formation in *S. oneidensis* MR-1 (Okamoto et al., 2013).

Deca-heme protein outer membrane cytochromes MtrC and OmcA form OMCs with MtrA by transmembrane barrel protein MtrB, which constructs an aisle for transferring electrons to the outside of cells. The crystal structures of the MtrCAB complex, MtrC, OmcA, and homologous protein MtrF were recently identified. Based on the crystal structure, authentic physicochemical electron transport energetics for electron conduction through redox heme centers have been extensively studied. *In silico* estimation using the crystal structure of MtrF, the redox potential of the terminal heme in the oxidized state is close to that of flavin, which is more positive than that of the reduced state, so flavin is more likely to bind to the reduced flavin for electron transfer (Watanabe et al., 2017). In addition, it was found that the Gibbs free energy of the oxidized OMCs binding to flavin is higher through molecular docking (Hong & Pachter, 2016), thermodynamically, the flavin binds more easily to the reduced OMCs (Figure 3-11).

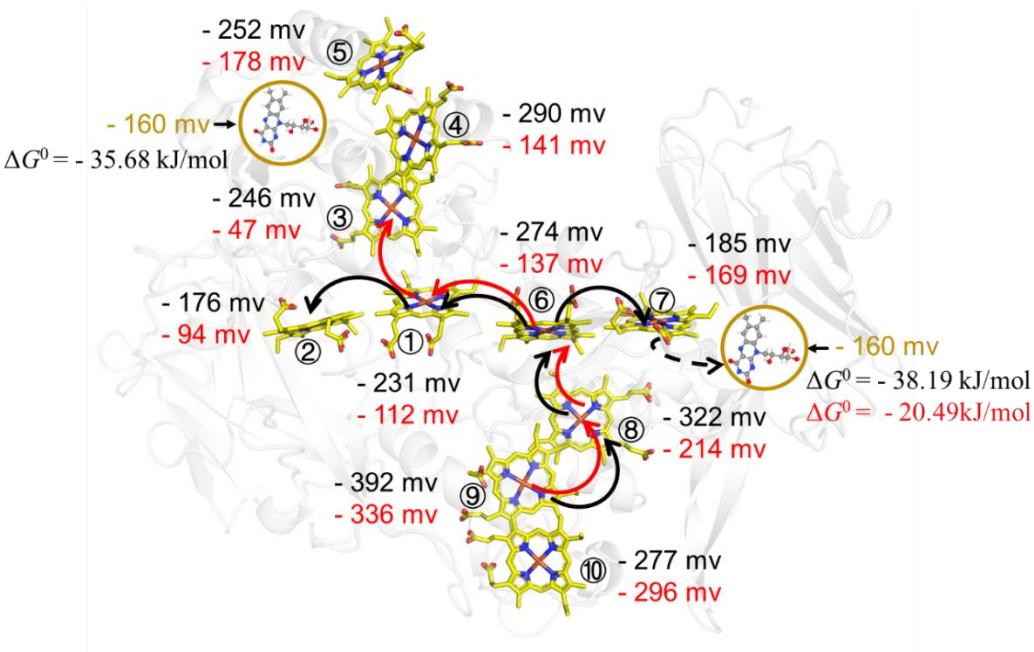

Figure 3-11 Electron transfer pathway in the oxidized and reduced MtrC with riboflavin (RF) binding

Electron transfer paths in MtrC simulated according to MtrF. The black arrow and red arrow indicated the reduced and oxidized heme electron flow, respectively. Brown cycles represent the binding site and binding energy of RF (black and red represent the binding energy of reduced and oxidized state MtrC with RF).

In addition to reduced heme centers, the well conserved structure of the CX_8C disulfide bond in MtrC was shown to be critical for flavin binding in MtrC and OmcA (Edwards et al., 2015). Edward, M. J. et al. demonstrated that the specific cleavage of disulfide bond stabilizes the bound flavin in purified MtrC and OmcA with oxidized heme centers. Meanwhile, the impact of heme reduction was not examined with disulfide bonds in MtrC and OmcA. In the present study, the hemes in OMCs were oxidized under anaerobic conditions. Because the redox of the disulfide bond was independent from the oxidation state of heme in purified MtrC, the fumarate or DMSO addition specifically oxidized the hemes in OMCs but not the two thiol groups of the reduced cysteines to recover the disulfide bond. Therefore, the observed flavin dissociation from the oxidized OMCs after the cleavage of a disulfide bond in the present study conflicts with the report with purified MtrC. The difference may be explainable by the structural difference of MtrC in an intact cell and purified state, due to the membrane or protein-protein

effects (Hunte & Richers, 2008; Levental & Lyman, 2022). The OMCs are flexible in structure, and the molar CD signal of MtrC is significantly altered in an intact cell (Johs et al., 2010; Tokunou et al., 2018). Alternatively, RF may weakly bound to MtrC not as semiquinone but as hydroquinone state to shuttle electrons in purified MtrC without a disulfide bond, as previously speculated.

Fumarate showed a stronger ability to oxidize OMCs than DMSO in both spectroscopy and electrochemistry. However, fumarate reductase to generate succinate has more negative redox potential than DMSO reductase (Kracke et al., 2015). The electron transport pathway in the periplasmic space has been investigated using gene editing, NMR and small-angle neutron scattering extensively (Alves et al., 2015; Edwards et al., 2018; Fonseca et al., 2013; Schuetz et al., 2009). While the FccA protein can exchange electrons with even MtrA, DMSO reductase bound to the outer membrane needs some electron transfer intervals for receiving an electron from OMCs. Therefore, a potential explanation is that fumarate is more kinetically prone to act as an electron acceptor because FccA is closer to the CymA (Figure 3-1).

For sustaining the high EET efficiency, mediators were used to enhance the electron transfer, flavin secreted by bacteria is a natural and non-toxic mediator of increasing the power generation in the mediator-less MFCs. If electron acceptors like fumarate or DMSO contaminate in MFCs, these not only compete for electrons with the anode but also promote the dissociation of the bound flavin cofactor even at less than 1 mM concentration (Figure 3-2F and H), resulting in the significant decrease in the power density of MFCs. Except for the electron acceptor which comes from the working environment, electron acceptors produced by the cell itself should also be taken into account. Fumarate can be synthesized by some biological processes during cell metabolism, suggesting that the fumarate synthesis pathway should be properly inhibited to enhance power output in MFCs. Given sufficient electron flow across OMCs is necessary for flavin binding, the stable flow of sufficient electron donors is essential for maintaining highly effective power output (Heilmann & Logan, 2006; Kim et al., 2003).

3.4. Conclusion

The present study shows that the reduced hemes are essential for OMCs to sustain high current efficiency via the bound flavin mechanism. Even less than 1 mM of fumarate or DMSO significantly oxidizes the hemes in the OMCs, indicating that the presence of an alternative electron acceptor could suppress the power generation even more than the stoichiometric ratio. A similar mechanism may control the affinity of RF to OMCs in *G. sulfurreducens* PCA. Therefore, the importance of deactivating alternative electron transport pathways would be a general strategy to sustain the critical effect of redox mediators in MFCs. Furthermore, the CD spectroscopy to monitor the oxidation state of OMCs in an intact cell would facilitate the exploration of the method to keep the reduced hemes in OMCs even in the presence of other electron acceptors.

Reference

Alves, M. N., Neto, S. E., Alves, A. S., Fonseca, B. M., Carrêlo, A., Pacheco, I., Paquete, C. M., Soares, C. M., & Louro, R. O. (2015). Characterization of the periplasmic redox network that sustains the versatile anaerobic metabolism of Shewanella oneidensis MR-1. *Front Microbiol*, *6*, 665. https://doi.org/10.3389/fmicb.2015.00665

Bretschger, O., Obraztsova, A., Sturm, C. A., Chang, I. S., Gorby, Y. A., Reed, S. B., Culley, D. E., Reardon, C. L., Barua, S., Romine, M. F., Zhou, J., Beliaev, A. S., Bouhenni, R., Saffarini, D., Mansfeld, F., Kim, B. H., Fredrickson, J. K., & Nealson, K. H. (2007). Current production and metal oxide reduction by Shewanella oneidensis MR-1 wild type and mutants. *Appl Environ Microbiol*, *73*(21), 7003-7012. https://doi.org/10.1128/aem.01087-07

Breuer, M., Rosso, K. M., & Blumberger, J. (2015). Flavin Binding to the Deca-heme Cytochrome MtrC: Insights from Computational Molecular Simulation. *Biophys J*, *109*(12), 2614-2624. https://doi.org/10.1016/j.bpj.2015.10.038

Bücking, C., Popp, F., Kerzenmacher, S., & Gescher, J. (2010). Involvement and specificity of Shewanella oneidensis outer membrane cytochromes in the reduction of soluble and solid-phase terminal electron acceptors. *FEMS Microbiology Letters*, *306*(2), 144-151. https://doi.org/10.1111/j.1574-6968.2010.01949.x

Coursolle, D., & Gralnick, J. A. (2010). Modularity of the Mtr respiratory pathway of Shewanella oneidensis strain MR-1. *Mol Microbiol*, *77*(4), 995-1008. https://doi.org/10.1111/j.1365-2958.2010.07266.x

Deng, X., Dohmae, N., Nealson, K. H., Hashimoto, K., & Okamoto, A. (2018). Multi-heme cytochromes provide a pathway for survival in energy-limited environments. *Sci Adv*, *4*(2), eaao5682. https://doi.org/10.1126/sciadv.aao5682

Edwards, M. J., White, G. F., Lockwood, C. W., Lawes, M. C., Martel, A., Harris, G., Scott, D. J., Richardson, D. J., Butt, J. N., & Clarke, T. A. (2018). Structural modeling of an outer membrane electron conduit from a metal-reducing bacterium suggests electron transfer via periplasmic redox partners. *J Biol Chem*, *293*(21), 8103-8112. https://doi.org/10.1074/jbc.RA118.001850

Edwards, M. J., White, G. F., Norman, M., Tome-Fernandez, A., Ainsworth, E., Shi, L., Fredrickson, J. K., Zachara, J. M., Butt, J. N., Richardson, D. J., & Clarke, T. A. (2015). Redox Linked Flavin Sites in Extracellular Decaheme Proteins Involved in Microbe-Mineral Electron Transfer. *Scientific Reports*, *5*, 11677. https://doi.org/10.1038/srep11677

Fonseca, B. M., Paquete, C. M., Neto, S. E., Pacheco, I., Soares, C. M., & Louro, R. O. (2013). Mind the gap: cytochrome interactions reveal electron pathways across the periplasm of Shewanella oneidensis MR-1. *Biochemical Journal*, *449*(1), 101-108. https://doi.org/10.1042/bj20121467

Fourmond, V. (2016). QSoas: A Versatile Software for Data Analysis. *Analytical Chemistry*, *88*(10), 5050-5052. https://doi.org/10.1021/acs.analchem.6b00224

Heilmann, J., & Logan, B. E. (2006). Production of electricity from proteins using a microbial fuel cell. *Water Environment Research*, *78*(5), 531-537. https://doi.org/10.2175/106143005x73046

Hong, G., & Pachter, R. (2016). Bound Flavin-Cytochrome Model of Extracellular Electron Transfer in Shewanella oneidensis: Analysis by Free Energy Molecular Dynamics Simulations. *Journal of Physical Chemistry B*, *120*(25), 5617-5624. https://doi.org/10.1021/acs.jpcb.6b03851

Huang, J., Cai, X. L., Peng, J. R., Fan, Y. Y., & Xiao, X. (2022). Extracellular pollutant degradation feedback regulates intracellular electron transfer process of exoelectrogens: Strategy and mechanism. *Science of the Total Environment*, *853*, 158630. https://doi.org/10.1016/j.scitotenv.2022.158630

Hunte, C., & Richers, S. (2008). Lipids and membrane protein structures. *Curr Opin Struct Biol*, *18*(4), 406-411. https://doi.org/10.1016/j.sbi.2008.03.008

Johs, A., Shi, L., Droubay, T., Ankner, J. F., & Liang, L. (2010). Characterization of the decaheme c-type cytochrome OmcA in solution and on hematite surfaces by small angle x-ray scattering and neutron reflectometry. *Biophys J*, *98*(12), 3035-3043. https://doi.org/10.1016/j.bpj.2010.03.049

Kim, B. H., Chang, I. S., Gil, G. C., Park, H. S., & Kim, H. J. (2003). Novel BOD (biological oxygen demand) sensor using mediator-less microbial fuel cell. *Biotechnol Lett*, *25*(7), 541-545. https://doi.org/10.1023/a:1022891231369

Kotloski, N. J., & Gralnick, J. A. (2013). Flavin electron shuttles dominate extracellular electron transfer by Shewanella oneidensis. *mBio*, *4*(1). https://doi.org/10.1128/mBio.00553-12

Kracke, F., Vassilev, I., & Krömer, J. O. (2015). Microbial electron transport and energy conservation - the foundation for optimizing bioelectrochemical systems. *Front Microbiol*, *6*, 575. https://doi.org/10.3389/fmicb.2015.00575

Levental, I., & Lyman, E. (2022). Regulation of membrane protein structure and function by their lipid nano-environment. *Nature Reviews: Molecular Cell Biology*. https://doi.org/10.1038/s41580-022-00524-4

Lloyd, J. R., & Lovley, D. R. (2001). Microbial detoxification of metals and radionuclides. *Current Opinion in Biotechnology*, *12*(3), 248-253. https://doi.org/10.1016/s0958-1669(00)00207-x

Logan, B. E., & Rabaey, K. (2012). Conversion of Wastes into Bioelectricity and Chemicals by Using Microbial Electrochemical Technologies. *Science*, *337*(6095), 686-690. https://doi.org/doi:10.1126/science.1217412

Long, X., & Okamoto, A. (2021). Outer membrane compositions enhance the rate of extracellular electron transport via cell-surface MtrC protein in Shewanella oneidensis MR-1. *Bioresource Technology*, *320*(Pt A), 124290. https://doi.org/10.1016/j.biortech.2020.124290

Lovley, D. R., & Phillips, E. J. (1988). Novel mode of microbial energy metabolism: organic carbon oxidation coupled to dissimilatory reduction of iron or manganese. *Applied and Environmental Microbiology*, *54*(6), 1472-1480. https://www.ncbi.nlm.nih.gov/pubmed/16347658

Myers, C. R., & Nealson, K. H. (1988). Bacterial manganese reduction and growth with manganese oxide as the sole electron acceptor. *Science*, *240*(4857), 1319-1321. https://doi.org/10.1126/science.240.4857.1319

Okamoto, A., Hashimoto, K., Nealson, K. H., & Nakamura, R. (2013). Rate enhancement of bacterial extracellular electron transport involves bound flavin semiquinones. *Proceedings of the National Academy of Sciences of the United States of America*, *110*(19), 7856-7861. https://doi.org/10.1073/pnas.1220823110

Okamoto, A., Kalathil, S., Deng, X., Hashimoto, K., Nakamura, R., & Nealson, K. H. (2014). Cell-secreted flavins bound to membrane cytochromes dictate electron transfer reactions to surfaces with diverse charge and pH. *Scientific Reports*, *4*, 5628. https://doi.org/10.1038/srep05628

Okamoto, A., Nakamura, R., Nealson, K. H., & Hashimoto, K. (2014). Bound Flavin Model Suggests Similar Electron-Transfer Mechanisms in Shewanella and Geobacter. *ChemElectroChem*, *1*(11), 1808-1812. https://doi.org/https://doi.org/10.1002/celc.201402151

Okamoto, A., Saito, K., Inoue, K., Nealson, K. H., Hashimoto, K., & Nakamura, R. (2014). Uptake of self-secreted flavins as bound cofactors for extracellular electron transfer in Geobacter species [10.1039/C3EE43674H]. *Energy & Environmental Science*, *7*(4), 1357-1361. https://doi.org/10.1039/C3EE43674H

Rowe, A. R., Rajeev, P., Jain, A., Pirbadian, S., Okamoto, A., Gralnick, J. A., El-Naggar, M. Y., & Nealson, K. H. (2018). Tracking Electron Uptake from a Cathode into Shewanella Cells: Implications for Energy Acquisition from Solid-Substrate Electron Donors. *mBio*, *9*(1). https://doi.org/10.1128/mBio.02203-17

Schröder, U. (2007). Anodic electron transfer mechanisms in microbial fuel cells and their energy efficiency. *Physical Chemistry Chemical Physics*, *9*(21), 2619-2629. https://doi.org/10.1039/b703627m

Schuetz, B., Schicklberger, M., Kuermann, J., Spormann, A. M., & Gescher, J. (2009). Periplasmic electron transfer via the c-type cytochromes MtrA and FccA of Shewanella oneidensis MR-1. *Appl Environ Microbiol*, *75*(24), 7789-7796. https://doi.org/10.1128/aem.01834-09

Shi, L., Dong, H., Reguera, G., Beyenal, H., Lu, A., Liu, J., Yu, H. Q., & Fredrickson, J. K. (2016). Extracellular electron transfer mechanisms between microorganisms and minerals. *Nat Rev Microbiol*, *14*(10), 651-662. https://doi.org/10.1038/nrmicro.2016.93

Tanaka, K., Yokoe, S., Igarashi, K., Takashino, M., Ishikawa, M., Hori, K., Nakanishi, S., & Kato, S. (2018). Extracellular Electron Transfer via Outer Membrane Cytochromes in a Methanotrophic Bacterium Methylococcus capsulatus (Bath). *Front Microbiol*, *9*, 2905. https://doi.org/10.3389/fmicb.2018.02905

Tokunou, Y., Chinotaikul, P., Hattori, S., Clarke, T. A., Shi, L., Hashimoto, K., Ishii, K., & Okamoto, A. (2018). Whole-cell circular dichroism difference spectroscopy reveals an in vivo-specific deca-heme conformation in bacterial surface cytochromes. *Chem Commun (Camb)*, *54*(99), 13933-13936. https://doi.org/10.1039/c8cc06309e

Tokunou, Y., & Okamoto, A. (2019). Geometrical Changes in the Hemes of Bacterial Surface c-Type Cytochromes Reveal Flexibility in Their Binding Affinity with Minerals. *Langmuir*, *35*(23), 7529-7537. https://doi.org/10.1021/acs.langmuir.8b02977

Tokunou, Y., Saito, K., Hasegawa, R., Nealson, K. H., Hashimoto, K., Ishikita, H., & Okamoto, A. (2019). Basicity of N5 in semiquinone enhances the rate of respiratory electron outflow in Shewanella oneidensis MR-1. *bioRxiv*, 686493. https://doi.org/10.1101/686493

Watanabe, H. C., Yamashita, Y., & Ishikita, H. (2017). Electron transfer pathways in a multiheme cytochrome MtrF. *Proceedings of the National Academy of Sciences of the United States of America*, *114*(11), 2916-2921. https://doi.org/10.1073/pnas.1617615114

Xu, S., Jangir, Y., & El-Naggar, M. Y. (2016). Disentangling the roles of free and cytochrome-bound flavins in extracellular electron transport from Shewanella oneidensis MR-1. *Electrochimica Acta*, *198*, 49-55. https://doi.org/https://doi.org/10.1016/j.electacta.2016.03.074

Chapter 4 Cell membrane potential controls binding effect between flavin and membrane cytochromes in the *Shewanella oneidensis* MR-1

4.1 Introduction

Extracellular electron transfer (EET) is a typical way for dissimilatory metal-reducing bacteria to obtain energy from environment minerals and sediment by anaerobic respiration, which was assumed to facilitate geochemical element cycle, bioremediation and clean energy generation(Lovley, 2011; Shi et al., 2016; Zhou et al., 2022). A well-studied electrochemically active model bacteria is *Shewanella oneidensis* MR-1 (Ikeda et al., 2021; Myers & Nealson, 1988). Three ways include outer membrane C-type cytochrome, nanowires, and redox mediators were used for *S.oneidensis* MR-1 to transfer electrons toward extracellular (Marsili et al., 2008; Pirbadian et al., 2014; Reguera et al., 2005; Shi et al., 2009). C-type cytochrome is a multi-heme aliments protein, which is responsible for electron transport reactions, especially in the bacteria membrane and mitochondria respiratory chains (Anraku, 1988; Hartshorne et al., 2007). Transmembrane cytochromes MtrCAB complex is employed by *S.oneidensis* MR-1 for transferring electrons across the insulated cell outer membrane. The porin protein MtrB sheaths ten hemes protein MtrA crossing the outer membrane while became MtrC localized to the outer membrane, another became C-type cytochromes OmcA expressed on the outer membrane nearby MtrC for electron transport as well (Edwards et al., 2020; Shi et al., 2006).

Bacterial secreted quinone compound flavin is involved in the bacterial EET process, it exhibits a brilliant effect on electron transport, not only EET but also extracellular electron uptake. Current production could be improved 10 times in the presence of micromolar amounts of flavin. The existence of flavin drives bacterial metabolism and elemental circulation greatly (Marsili et al., 2008; A. Okamoto et al., 2014; Okamoto et al., 2013). Mechanisms of flavin increased current production could be attributed to the interaction between flavin and outer membrane cytochromes (OMCs). Riboflavin (RF) and flavin mononucleotide (FMN) secreted by *S.oneidensis* MR-1 have been proven to enhance EET by binding with OmcA and MtrC respectively (Okamoto et al., 2013; Akihiro Okamoto et al., 2014). The redox potential of bound flavin shifted from -260mv to -145mv compared with free flavin, besides, the redox peak of flavin and outer membrane cytochromes fusion to one peak, which strongly suggested flavin could be as outer membrane cytochromes cofactor to enhance current production. Instead of a two-electron redox reaction model in free flavin, the bound flavin transfer electron by one-electron redox reaction via forming semiquinone (Okamoto et al., 2013).

Molecular docking simulations show flavin can access the heme center of OMCs, it has a 5.8 Å distance between RF and heme 5 of OmcA, besides, FMN bound MtrC with a 7 Å distance with heme 7 (Babanova et al., 2017). Flavin exerts a high enhancement effect by binding with outer membrane cytochromes which were proved by experimental investigation and computational simulation. Factors that influence flavin binding with outer membrane cytochromes are still poorly understood.

A reversible transition state of flavin interacted with outer membrane cytochromes was controlled by a conserved redox-active disulfide, which was influenced by the oxygen as well (Edwards et al., 2015; Akihiro Okamoto et al., 2014). However, there is a transient interaction between the purified outer membrane cytochrome and FMN (Paquete et al., 2014), the reduced state of purified outer membrane cytochromes has a low binding affinity with flavin compared with intact cells which were in the anaerobic condition, which strongly indicated the redox state of OMCs affects binding affinity of OMCs with flavin. Furthermore, the electron flux controls OMC's redox state has been proved in physiological conditions, in addition, flavin binding with OMCs was inhibited in the absence of lactate, which proved the electron flux is important for stabilizing bound flavin due to the redox state of heme (Okamoto et al., 2013).

Recently, a study showed membrane potential changes as the electron flux. During the EET process, electrons and protons are transferred to the periplasm, subsequently, electrons were transported to the extracellular. As the electron flux increases, more protons were accumulated in the periplasm, which results in membrane hyperpolarization. The membrane potential probe thioflavin T (Tht) can be accumulated on the inside of the membrane due to hyperpolarization (Pirbadian et al., 2020; Prindle et al., 2015). The hyperpolarization of the inner membrane was attributed to the proton translocation which resulted from the quinone cycling by the inner-membrane-anchored c-type cytochrome CymA redox loop. Besides, the proton pump NADH dehydrogenases Nuo play a vital role in the hyperpolarization of the membrane when high potential electron acceptors were utilized in the *S.oneidensis* MR-1. The electron from the CymA was transferred to the extracellular electron acceptor, which suggests electron flow is important for membrane potential formation (Kane et al., 2016; Madsen & TerAvest, 2019).

While the membrane potential has been considered for the inner membrane only, some evidence suggests proton localization in the periplasmic space as well during EET. Under the anaerobic condition, substrate-level phosphorylation is dedicated to the production of ATP rather than F-type ATPase in the *S.oneidensis,* which suggested the proton should be localized in the periplasm (Hunt et al., 2010; Tokunou et al., 2015). As the proton was transferred into the periplasm, which not only cause the inner membrane to hyperpolarize but also limits the electron transport to extracellular. Due

to the same amount of electrons and protons produced by the NADH dehydrogenase, the proton transfer rate should be the same as electron transfer, however, the proton diffusion ratio across the outer membrane is five thousand-folds less than the electron flux, so that, excessive protons are accumulated in the periplasm, which results in the limitation of EET by the proton transfer (Okamoto et al., 2017; Okamoto et al., 2016). Those pieces of evidence strongly indicate that inner membrane hyperpolarization and depolarization can affect the EET process.

The electron flux affects the formation of flavoprotein complexes, which may be caused by the redox state of heme in the outer membrane cytochromes. Although the electron flux exists, the binding between OMCs and flavin still was decreased in the presence of low concentrations of CCCP. As CCCP is a membrane potential disruptor, herein, the membrane potential change was assumed as the reason which affects the flavin bind with OMCs. In the present study, we demonstrate the relationship between membrane potential and the binding affinity of flavin with outer membrane cytochromes. The whole intact cell was used to carry out the electrochemical measurement, the evidence shows membrane hyperpolarization could enhance binding affinity between flavin and outer membrane cytochromes, which bridges the gap between microbial electrochemistry and microbial electrophysiology.

4.2 Materials and Methods

4.2.1 Cell preparation

S. oneidensis MR-1 was cultured in Luria-Bertani (LB) medium with shaking overnight under 30℃, and then cells were washed with defined medium (DM; $NaHCO_3$ [2.5 g], $CaCl_2 \cdot 2H_2O$ [0.08 g], NH_4Cl [1.0 g], $MgCl_2 \cdot 6H_2O$ [0.2 g], NaCl [10 g], [HEPES; 7.2 g], 0.5 g yeast extract) for 2 times, 6000 rpm 10min for each time, cell numbers were adjusted to the appropriate concentration for next experiment by measuring OD_{600}.

4.2.2 Electrochemical Measurements

Electrochemical measurement was carried out by a three-electrode system single chamber, Tin-doped In2O3 (ITO) sprayed glass (3.1 cm^2, and thickness 1.1 mm) Ag/AgCl (sat. KCl) and platinum wire was used as working electrode (WE) reference electrode (RF) and counter electrode (CE), respectively. 5 mL DML (DM with 10 mM lactate) was added to the reactor as an electrolyte and then N_2 was purged for 30 mins in a sealed reactor. Keep the temperature at 30 ℃ when the electrochemical measurement was running. The working electrode was poised at a potential of +0.2 V vs. Ag/AgCl.

Differential pulse voltammetry was run using an automatic polarization system (VMP3, Bio Logic Company), the DPV set from the initial potential -0.8 V to a limit potential +0.5 V and the pulses height pulses width and step height were set as 50 mV 300 ms and 5 mV, respectively.

4.2.3 Fluorescence Measurements

Cells were cultured at the transparent anaerobic electrochemical reactor for 24 hours, and the fresh DM-lactate containing 10 μM Tht was transferred to the reactor under anaerobic conditions. Then, the reactor was placed on the fluorescent microscope to observe membrane potential changes under different electrode potentials. (The different potential was controlled by the potentiostat.)

4.2.4 Dissociation constant (Kd) estimation

The Kd value of complex formation between OMCs and each flavin was calculated according to a previous study (Tokunou et al., 2019), in brief, the cells were incubated at +0.2 V overnight with the OD_{600} = 0.1, subsequently, the 2 μM flavin was supplied in the reactor for each hour, after adding the flavin 1 hour, the DPV was measured. According to the equation as follow.

$$\alpha - 1 = K_{\mathrm{d}}\left(\frac{1}{[\mathrm{L}]_1} - \frac{\alpha}{[\mathrm{L}]_2}\right)$$

α is the fold changes of the peak current from the flavin concentration $[L]_1$ to $[L]_2$, here the flavin concentration was chosen from 2 μM to 12 μM.

4.2.5 Rhodopsin expression and western blot

Genes of PR (Song et al., 2019) and XR (Shevchenko et al., 2017) whose codons were optimized for an *E. coli* expression system, were synthesized (Eurofins Genomics Inc.) and subcloned into a pETSXM vector with C-terminal 6 × His-tag (Ng et al., 2018). And then using the electroporation transfer to the plasmid to the *S. oneidensis* MR-1, lactose was used as an inducer.

The expression of PR and XR was detected by Western blot. After induction of rhodopsin, cells were sonicated to load protein to prepare protein samples. Use SDS-PAGE to separate proteins by weight before transferring them to PVDF membranes. Afterward, they were incubated with primary and secondary antibodies, respectively. Finally imaged with ECL Plus Western Blotting substrate and exposure machine.

4.3 Results and Discussion

4.3.1 The effect of CCCP on the binding of flavin with OMCs.

S.oneidensis MR-1 membrane potential can be formed during the EET process, CCCP also can change the membrane potential by decreasing electron flux. For controlling membrane potential, we used the 20 μM CCCP to treat cells (Felle & Bentrup, 1977), as shown in Figure 4-1A and 4-1B, CCCP can decrease membrane potential significantly which showed by Tht fluorescence. To further study the effect of CCCP on flavoprotein formation, wild-type cells were incubated at +200 mV overnight, and then, the fresh medium which contains different concentrations of CCCP was supplied. As shown in Figure 4-1C, the current production significantly increased after adding 8 μM RF in the absence of CCCP. The effect of RF in enhancing current production was, however, impaired by CCCP. The current production without CCCP is 7 times higher than the current production with CCCP, which suggested CCCP has a strong effect on repressing the current increment induced by flavin.

For clarifying details of CCCP on flavin binding with OMCs, we applied the whole-cell differential pulse voltammetry measurements in monolayer biofilms of *S. oneidensis* MR-1 which is attached on the electrode surface. The result shown in Figure 4-1D-F, showed two redox peaks at -360 mv (free flavin) and -50 mv (unbound OMCs), although it lacks CCCP and only contains solvent DMSO. On the other hand, the DP voltammograms of the CCCP group showed significant two peaks at -360 mv and -50 mv as well.

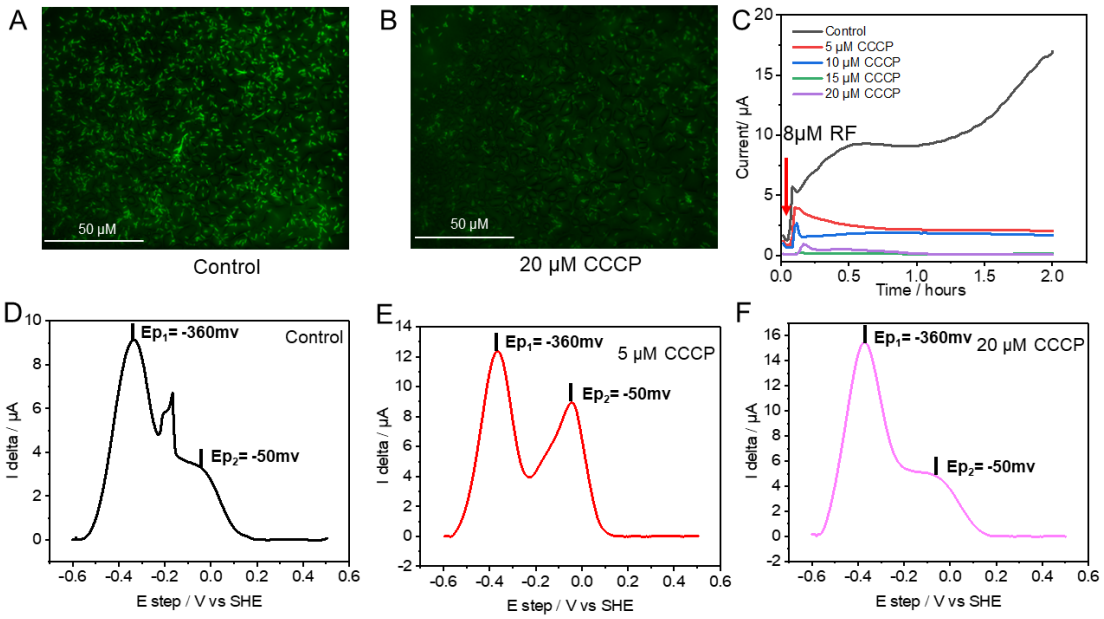

Figure 4-1 CCCP impeded the flavoprotein complex formation in the wild type of *S.oneidensis*

MR-1

Membrane potential was shown by Tht fluorescence without CCCP (A) and with 20 μM CCCP (B) in the *S.oneidensis* MR-1 wild type. (C) Current production of *S.oneidensis* MR-1 wild type in the presence of different concentrations CCCP (0 5 10 15 20 μM) under +0.2 V potential. The DP voltammograms of wild type *S.oneidensis* MR-1 wild type without CCCP (D) and 5 μM CCCP (E) 20 μM CCCP (F).

Herein, the mutant strain *Δdms*-all was used to explore the effect of flavin binding with OMCs. Cells were incubated with +200 mV overnight to form a biofilm, and then, the medium containing 5 μM CCCP was used as an electrolyte after removing planktonic cells. Current production could be enhanced greatly by adding flavin that functions as a cofactor of OMCs, which results in the two-electron redox reaction turning into one electron redox reaction. However, the effect of flavin not only RF but FMN in the current increment was inhibited by CCCP, the result shown in Figure 4-2A and 4-2D, which indicated CCCP inhibited the current increment induced by flavin. Although the current production was inhibited by CCCP in the presence of 8 μM RF, still current production arrived at 15 μA in the 5 μM CCCP with 8 μM RF, suggesting the electron flux across MtrCAB is still existence.

To confirm the membrane potential changes that could affect flavin binding with OMCs, we applied the whole-cell differential pulse voltammetry measurements in monolayer biofilms of mutant strain *Δdms*-all. The DPV measurements were carried out in the presence of 8 μM RF and FMN. The DPV of mutant *Δdms*-all. showed one peak position at -130 mV (Figure 4-2B) and-200 mV (Figure 4-2E) in the presence of RF and FMN, however, two redox peaks appeared in the presence of 5 μM CCCP at -210 mV and -50 mV, which was assigned as free RF and OMCs peak respectively (Figure 4-2C) besides, the DPV shows two peaks at -230 mV and -50 mV (Figure 4-2F) in the presence of FMN. Those results demonstrated flavin binding with OMCs was inhibited by CCCP, and it further indicated the flavin binding affinity could be disrupted by the membrane potential change although the electron flux existed.

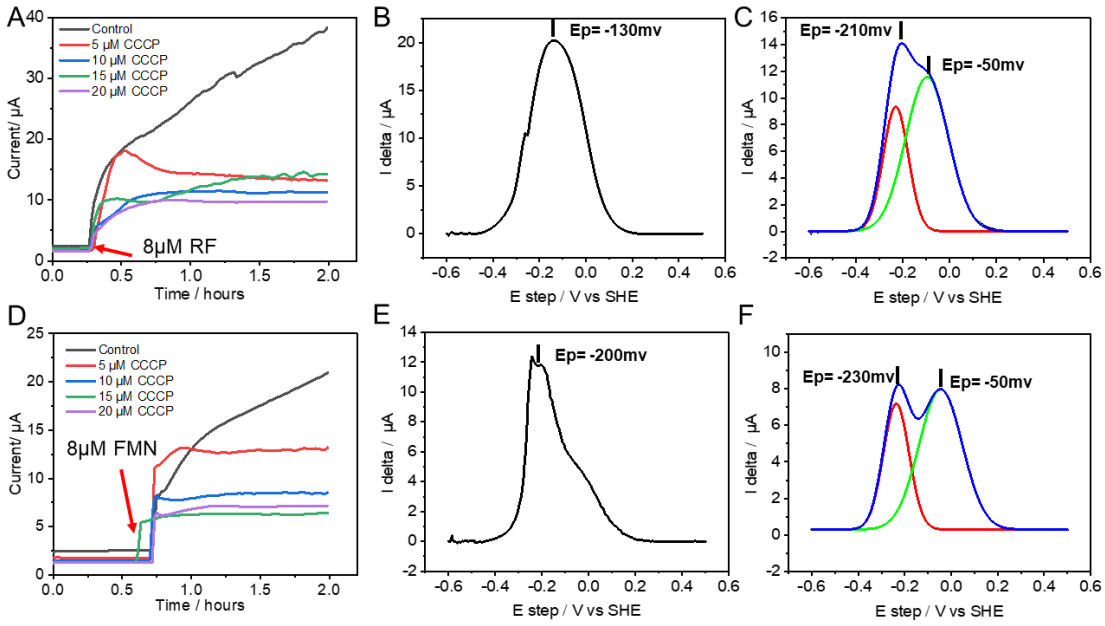

Figure 4-2 CCCP inhibited RF and FMN binding with OMCs in the mutant strain *Δdms-all*

The mutant strain of *Δdms-all.* The cell was incubated at +0.2 V potential overnight, then, planktic cells were removed by changing the fresh medium with different concentrations of CCCP carefully. For current production measurements of cells (A), the arrow shows 8 μM RF was added into the reactor. The DP voltammograms for the monolayer were measured in the presence of 8 μM RF without CCCP (B) and with 5 μM CCCP (C). The current production for cells after adding 8 μM FMN (D). The DP voltammograms for monolayer were measured in the presence of 8 μM FMN without CCCP (E) and with 5 μM CCCP (F)

4.3.2 The effect of different electrode potentials on the membrane potential and cell metabolism.

As the CCCP is a chemical solved in the DMSO, which may bring unknown chemical side effects, for excluding chemical effects and elucidating details of membrane potential on flavoprotein formation, membrane potential was controlled by applying different electrode potential. A transparent three-electrode electrochemical system was applied as shown in Figure 4-3A to image cell membrane potential by applying different electrode potentials. The indium tin oxide (ITO) was used as the working electrode. Cells were resuspended by DML with 10 μM Tht and then placed into the electrochemical reactor with anaerobic condition and +200 mV (vs. Ag/AgCl KCl saturated) potential to the working electrode for 2 hours for allowing cells attached on the electrode surface. During the period of imaging live cells attached to the electrode, three-electrode potentials (+500 mV 0mV, and

-500 mV vs. Ag/AgCl KCl saturated) were chosen to monitor membrane potential by Tht fluorescence. The result shown in the Figure 4-3B-D, the fluorescence of cells attached to the electrode surface was increased gradually with the electrode potential increased from -500 mV to +500 mV, which suggested cell membrane potential could be controlled by the electrode potential when the electrode was solely electron acceptor.

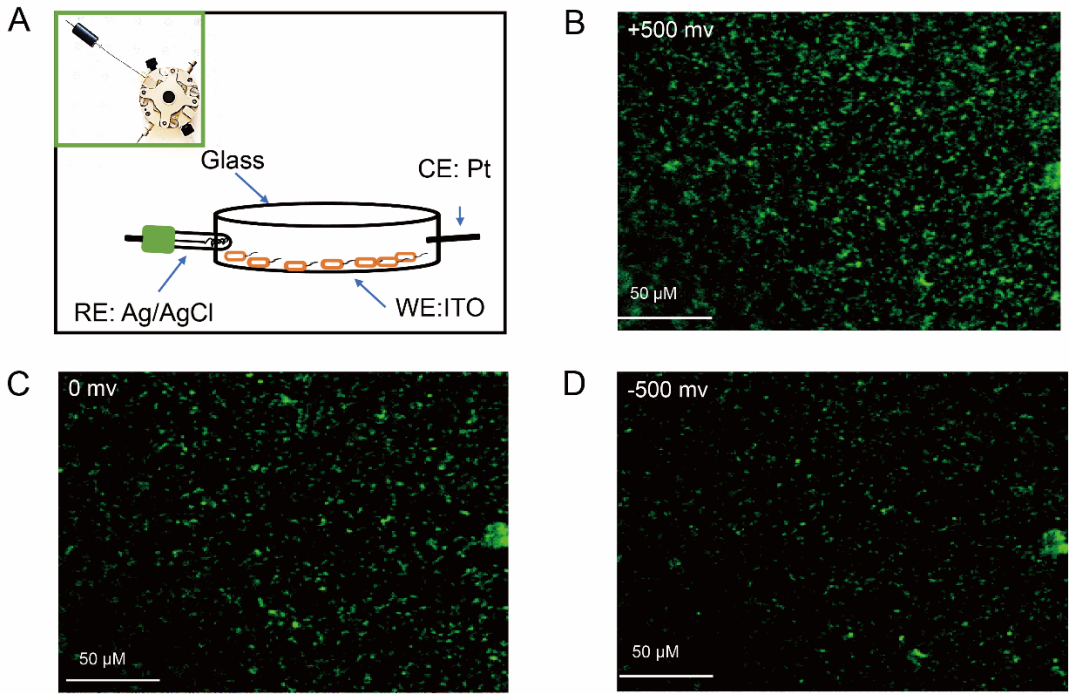

Figure 4-3 Membrane potential can be changed by CCCP and different electrode potential

(A)The anaerobic electrochemical reactor with a three-electrode system, working electrode (WE) reference electrode (RE), and count electrode (CE) are ITO Ag/AgCl and platinum wire, respectively, transparent glass was used as the cover of the reactor. The real reactor was shown at the green square. The membrane potential was shown under +500mv (B) 0mv (C) and -500mv (D) (vs.Ag/AgCl KCl saturated) by Tht fluorescence.

Since the different electrodes showed good performance for changing membrane potential, the different electrode potential here was used to control membrane potential. To exclude the effect of different electrode potentials on cell metabolisms, cells were incubated at the +0.2V for overnight, and the fresh medium was changed to remove the planktic cells, after that, the electrode was changed allows +200 mV→different potentials→+200 mV, as shown in the Figure 4-4A, the current production was increased immediately after adding 8 μM RF except the -500 mV, however, when the

electrode potential turned to +200 mV, the current production of different potential recovered to the same level, as shown in the Figure 4-4B.

To further investigate the effect of different electrode potentials on the cell internal metabolism, the lacking of all the outer membrane cytochromes strain (Δ*omc*-all) was used. The current production of Δ*omc*-all directly reflects the cell's metabolism due to the electron can be transferred from the inner membrane rather than the outer membrane shown in Figure 4-5. The Δ*omc*-all was cultured at the +200 mV for overnight, subsequently, the electrode potential was changed (-300 mV, 0 mV, +300 mV) before 100 μM RF was added, the result shown in the Figure 4-4C, the current production was increased after adding RF, but the current under -300 mV shows comparable with 0 mV and +300 mV. Those results showed the effect of the current decrease was attributed to the different electrode potential changes rather than cell upstream metabolism.

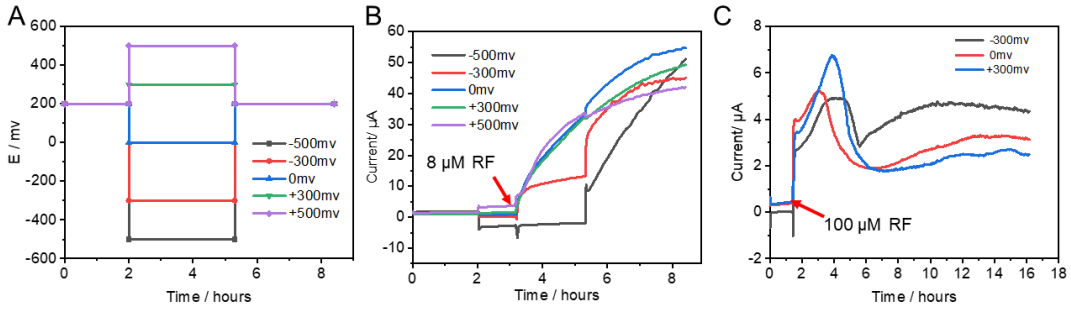

Figure 4-4 Effects of different electrode potentials on cell metabolism.

(A) The different electrode potentials poised at *S.oneidensis* MR-1 monolayer on the ITO electrode, 5 electrode potentials (-0.5 V, -0.3 V, 0 V, +0.3 V, +0.5 V (vs. Ag/AgCl KCl saturated) were used for 5.5 hours, the current production shows at (B), the arrow shows the point that adds 8μM RF. Next, the voltage is uniformly adjusted to +0.2 V. (C) The schematic illustration of EET for the mutant strain Δ*omc*-all strain EET in the presence of flavin. (D) The current production of Δ*omc*-all under different electrode potentials (-0.3 V, 0V, +0.3 V (vs.Ag/AgCl KCl saturated)) in the presence of 100 μM RF.

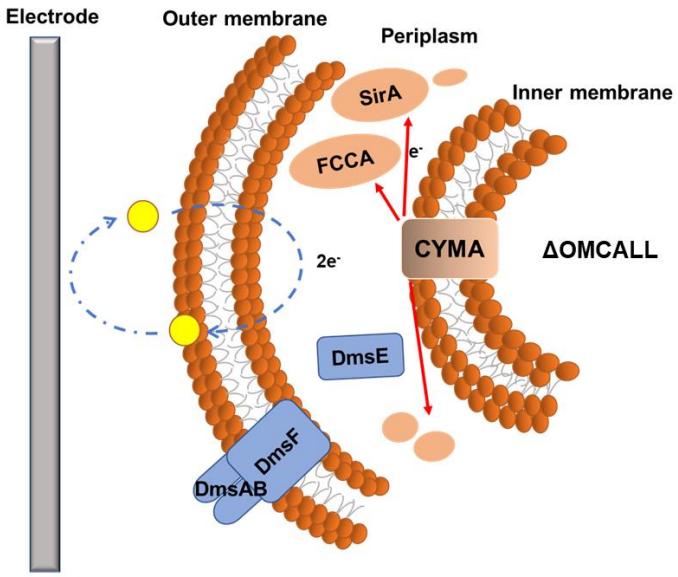

Figure 4-5 The schematic of extracellular electron transfer in the Δ*omc*-all strain with flavin

The mutant strain of Δ*omc*-all transfer electron to the extracellular for the shuttling process by a two-electron redox reaction of free-form flavin independent on outer membrane cytochromes.

4.3.3 The effect of the different electrodes on the current production increasement by flavin

Different electrode potentials have been shown to well alter the cell membrane potential without changing the upstream metabolism of the cell. The affinity of flavin with OMCs was evaluated under different electrode potentials. *S.oneidensis* MR-1 wild type was incubated at +200 mV (vs. Ag/AgCl KCl saturated) for overnight, before changing the electrode potential, planktonic cells were removed by fresh DM with 10 mM lactate. Subsequently, various potentials (-500 mV, -300 mV, 0 mV, +300 mV +500 mV) were applied on the electrode surface.

To explore the flavin effect under different membrane potentials, 2 μM RF and FMN were added into the reactor under different electrode potentials from -500 mV to +500 mV each hour, the result is shown in the Figure 4-6A and 4-6B, compared with the positive potential group (+500 mV, +300 mV, and 0 mV), the current increasement of bacteria which poised at -300 mV potential is in the low level, which suggested flavin does not fully exert the ability to increase current. The current did not increase under the -500 mV potential in the presence of flavin, which may be due to the lack of flavin binding to OMCs. Here, results showed the current increasement which caused by flavin could be inhibited by membrane potential decrease.

To evaluate the binding affinity between flavin and OMCs, the dissociation constant (Kd) was

calculated according to the previous description. Cells were cultured at +200 mV (vs. Ag/AgCl KCl saturated) for overnight, and then, 2 μM flavin was supplied for each hour, the DPV was measured 1 hour later after adding flavin. Result shown in Figure 4-6C and 4-6D, the negative electrode potential (-300 mV) showed a high Kd value, which indicted the binding affinity of flavin with OMCs was low, in the contrast, the positive potential (0 mV +300 mV and +500 mV) showed low Kd value, which suggested flavin binding with OMCs is easy under positive electrode potential.

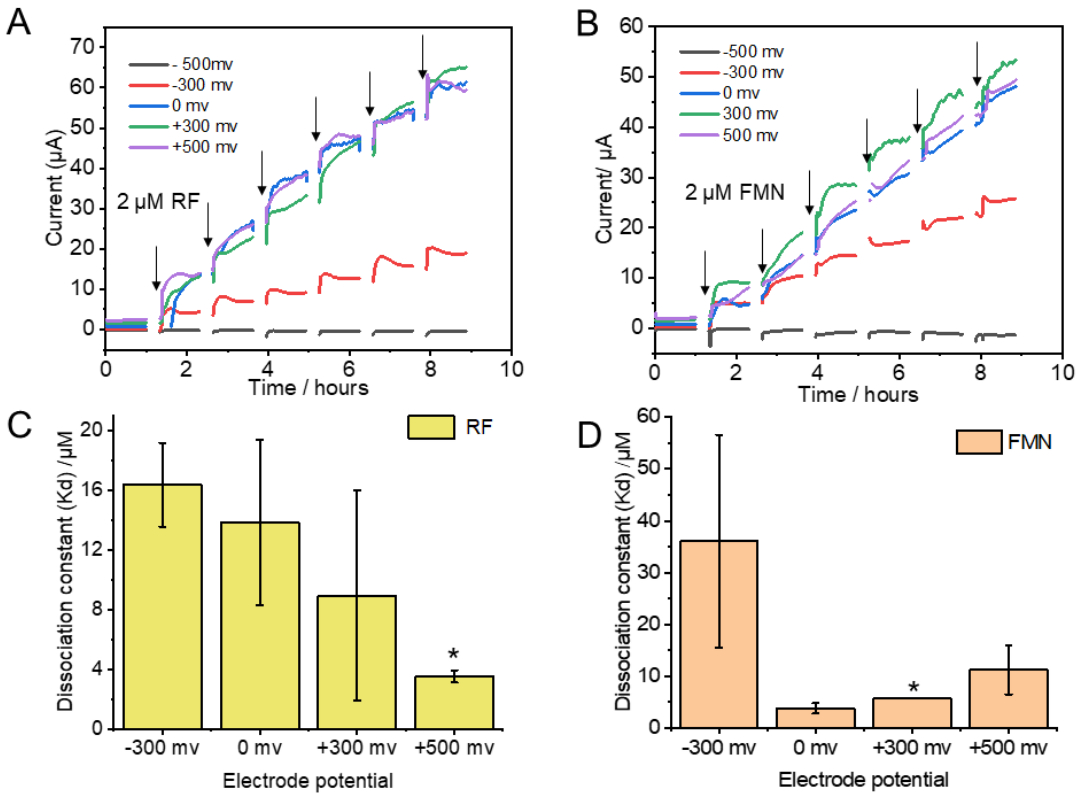

Figure 4-6 Flavin binding affinity with OMCs was inhibited by negative electrode potential

The *S.oneidensis* MR-1 was incubated at +0.2 V (vs. Ag/AgCl KCl saturated) for overnight for better-forming biofilm, and then the different electrode potentials were applied to the cells. current production for the cell which was supplied with 2 μM RF (A) and 2 μM FMN (B) each hour, differential pulse voltammetry was used for each hour after adding flavin. The dissociation constant (Kd) value about complex formation between RF (C) or FMN (D) and OMCs under various electrode potentials (+0.5 V +0.3V 0V -0.3 V (vs. Ag/AgCl KCl saturated)).

Herein, the cell membrane potential is decreased by CCCP and negative electrode potential, which leads to a decrease in binding affinity between flavin and OMCs. Since the free flavin shows more

negative redox potential, here, redox potential under -300 mV and +300 mV were measured using DP voltammetry and linear sweep voltammetry (LSV). As shown in Figure 4-7A, the electrode potential was at +200 mV for 1 hour, then +300 mV or -300 mV without RF for 1 hour, after that, RF was added in to reactor for 1 hour. The result shown in Figure 4-7B, the current production under +300 mV is 4 times more than the current production of -300 mV in the presence of RF. Compared with -300 mV, the redox potential of +300 mV is more positive, and the redox potential from -176 mV shifts to -156 mV as shown in the Figure 4-7C which is measured by DPV, correspondingly, the LSV data shows the redox potential under +300 mV is more positive than -300 mV as well (Figure 4-7D). These results suggested that the higher the membrane potential, the more flavin binds to OMCs.

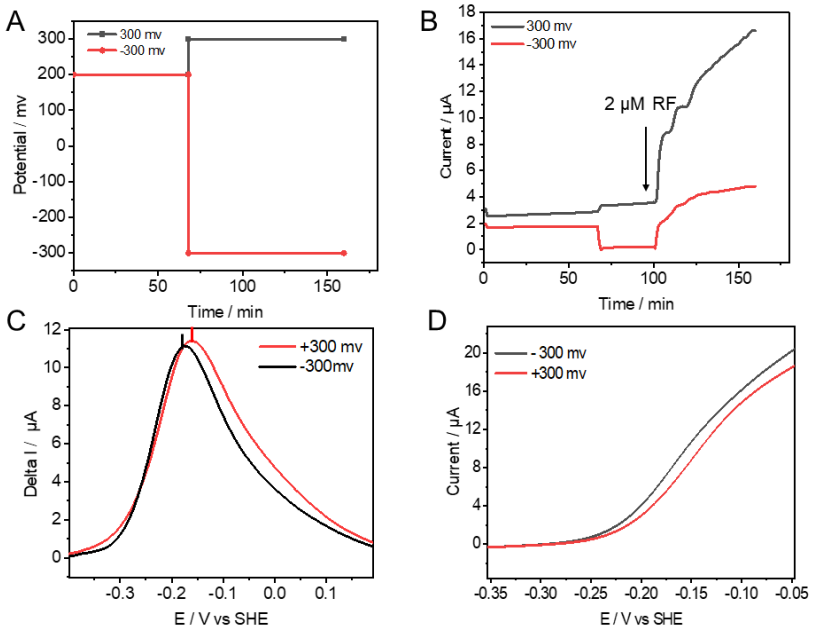

Figure 4-7 Redox potential is more positive under positive electrode potential.

(A)The electrode potential setting for *S.oneidensis* MR-1, +0.2 V (vs. Ag/AgCl KCl saturated) electrode potential was applied on the *S.oneidensis MR-1* monolayer for 1 hour, then, the electrode potential was changed to +0.3 V/-0.3 V for 2 hours. (B) Current production of *S.oneidensis* MR-1 under +0.3 V and -0.3 V, the arrow shows 2 μM RF was added into the reactor. DP voltammograms (C) and linear sweep voltammograms (D) of *S.oneidensis* MR-1 after supplying RF under +0.3 V and -0.3 V.

To elucidate the effect of different electrode potential on the flavin binding with OMCs, 2 μM flavin were supplied for each hour, subsequently, whole cell DPV was used to check the flavin binding with OMCs. As shown in the Figure 4-8A and 4-8C, under +500 mV electrode potential, there is one peak that appeared at -150 mV in the presence of RF, meanwhile, only one peak appeared at -210 mV

with FMN, this single peak is considered to be the binding peak of flavin with OMCs, the binding peak was increased by the flavin concentration from 2 µM to 12 µM. However, under -0.5 V electrode potential, there are two peaks shown in Figure 4-8B, -210 mV and -50 mV which should be free RF and OMCs. Although the RF concentration increased, the peak at -0.2 V still existed. While, the -240 mV and -20 mV which assigned as free FMN and free OMCs respectively, as shown in the Figure 4-8D, the free OMCs peak current at -20 mV keep at the same level even though the FMN concentration increased 6 times, in the contrast, the free FMN peak (-240 mV) was increased by the supplement of FMN. That evidence strongly proved the different electrode potentials inhibited the formation of a complex between flavin and OMCs.

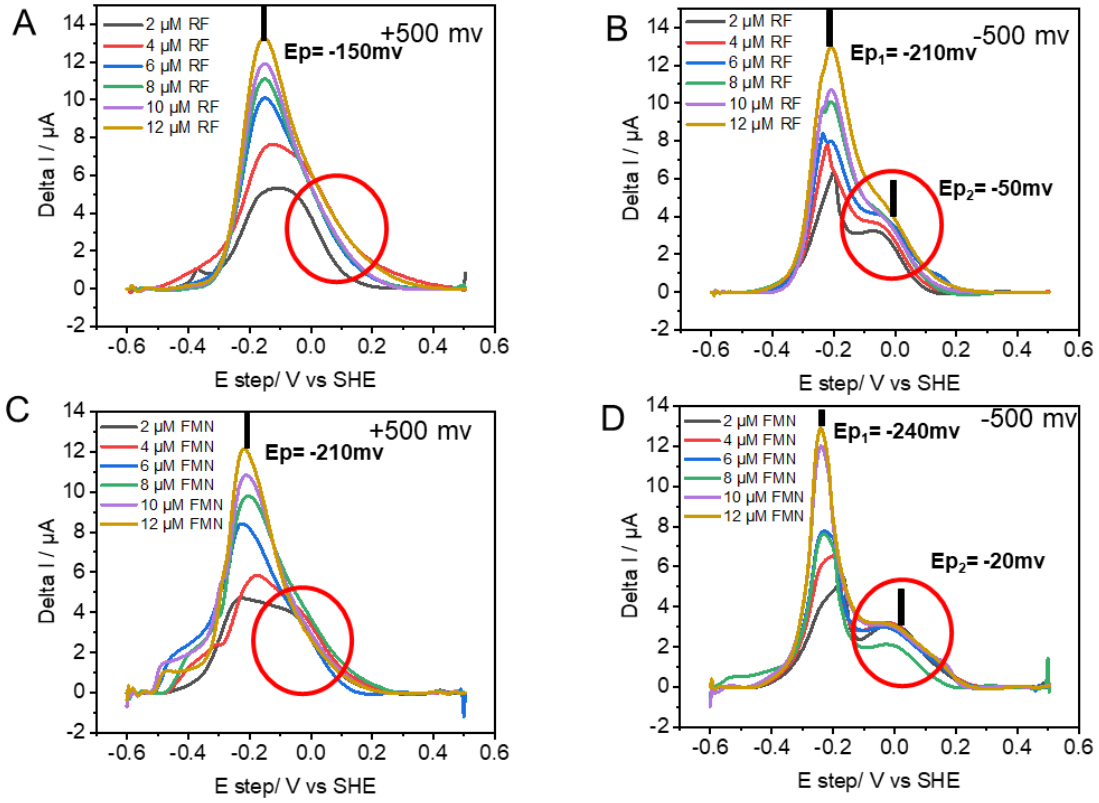

Figure 4-8 Flavin cannot bind with OMCs under +500mv and -500mv

The DP voltammograms of the monolayer were measured after different concentrations of RF (2-12 µM) were added into the reactor under +0.5 V (A) and -0.5 V (B) (vs.Ag/AgCl KCl saturated) electrode potential. DP voltammograms in the presence of different concentrations FMN under the +0.5 V (C) and -0.5 V (D).

4.3.4 Expression and Characterization of Rhodopsin

As the proton limits the EET ability in the *S. oneidensis* MR-1 has been proved, and also, the proton gradient is an important factor for the membrane potential. To explore the direct effect of membrane potential on the EET, here, two proton antiporters were expressed to enhance the membrane potential. Proteorhodopsin (PR) is a light-activated protein, which can transfer the proton from the inside of the cell to the outside, meanwhile, xanthorhodopsin (XR) is an inward proton transporter. As the plasmid that using the lactose indue has a good effect, herein, the different concentrations of lactose were used to induce the rhodopsin expression in the aerobic condition, the results shown in Figure 4-9A, after 12 hours, compared with that without lactose, the 0.1% to 0.5% lactose shows the deeper pink, which suggests that the PR had expressed (PR itself is pink). However, the XR did not show any color change. As the XR is an inward proton transporter, it has the same proton transfer direction as the F-type ATPase, so the expression of XR will impair the F-ATPase function, which leads to the difficulty of the XR expression. According to a previous study of our laboratory, F-ATPase will not work during the EET process, so herein, the anaerobic condition was used to express XR, the result shown in Figure 4-9 B, the XR with plasmid and lactose showed deep color than the control group, which means the XR can be induced under the anaerobic condition. As we put a 6X His-tag in front of rhodopsin, herein, we checked 6X His-tag to confirm the rhodopsin expression by the western blot. Results shown in Figure 4-9 C and 4-9D, the PR and XR can express under aerobic and anaerobic conditions, respectively.

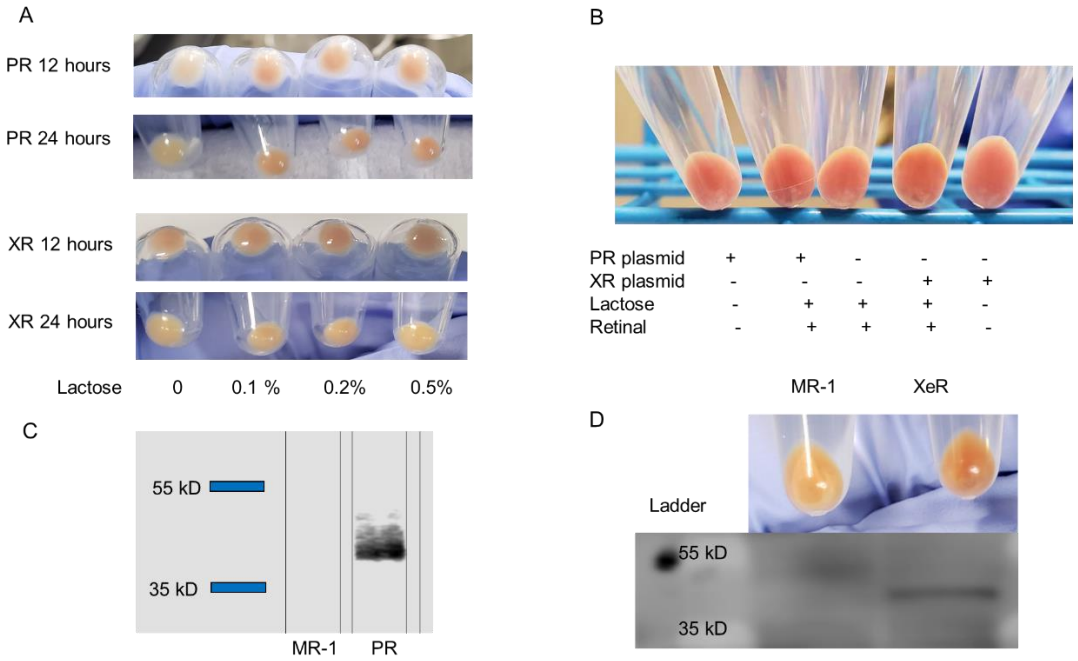

Figure 4-9 The expression of rhodopsin. (A) Different concentrations of lactose for inducing the rhodopsin expression under aerobic conditions. (B) Anaerobic condition for inducing the rhodopsin expression under 0.2% lactose. Western blot for PR (C) and XR (D).

4.3.5 The effect of Rhodopsin on electricity generation

As we expressed the rhodopsin on the cell membrane, we constructed an electrochemical combined with light systems. As shown in Figure 4-10, cells were incubated at +200 mV in the traditional electrochemical reactor, since the working electrode is transparent, so that the light can arrive at the cell surface to activate the rhodopsin.

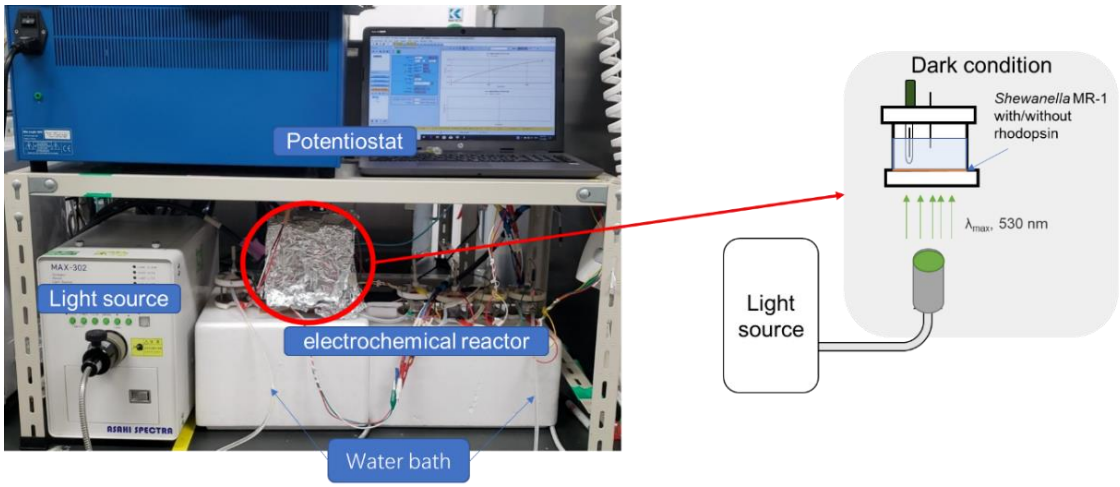

Figure 4-10 The schematic of electrochemical combined with light system

After the system was successfully built, the effect of rhodopsin on the current output was studied. As shown in Figure 4-11A, the PR appears to be very effective for the current enhancement. The current production of strains expressing PR increased immediately after light supplementation, suggesting that increased proton transfer could enhance extracellular electron transfer. However, strains expressing XR showed very little effect (Figure 4-11B), possibly due to difficulties in expression, as there was less amount of XR on the membrane, so less current was produced. Those results demonstrated that rhodopsin can enhance the current production immediately, this cannot be attributed to an increase in metabolic activity, since the current increase immediately after the addition of light stimulation.

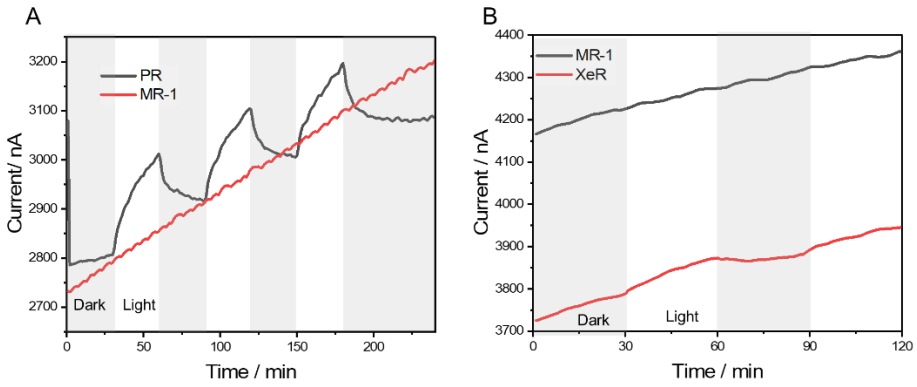

Figure 4-11 Light-dependent current increases in electrochemical chambers containing *S. oneidensis* expressing PR and XR.

(A) Current production increased after giving light on the strain with PR. (B) Current production increases after giving the light in the strain with XR

To further explore the effect of rhodopsin on outer membrane proton transfer, deuterium water was used to detect proton transfer in the outer membrane. The results are shown in Figures 4-12C and D. Compared with the PR strain without light, the time for the current production of the PR strain to increase to the original level during the light period was shorter after adding 4% D_2O. These results suggest that membrane potential can enhance outer membrane proton transfer, resulting in increased current production due to proton transfer limiting EET in *S. oneidensis* MR-1.

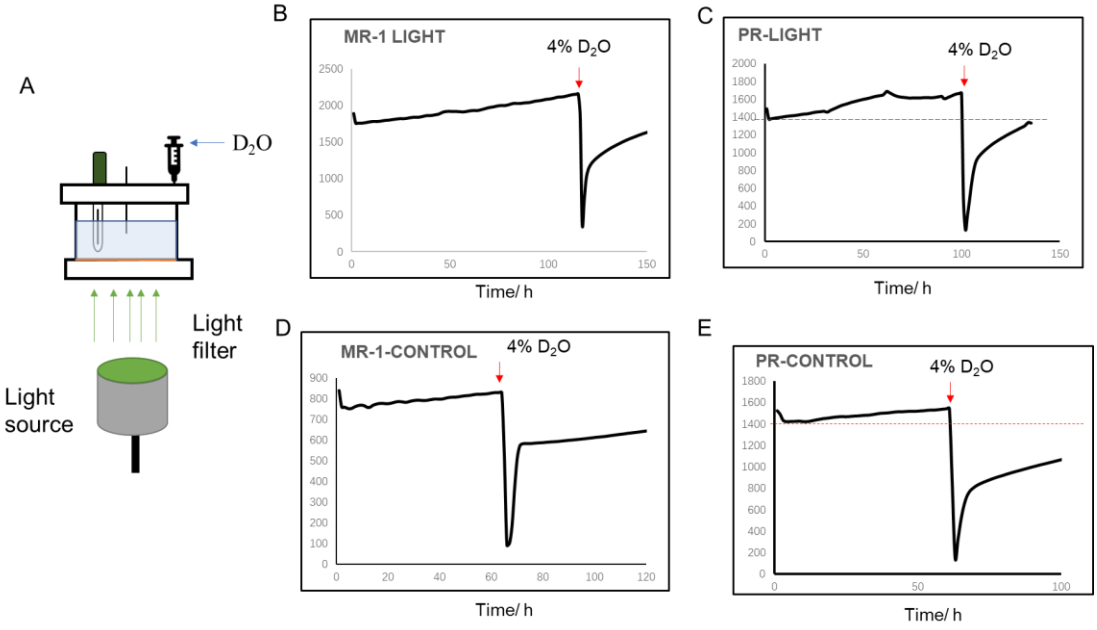

Figure 4-12 Kinetic isotope effect of PR expressed MR-1. (A) The scheme of D_2O injection. Time

versus current production (I_c) for a monolayer biofilm of *S. oneidensis* MR-1 in an electrochemical system with the addition of D_2O. (A) MR-1 with light and (B) MR-1expressed PR with light. (C) and (D) MR-1 and MR-1expressed PR without light, respectively.

We also checked the effect of rhodopsin on RF enhancing current production. The result shown in the Figure 4-13A, the PR with light showed a higher enhancement factor (7.6) than the MR-1(5), which suggests rhodopsin can promote the semiquinone formation for increasing current production because PR can hyperpolarize cells by transporting protons. It is consistent with the above study. Additionally, activated rhodopsin can increase the redox ability of OMCs (Figure 4-13 B), which is also another reason for increasing the current production.

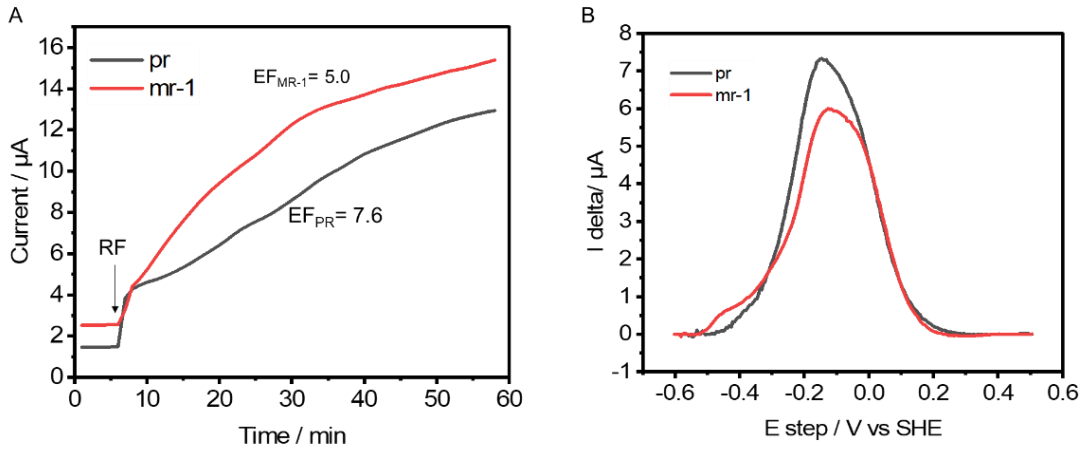

Figure 4-13 Rhodopsin enhance the flavin effect and outer membrane cytochrome redox ability. (A) current production increased by the riboflavin in the strain MR-1 and MR-1 with PR. (B) The DP voltammograms of a monolayer of MR-1 and MR-1 with PR in the presence of light.

4.3.6 Discussion

Extracellular electron transfer efficiency can be improved largely by flavin supplementation. Flavin could transfer the electron from outer membrane cytochromes to the insoluble substrate such as an electrode by two-electron redox reaction (FMN/RF $+2e^{-}+2H^{+}\rightarrow FMNH_2/RFH_2$), however, the purified protein in vitro binding experiments show FMN and RF could be a cofactor of MtrC and OmcA, additionally, whole cells electrochemical measurement showed the FMN and RF could bind MtrC and OMCA, respectively. This bound pattern increases the extracellular electron transfer by one electron transfer way via forming semiquinone (FMN/RF $+e^{-}+H^{+}\rightarrow$FMNH/RFH), which is more thermodynamically feasible (Okamoto et al., 2013).

Since the vital role of bound flavin plays in extracellular electron transfer, factors that affect flavin binding with OMCs should be explored more. Although previous evidence demonstrated that flavin can bind with OMCs in the intact cell, the purified protein shows it is a transient state of flavin with OMCs, besides, research points out that the binding of flavin with OMCs was controlled by a disulfide bond, this disulfide bound can be reformed by aerobic condition, which indicated the binding state dominated by heme center redox state (Edwards et al., 2015; Okamoto et al., 2013). However, even absence of oxygen, the flavin cannot bind with OMCs under negative electrode potential, which was attributed to the heme redox state that is controlled by the electron flux. One of the important functions of electron flux is to maintain membrane potential. Here, the flavin-bound OMC was inhibited even though electron flux persisted, which was attributed to the change in membrane potential. The role of membrane potential in extracellular electron transfer is rarely studied.

In the present study, the membrane potential is shown to play an important role in the binding of flavin to OMCs. To examine our hypothesis, the monolayer of *S.oneidensis* MR-1 was used to measure electrochemical properties. A chemical for disrupting membrane potential CCCP and different electrode potential was used to change the membrane potential in this study. The membrane potential was shown by the Tht fluorescence as described in the previous study (Pirbadian et al., 2020). After the cells were treated with CCCP and negative potential, the cell membrane was depolarized which showed by the Tht fluorescence, in the contrast, under the positive electrode, the cell membrane was hyperpolarized. For exploring the state of flavin binding with OMCs under different membrane potentials, 8μM flavin was added into the electrochemical reactor, in the presence of CCCP and negative electrode condition, the effect of flavin on the current increment was inhibited, to further study reason, the whole cell DPV and LSV were carried out when the flavin binds with OMCs, the peak of flavin and OMCs will be fusion to one peak, but, under membrane depolarization condition,

it still shows two peaks, which suggested the free flavin and unbound OMCs existed in the electrolyte, it further indicated parts of the flavin are free to form rather than bound state, and the binding affinity was evaluated by Kd value according to a previous study (Tokunou et al., 2019), it shows flavin binding with OMCs is easier when the membrane was hyperpolarized. However, the depolarization of the membrane caused a difficult situation for flavin binding with OMCs.

Although the extracellular electron transfer in *S.oneidensis* MR-1 has been studied a lot, the relationship between membrane potential and extracellular electron transfer is still poorly understood. Recently, membrane potential could be an indicator for extracellular electron transfer reported, it shows membrane potential can respond to extracellular electron transfer, however, the mutant Δ*bfe* membrane potential shows no significant difference with the wild type even though the current production of Δ*bfe* was low than wild type (Kotloski & Gralnick, 2013; Pirbadian et al., 2020), additionally, in the presence of 5 μM RF, the fluorescence shows same level with absence of RF, but, when the high electrode potential was poised, the fluorescence will be largely increased. In the contrast, when the membrane potential changes, the current production also changed, which provided a new sight for membrane potential with extracellular electron transfer, in this study, membrane potential controls the binding of flavin with OMCs explaining.

How the membrane potential controls flavin binding with OMCs, still needs more research. Although the current knowledge believes bacteria's outer membrane has no membrane potential and the bacterial outer membrane is permeable, which cannot form the ion gradient and electrochemical gradient, electrochemical active bacteria may be different, the proton transfer across to the outer membrane has been proved as a limitation for extracellular electron transfer. This study indicated the proton cannot cross the outer membrane freely, it is proved that a cation gradient between the extracellular and periplasmic exists.

In the present study, when the membrane potential was decreased, the proton gradient will be destroyed, which led to the proton do not accumulate in the periplasm, meanwhile, the proton transfer to outside across the outer membrane will be decreased, as we know the flavin could transfer one proton and one electron when it binding with OMCs, here, there is no need for so much flavin to transport proton, and the flavin binding with OMCs will be inhibited. However, the membrane potential is enhanced, while, the rate of proton transfer at the outer membrane increases, which results in more flavin needing to bind OMCs to transfer the protons.

Although flavin is a cofactor for cytochromes, its binding to cytochromes still requires cytochromes with the proper conformation. Changes in the conformation of OMCs may affect the dissociation between flavin and OMCs. Our findings demonstrated the flavin binding with OMCs

could be controlled by membrane potential, which showed in Figure 4-14, the cell membrane hyperpolarization by positive electrode potential, the more flavin binding with OMCs, on the other hand, cell membrane depolarization by CCCP and negative electrode potential, the less flavin binding with OMCs.

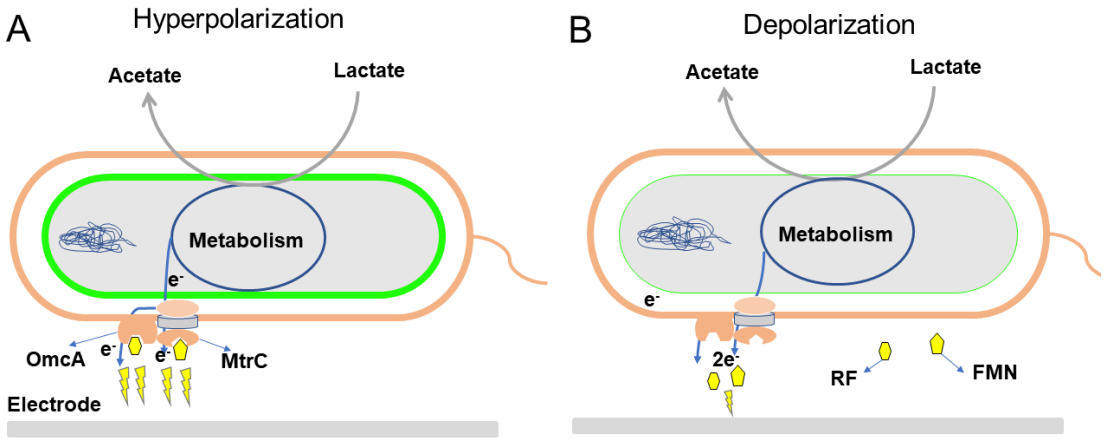

Figure 4-14 The schematic of flavin binding under different potential

Hypothetical model of flavin binding with OMCs under different potentials. The membrane could be hyperpolarized by positive electrode potential which results in the strong binding between the flavin and OMCs (A), however, the membrane potential could be depolarized by negative electrode potential, meanwhile, flavin binding with OMCs was inhibited (B).

To further prove the effect of membrane potential effect on the *S.oneidensis* MR-1 EET ability, the rhodopsin was expressed on the cell membrane to specific polarized cells, besides the activated rhodopsin, the isotope effect of PR expressed MR-1 was measured. Those results showed that activated rhodopsin can increase the current production by the polarized cell due to its proton transfer ability. Activated rhodopsin can enhance the flavin function on increasing EET, proving the membrane potential can affect the semiquinone formation. Those results are consistent with a different potential date and CCCP data. Here, this study shows that the membrane potential can control the EET in two ways, the first way is affecting semiquinone formation, and also it can directly affect EET by the proton transfer. However, the underlying mechanism still needs study.

Membrane potential was considered the important electrical signal to regulate bacterial behavior, which could be sorted into microbial electrophysiology (Stratford et al., 2019). From the microbial electrophysiology sight, the relationship between microbial electrophysiology and microbial extracellular electron transfer was established in this study. Bacteria always choose the most energy-

saving way to effectively obtain energy from the outside, for keeping the best efficiency of anaerobic respiration, the extracellular respiration bacteria not only secrete flavin for enhancing extracellular electron transfer but also control the flavin binding with OMCs by an electric signal which provided by membrane potential. This study gives new sight into bacteria electrophysiology to control its behavior.

5. Conclusion

In summary, this study suggested membrane potential play a vital role in the formation of flavin-outer membrane cytochromes complex, the binding affinity can be decreased by disturbing membrane potential. This study connects microbial electrophysiology and microbial extracellular electron transfer, which provide new insight into microbial electrophysiology and control cell behavior. Nonetheless, our study still needs more evidence to prove the details.

Reference

Anraku, Y. (1988). Bacterial electron transport chains. *Annual review of biochemistry*, *57*(1), 101-132.

Babanova, S., Matanovic, I., Cornejo, J., Bretschger, O., Nealson, K., & Atanassov, P. (2017). Outer membrane cytochromes/flavin interactions in Shewanella spp.-A molecular perspective. *Biointerphases*, *12*(2), 021004. https://doi.org/10.1116/1.4984007

Edwards, M. J., White, G. F., Butt, J. N., Richardson, D. J., & Clarke, T. A. (2020). The crystal structure of a biological insulated transmembrane molecular wire. *Cell*, *181*(3), 665-673. e610.

Edwards, M. J., White, G. F., Norman, M., Tome-Fernandez, A., Ainsworth, E., Shi, L., Fredrickson, J. K., Zachara, J. M., Butt, J. N., & Richardson, D. J. (2015). Redox-linked flavin sites in extracellular decaheme proteins involved in microbe-mineral electron transfer. *Scientific reports*, *5*(1), 1-11. https://doi.org/10.1038/srep11677

Felle, H., & Bentrup, F. W. (1977). A study of the primary effect of the uncoupler carbonyl cyanide m-chlorophenylhydrazone on membrane potential and conductance in Riccia fluitans. *Biochimica et biophysica acta*, *464*(1), 179-187.

Hartshorne, R. S., Jepson, B. N., Clarke, T. A., Field, S. J., Fredrickson, J., Zachara, J., Shi, L., Butt, J. N., & Richardson, D. J. (2007). Characterization of Shewanella oneidensis MtrC: a cell-surface decaheme cytochrome involved in respiratory electron transport to extracellular electron acceptors. *JBIC Journal of Biological Inorganic Chemistry*, *12*(7), 1083-1094.

Hunt, K. A., Flynn, J. M., Naranjo, B., Shikhare, I. D., & Gralnick, J. A. (2010). Substrate-level phosphorylation is the primary source of energy conservation during anaerobic respiration of Shewanella oneidensis strain MR-1. *J Bacteriol*, *192*(13), 3345-3351. https://doi.org/10.1128/jb.00090-10

Ikeda, S., Takamatsu, Y., Tsuchiya, M., Suga, K., Tanaka, Y., Kouzuma, A., & Watanabe, K. (2021). Shewanella oneidensis MR-1 as a bacterial platform for electro-biotechnology. *Essays in Biochemistry*, *65*(2), 355-364.

Kane, A. L., Brutinel, E. D., Joo, H., Maysonet, R., VanDrisse, C. M., Kotloski, N. J., & Gralnick, J. A. (2016). Formate Metabolism in Shewanella oneidensis Generates Proton Motive Force and Prevents Growth without an Electron Acceptor. *J Bacteriol*, *198*(8), 1337-1346. https://doi.org/10.1128/jb.00927-15

Kotloski, N. J., & Gralnick, J. A. (2013). Flavin electron shuttles dominate extracellular electron transfer by Shewanella oneidensis. *mBio*, *4*(1). https://doi.org/10.1128/mBio.00553-12

Lovley, D. R. (2011). Live wires: direct extracellular electron exchange for bioenergy and the

bioremediation of energy-related contamination. *Energy & Environmental Science*, *4*(12), 4896-4906.

Madsen, C. S., & TerAvest, M. A. (2019). NADH dehydrogenases Nuo and Nqr1 contribute to extracellular electron transfer by Shewanella oneidensis MR-1 in bioelectrochemical systems. *Sci Rep*, *9*(1), 14959. https://doi.org/10.1038/s41598-019-51452-x

Marsili, E., Baron, D. B., Shikhare, I. D., Coursolle, D., Gralnick, J. A., & Bond, D. R. (2008). Shewanella secretes flavins that mediate extracellular electron transfer. *Proceedings of the National Academy of Sciences*, *105*(10), 3968-3973.

Myers, C. R., & Nealson, K. H. (1988). Bacterial manganese reduction and growth with manganese oxide as the sole electron acceptor. *Science*, *240*(4857), 1319-1321.

Ng, I. S., Guo, Y., Zhou, Y., Wu, J.-W., Tan, S.-I., & Yi, Y.-C. (2018). Turn on the Mtr pathway genes under pLacI promoter in Shewanella oneidensis MR-1. *Bioresources and Bioprocessing*, *5*(1), 35. https://doi.org/10.1186/s40643-018-0221-9

Okamoto, A., Hashimoto, K., & Nealson, K. H. (2014). Flavin redox bifurcation as a mechanism for controlling the direction of electron flow during extracellular electron transfer. *Angew Chem Int Ed Engl*, *53*(41), 10988-10991. https://doi.org/10.1002/anie.201407004

Okamoto, A., Hashimoto, K., Nealson, K. H., & Nakamura, R. (2013). Rate enhancement of bacterial extracellular electron transport involves bound flavin semiquinones. *Proceedings of the National Academy of Sciences*, *110*(19), 7856-7861. https://doi.org/doi:10.1073/pnas.1220823110

Okamoto, A., Kalathil, S., Deng, X., Hashimoto, K., Nakamura, R., & Nealson, K. H. (2014). Cell-secreted flavins bound to membrane cytochromes dictate electron transfer reactions to surfaces with diverse charge and pH. *Scientific reports*, *4*(1), 1-8. https://doi.org/10.1038/srep05628

Okamoto, A., Tokunou, Y., Kalathil, S., & Hashimoto, K. (2017). Proton Transport in the Outer-Membrane Flavocytochrome Complex Limits the Rate of Extracellular Electron Transport. *Angew Chem Int Ed Engl*, *56*(31), 9082-9086. https://doi.org/10.1002/anie.201704241

Okamoto, A., Tokunou, Y., & Saito, J. (2016). Cation-limited kinetic model for microbial extracellular electron transport via an outer membrane cytochrome C complex. *Biophys Physicobiol*, *13*, 71-76. https://doi.org/10.2142/biophysico.13.0_71

Paquete, C. M., Fonseca, B. M., Cruz, D. R., Pereira, T. M., Pacheco, I., Soares, C. M., & Louro, R. O. (2014). Exploring the molecular mechanisms of electron shuttling across the microbe/metal space [Original Research]. *Frontiers in Microbiology*, *5*. https://doi.org/10.3389/fmicb.2014.00318

Pirbadian, S., Barchinger, S. E., Leung, K. M., Byun, H. S., Jangir, Y., Bouhenni, R. A., Reed, S. B.,

Romine, M. F., Saffarini, D. A., & Shi, L. (2014). Shewanella oneidensis MR-1 nanowires are outer membrane and periplasmic extensions of the extracellular electron transport components. *Proceedings of the National Academy of Sciences*, *111*(35), 12883-12888.

Pirbadian, S., Chavez, M. S., & El-Naggar, M. Y. (2020). Spatiotemporal mapping of bacterial membrane potential responses to extracellular electron transfer. *Proceedings of the National Academy of Sciences*, *117*(33), 20171-20179. https://doi.org/doi:10.1073/pnas.2000802117

Prindle, A., Liu, J., Asally, M., Ly, S., Garcia-Ojalvo, J., & Süel, G. M. (2015). Ion channels enable electrical communication in bacterial communities. *Nature*, *527*(7576), 59-63. https://doi.org/10.1038/nature15709

Reguera, G., McCarthy, K. D., Mehta, T., Nicoll, J. S., Tuominen, M. T., & Lovley, D. R. (2005). Extracellular electron transfer via microbial nanowires. *Nature*, *435*(7045), 1098-1101.

Shevchenko, V., Mager, T., Kovalev, K., Polovinkin, V., Alekseev, A., Juettner, J., Chizhov, I., Bamann, C., Vavourakis, C., Ghai, R., Gushchin, I., Borshchevskiy, V., Rogachev, A., Melnikov, I., Popov, A., Balandin, T., Rodriguez-Valera, F., Manstein, D. J., Bueldt, G., Bamberg, E., & Gordeliy, V. (2017). Inward H⁺ pump xenorhodopsin: Mechanism and alternative optogenetic approach. *Science Advances*, *3*(9), e1603187. https://doi.org/doi:10.1126/sciadv.1603187

Shi, L., Chen, B., Wang, Z., Elias, D. A., Mayer, M. U., Gorby, Y. A., Ni, S., Lower, B. H., Kennedy, D. W., Wunschel, D. S., Mottaz, H. M., Marshall, M. J., Hill, E. A., Beliaev, A. S., Zachara, J. M., Fredrickson, J. K., & Squier, T. C. (2006). Isolation of a High-Affinity Functional Protein Complex between OmcA and MtrC: Two Outer Membrane Decaheme c-Type Cytochromes of Shewanella oneidensis MR-1. *Journal of Bacteriology*, *188*(13), 4705-4714. https://doi.org/doi:10.1128/JB.01966-05

Shi, L., Dong, H., Reguera, G., Beyenal, H., Lu, A., Liu, J., Yu, H. Q., & Fredrickson, J. K. (2016). Extracellular electron transfer mechanisms between microorganisms and minerals. *Nat Rev Microbiol*, *14*(10), 651-662. https://doi.org/10.1038/nrmicro.2016.93

Shi, L., Richardson, D. J., Wang, Z., Kerisit, S. N., Rosso, K. M., Zachara, J. M., & Fredrickson, J. K. (2009). The roles of outer membrane cytochromes of Shewanella and Geobacter in extracellular electron transfer. *Environmental microbiology reports*, *1*(4), 220-227.

Song, Y., Cartron, M. L., Jackson, P. J., Davison, P. A., Dickman, M. J., Zhu, D., Huang, W. E., & Hunter, C. N. (2019). Proteorhodopsin Overproduction Enhances the Long-Term Viability of Escherichia coli. *Appl Environ Microbiol*, *86*(1). https://doi.org/10.1128/aem.02087-19

Stratford, J. P., Edwards, C. L. A., Ghanshyam, M. J., Malyshev, D., Delise, M. A., Hayashi, Y., &

Asally, M. (2019). Electrically induced bacterial membrane-potential dynamics correspond to cellular proliferation capacity. *Proc Natl Acad Sci U S A*, *116*(19), 9552-9557. https://doi.org/10.1073/pnas.1901788116

Tokunou, Y., Hashimoto, K., & Okamoto, A. (2015). Extracellular Electron Transport Scarcely Accumulates Proton Motive Force in Shewanella oneidensis MR-1. *Bulletin of the Chemical Society of Japan*, *88*(5), 690-692. https://doi.org/10.1246/bcsj.20140407

Tokunou, Y., Saito, K., Hasegawa, R., Nealson, K. H., Hashimoto, K., Ishikita, H., & Okamoto, A. (2019). Basicity of N5 in semiquinone enhances the rate of respiratory electron outflow in Shewanella oneidensis MR-1. *bioRxiv*, 686493. https://doi.org/10.1101/686493

Zhou, E., Lekbach, Y., Gu, T., & Xu, D. (2022). Bioenergetics and extracellular electron transfer in microbial fuel cells and microbial corrosion. *Current Opinion in Electrochemistry*, *31*, 100830.

Chapter 5 Anomaly detection narrowed down genes identified by whole mutant library screening with carbon electrode-based high-throughput electrochemistry

5.1 Introduction

Extracellular electron transfer (EET) is a type of respiration, which can use extracellular solid electron acceptors (Hernandez & Newman, 2001). Many bacteria in nature can utilize EET to survive under anaerobic conditions. Microbial fuel cells (MFCs) which are based on the EET are a promising way to solve the energy crisis (Logan et al., 2006). However, the EET rate still limits the real application for the MFCs. Exploring the EET limitation is important for developing EET-based technology and understanding the survival mechanism of microorganisms in extreme environments.

The well-studied EET model of bacteria is *Shewanella oneidensis* MR-1, although it is model bacteria, the over 50% gene in *S. oneidensis* MR-1 is still unknown (Deutschbauer et al., 2011). To better understand and control the EET process, exploring the gene which limits EET is an effectivity way to solve this issue. Buz et al. constructed a mutant library that contains whole-genome mutants, a colorimetric assay was used to explore EET genes by screening the whole mutant library in *S. oneidensis* MR-1, a colorless compound AQDS can be reduced to yellow due to AHDS to the EET ability of *S. oneidensis* MR-1 (Baym et al., 2016). However, the mechanism of redox dye reduction is not the same with EET on an electrode, even the MtrC and OmcA mutants show effectiveness on the reduced AQDS. Besides, this colorimetric assay cannot screen the biofilm and nanowire-related EET gene as well.

Herein, a high High-throughput Electrochemistry system was developed in this study for screening the whole mutant library in *S. oneidensis* MR-1. It is rapid to narrow the range of EET-related genes, and also it gives us direct evidence for the factor which limits EET on the electrode surface.

5.2. Materials and Method

5.2.1 High throughput electrochemical system

The high throughput electrode system consisted of the potentiostats control computer, for keeping the anaerobic condition, the high throughput system was installed in an anaerobic chamber. Carbon Ag/AgCl and carbon were used as working electrode (WE) reference electrodes (RF) and counter electrodes (CE) for each well, respectively. 96 wells are independent and each well is an individual three-electrode system, each single potentiostat consists of 96 channels.

5.2.2 Cell preparation

The single colony of *S. oneidensis* MR-1 wild-type strain which was kept in our laboratory was picked from the agar plate and then cultured in Luria-Bertani (LB) medium with 30℃. After 18 hours, cells were washed 2 times by the defined medium (DM; NaHCO3 [2.5 g], CaCl2·2H2O [0.08 g], NH4Cl [1.0 g], MgCl2·6H2O [0.2 g], NaCl [10 g], [HEPES, 7.2 g], 0.5 g yeast extract), and then cells were used to electrochemical experiment after adjusting cell numbers by OD_{600}.

S.oneidensis MR-1 mutant library was kindly given by professor Buz Barstow and was constructed by Sudoku knockout procedure. Mutants were cultured in the 96-well plate in LB medium which contains 50 μg mL−1 kanamycin for 24 hours under 30 ℃ conditions, cells were washed by the defined medium twice using a 96-well plate centrifuge before measuring the OD_{600} by 96-well plate reader. Cells were seeded in the 96-well electrode plate to measure the ability to produce current. After wild-type cells were prepared, cells were diluted into 24 different concentrations from OD_{600} = 1.3 to OD_{600} = 0, before measuring the current production by high throughput electrode system, cells were seeded into the 96-well electrode plate and covered with aluminum cover for avoiding evaporation.

5.2.3 Data analysis

As the 24-hour OD_{600} of mutants varies from each other, it is unreliable to compare current production without consideration of cell numbers. For solving the growth difference problem, the machine learning anomaly detection algorithm used in this study, to detain, the current production of a wild-type different OD_{600} was measured by high throughput electrochemical system to construct an OD-current dependent database, the mutant current production could be compared based on this database.

In the present study, three parameters were used to analyze the EET ability of mutants, 10 hours

of current production 24 hours of current production, and maximum slop. 10 hours is a watershed for current production, the current increased quickly during the 10 hours, and after that, current production becomes stable gradually. The current production is close to the maximum current due to the limitation of carbon sources at 24 hours, so the 24-hour current production was chosen as one of the parameters. Additionally, for making sure the speed of current production, the maximum slope was calculated in this study.

5.3 Results and Discussion

5.3.1 Process for the high throughput system for screening the mutant library

To screen the mutant library, we developed a high-throughput system, the standard procedure is shown in Figure 5-1. In the beginning, mutants were cultured at LB medium for 24 hours at 30 degrees, and then, cells were washed and resuspended by the defined medium before measuring the cell OD with 96 well plate reader. And then cells were transferred to the 96-well electrode plate before putting into the potentiostat, and we can keep monitoring it.

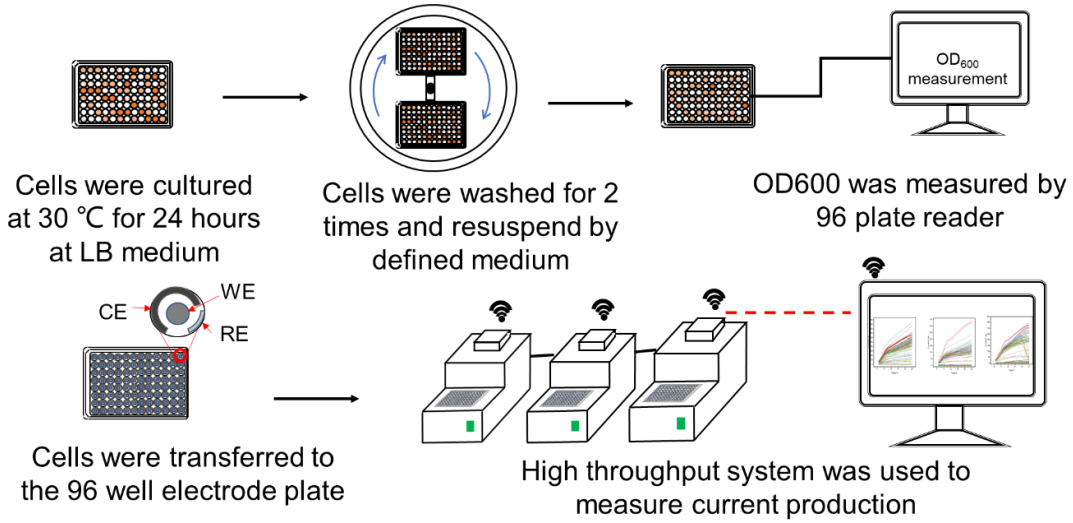

Figure 5-1 Procedure of mutant library screening

5.3.2 The correlation between current production and OD difference

To screen the mutant which shows the anomaly gene, firstly, we optimize the procedure to screen the mutant library, then, the mutant strain in the mutant library was applied to the 96-well high throughput system. Cells were incubated at +200 mV (vs. Ag/AgCl) for 24 hours, the real-time current production was recorded. The result is shown in Figure 5-2A, as time goes on, most strains show an increase in current production. However, compared with the wild type (red line), most of them show low current production. Besides, the current production before 10 hours exhibited a fast increase, and the I_c gradually become stable after 10 hours. To confirm the I_c difference is due to the gene function lost rather than the cell number. We measured the cell OD before the electrochemical measurement. The result is shown in Figure 5-2B, different mutants have different OD, after 24 hours of culture, and some strains OD_{600} = 1.3, however, some strains' OD_{600} is very low, which may be caused by the gene function loss.

Those results suggest that cell number is an issue for I_c measurement in our high throughput system due to the different growth abilities of mutants. It is impossible to directly apply it to measure the whole mutant library. Bacteria genes responses different functions, and, normally, lacking some genes can affect cell growth. However, we have to keep the same OD to measure the current production for screening gene that limits EET. However, adjusting cell OD to the same level is a time-consuming and impossible thing due to over 3000 mutants in the mutant library and the growth rate of some mutants is too low. To successfully use the high throughput system the problem should be solved.

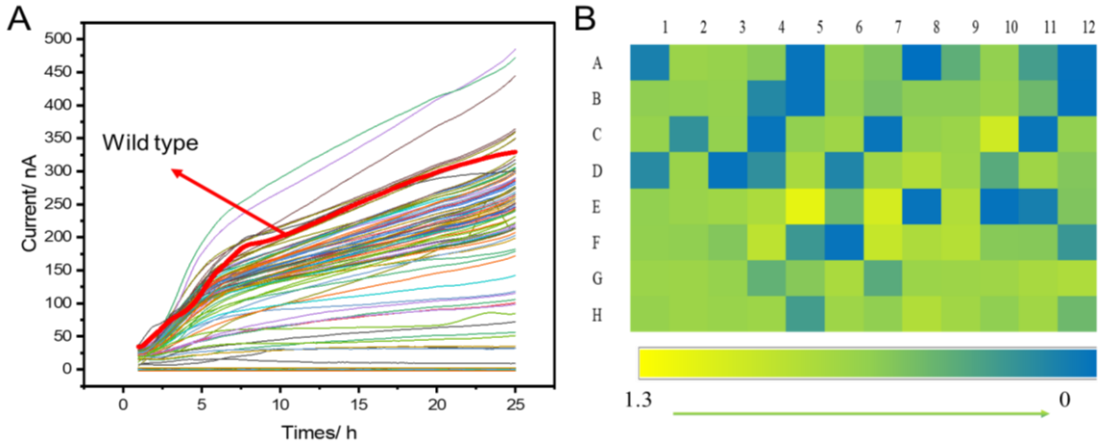

Figure 5-2 Current production and cell growth of mutants. (A) Current production of 96 mutant strains for 25 hours. (B) Cell OD_{600} of 96 mutants after culturing 24 hours.

5.3.3 Cell number dependence on current production

To solve the problem of the different growth effects of the current production in the mutant strain, we use the different cell density gradients to check the current production. As shown in Figure 5-3, the current gradually increased with time dependence. Besides, at a specific time, the current production showed a correlation with cell OD_{600}. After 24 hours the current production gradually stable. Under the high OD_{600} condition, the current production increases fast, which is contributed to the cell numbers. In the beginning, more cells, and high current production, however, due to the consumption of electron donors, the current gradually decreases at 17 hours for the high OD_{600} group.

As we know the cell OD and current production showed a good correlation, so we can use different OD of wild-type current to set a standard database to solve the different growth problems in the mutant strain.

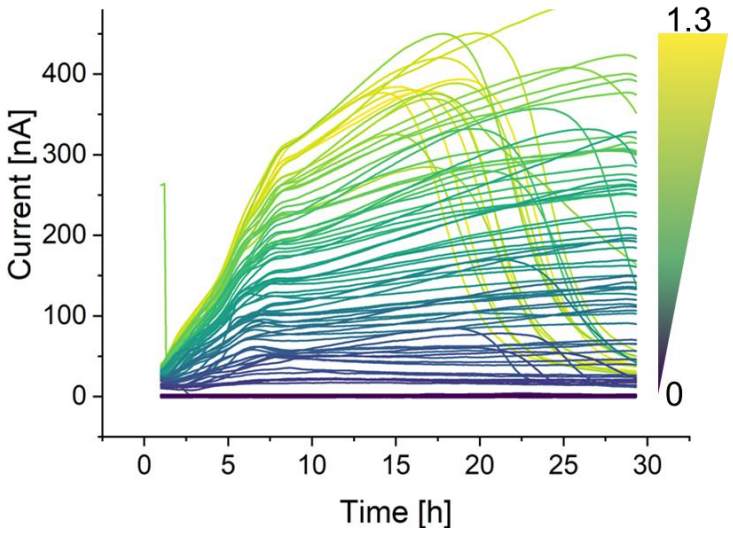

Figure 5-3 Current production of different cell densities in the wild type. Current production with a time curve, the inverted triangle means the cell OD_{600} from 1.3 (top) to 0 (bottom).

5.3.4 Anomaly detection and anomaly threshold

To set the database of current production with cell OD in the wild type. We selected three parameters for constructing the database. Current production at 10 hours, current production at 24 hours, and maximum slop. The reason why we choose these three parameters is as follows, firstly, as shown in Figure 5-4 current production growth is fast before 10 hours, it arrives at the first stable stage, so we choose 10 hours current as the first parameter. After 24 hours, the current production increase rate decreased, which means current production almost arrive at peak current because of the high OD conditions the current production already decrease. The maximum slope shows the maximum current increase rate, which is an important parameter in real applications. So herein, three parameters were used to build the database.

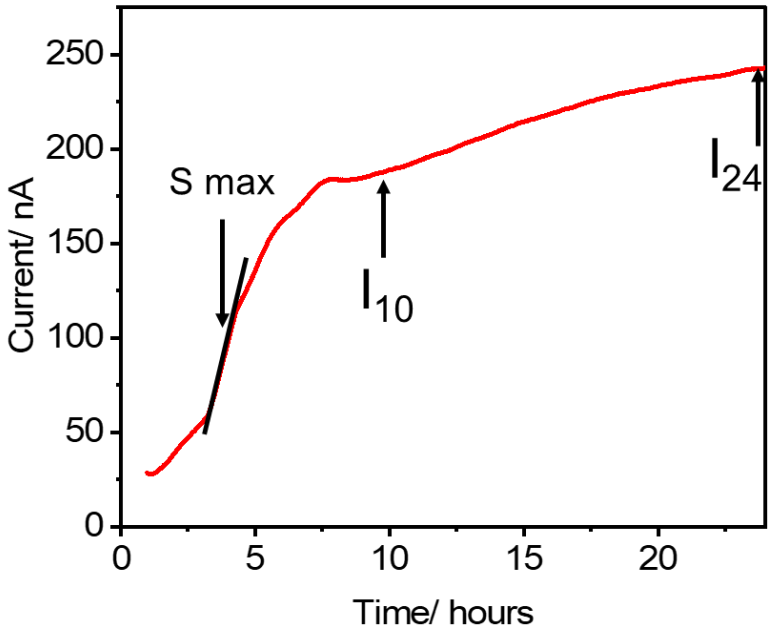

Figure 5-4 Current production of the wild type. *I-t* curve of wild type. Arrows indicated the maximum slop, 10 hours of current production, and 24 hours of production.

Next, we checked the correlation between OD_{600} and three parameters. The results showed three parameters have a good linear relationship with cell OD_{600} (Figure 5-5A, B, and C). we can use these three parameters to set a threshold for specific pick-up mutants which show abnormal current production. For the data analysis, we used the residual sum of squares to set the boundary for normal and abnormal. Herein the RMSE was used for anomaly detection.

Residual=Actual Y value−predicted Y value

$$RMSE = \sqrt{\frac{\sum(\text{residual}^2)}{n-1}}$$

The results shown in Figure 5-5D, RMSE was used to set the upper limit and lower limit by the OD_{600} gradient of current production in wild type (yellow line). Over 1000 mutants were applied to detection, which showed by blue points. Some points beyond the boundary can be considered abnormal genes.

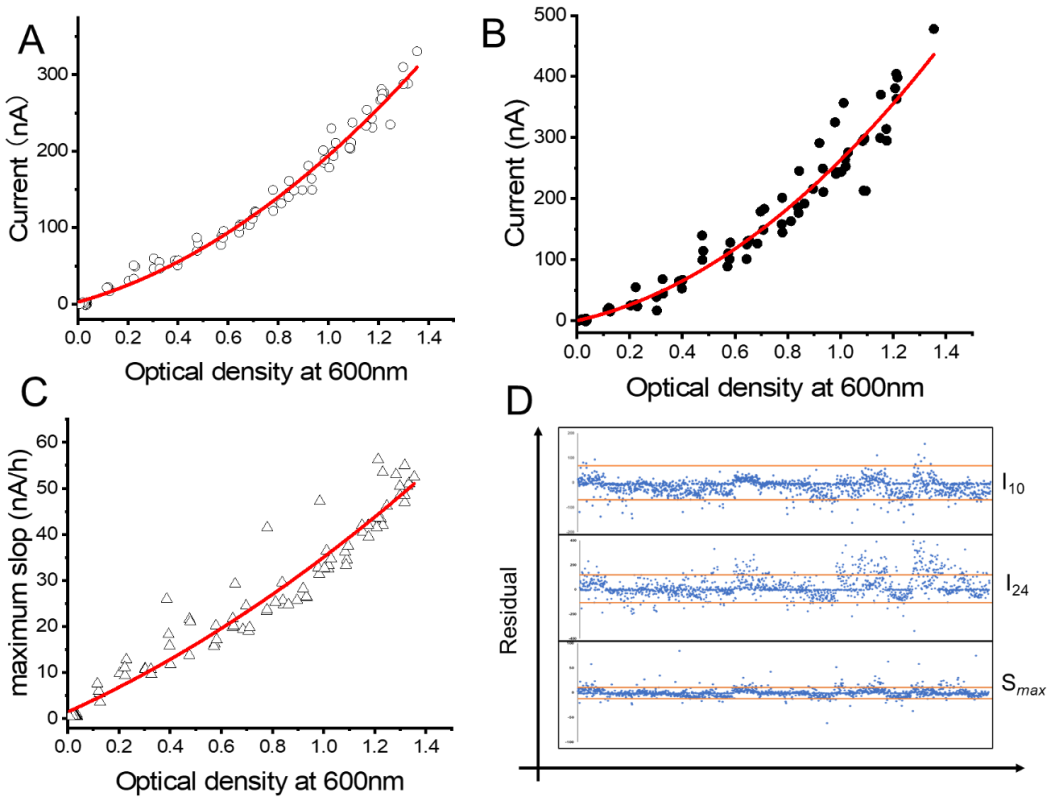

Figure 5-5 Anomaly threshold setting by combining mutant data.

The relationship of different OD_{600} with current production for (A)10 hours, (B) 24 hours, and (C) maximum slope. (D) 1000 mutant strains of I_{10} I_{24} and S_{max} were applied to anomaly detection. The yellow line means the Residual boundary.

5.3.5 The application of anomaly detection on the mutant library

To better visualize the mutant which showed abnormal behaviors in the current production and maximum slope. We show the relationship between current production with OD_{600} and we set the boundary by the anomaly detection described above. As shown in Figure 5-6A, we divide it into 3 parts, the red circle is the high current area, which suggests that the mutant strain shows higher current production than the wild type at the same cell number. The comparable area is the black circle, the mutant that appeared here means they have similar EET ability with the wild type. Meanwhile, the blue circle shows the mutant strain which has lower current production compared with the wild type. To further confirm the feasibility of our system and anomaly detection. The mutant strain Δ*mtrC* was used as the control for low EET ability strain. As expected, the Δ*mtrC* appears at the low current area as pointed out in Figure 6A. Additionally, 24 hours current and maximum slope showed similar results

(Figure 5- 6B, 6C, and 6D).

The mutant strain showed similar results at 10 hours current, 24 hours current, and maximum slope. However, as we can know from the figures low current area, 10 hours of current production showed 56 abnormal mutants, however, the 24 hours of current showed 53 abnormal mutants, besides, the maximum slope has 46 anomaly mutants. Those results mean we cannot use only one parameter to judge the EET ability due to the behavior being different in the three parameters.

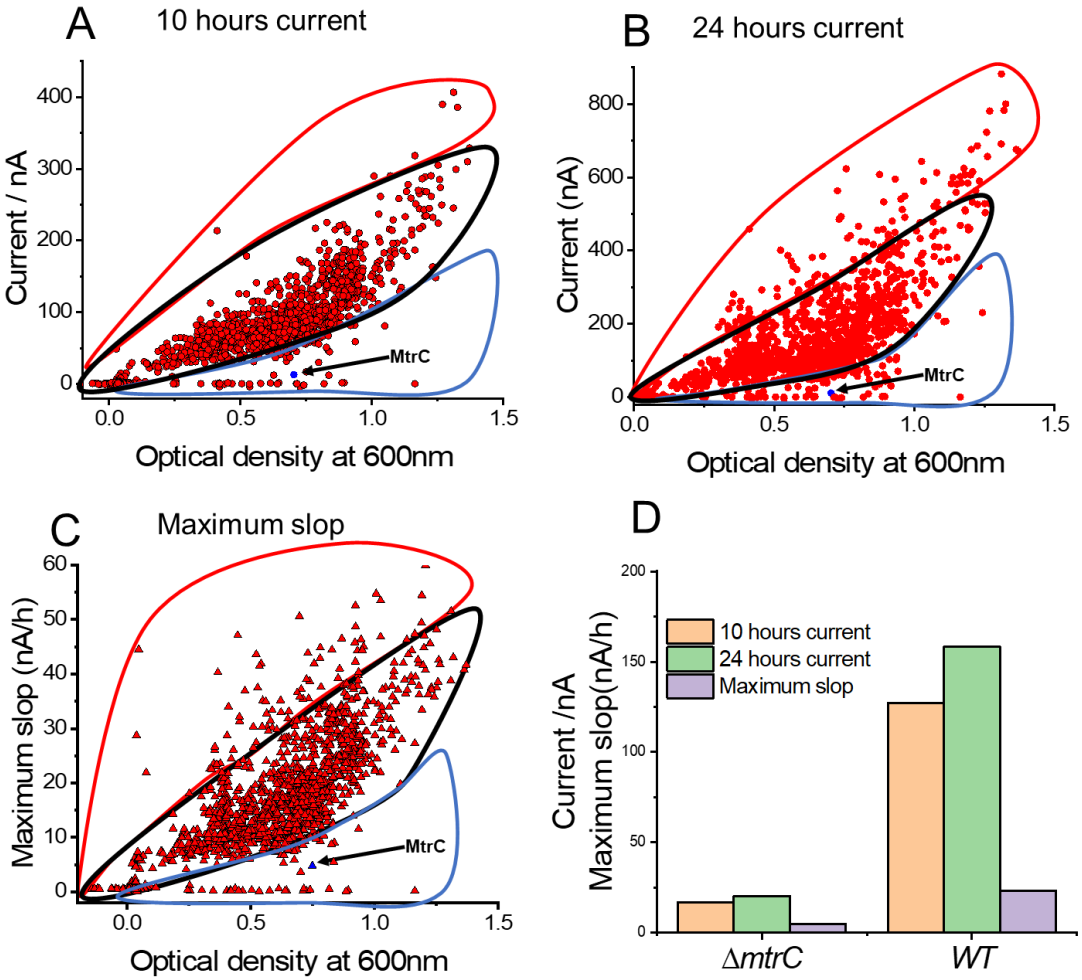

Figure 5-6 Anomaly detection for 1000 mutants.

Compared between mutants and WT of OD with (A) 10 hours current (B) 24 hours current (C) maximum slope. (D) compared between wild with the mutant strain Δ*mtrC*.

5.3.6 Analysis of anomaly genes

For getting more accurate data, we combined three parameters to decrease the error. The result

is shown in Figure 5-7A, 25 mutants appeared in the common area, which means these 25 mutants showed low current all the time. besides, there are 10 mutants shared by the 10 hours current and 24 hours current, the current production is less but the increase rate is similar to the wild type. 7 mutants appeared at 10 hours current and maximum slope, it is unlike the wild type only before10 hours current increased fast, which suggests the current should be kept at a medium increase rate (less than the maximum slope but higher than the slope after 10 hours in wild type) to generate current. There are 14 mutants which are appeared only at 10 hours, for those strains should have a lag time on the current production, and then, after 10 hours it increased fast and arrive at a similar level to the wild type. 17 mutants only appeared at 24 hours current, which may be due to the current decreasing at 24 hours after arriving at the highest current. Some strains may use the electron donor to grow or some other pathway not only for the producing current, so, the current at 24 hours shows low current but the maximum slope and 10 hours current show normal phenomenon.

Additionally, we analyzed the 25 mutants which showed low current production by Gene Ontology for gene function clustering (Figure 5-7B). It shows that those genes are related to some cellular metabolism and also some molecule synthesis, besides, it is also related to quinone and lipid synthesis. Those results provided a lot of information that is new to the EET mechanism.

The gene list shown in table 1 shows low current production. To further confirm the reliability of the high throughput system and anomaly detection. We picked up that gene and then used the traditional electrochemical reactor to verify. Herein, the cell OD_{600} was adjusted to 1, and then, incubated for 24 hours at the ITO electrode (working electrode). The current production shows 15 mutants has low current production in 22 mutants, it is around 70 % similar to the high throughput system. Besides, the working electrode in the 96 well is carbon, but in the traditional reactor is ITO, which may cause the different EET behaviors, so that, 7 mutants may be due to the difference of working electrode.

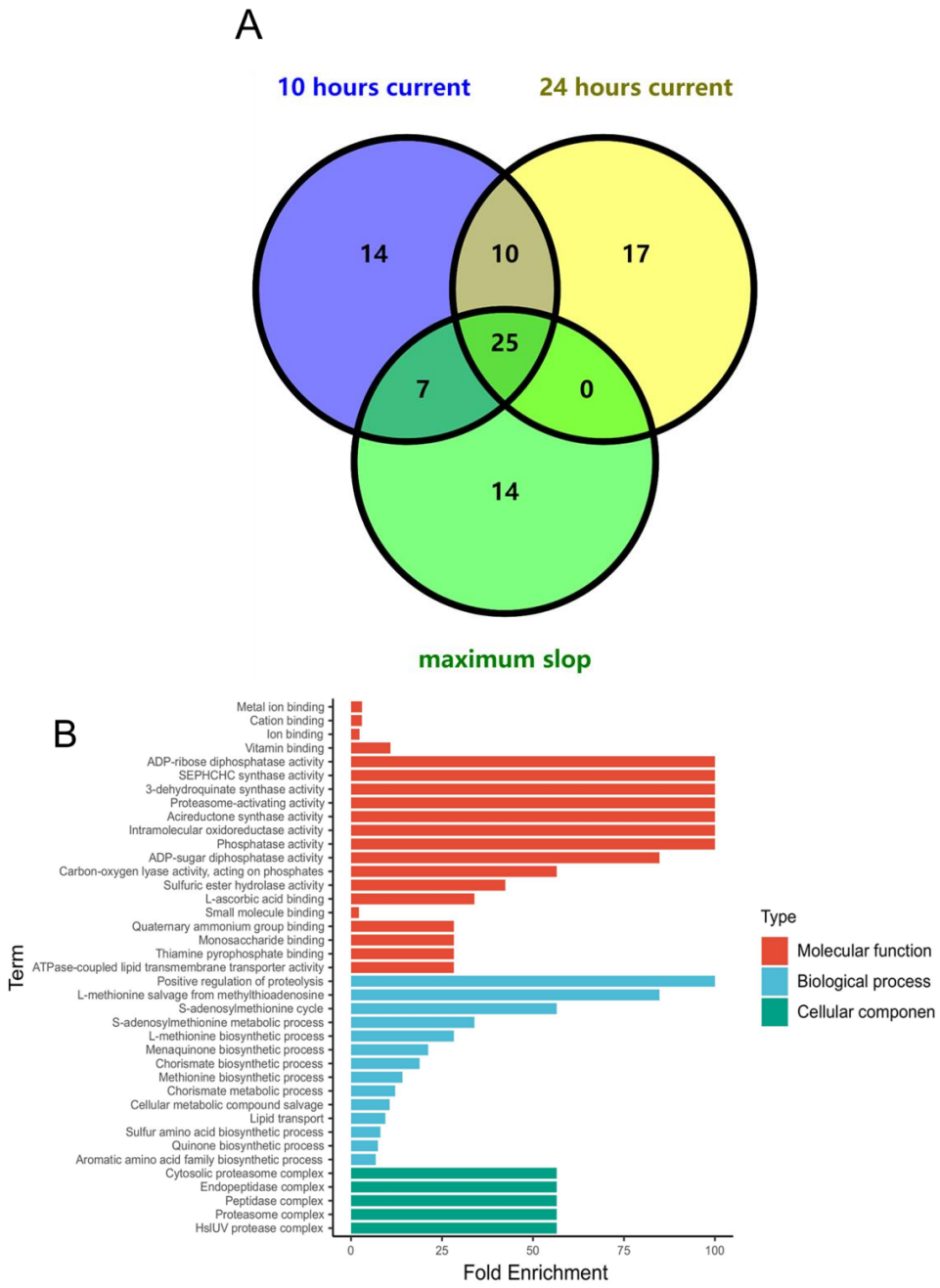

Figure 5-7 Analysis of low current mutants.

(A) Venn diagram showing overlap of genes among three parameters. (B) Gene function clusters of 25 low current production genes.

Table1 mutants which showed low current production

Gene name	Function	Current production (μA)(ITO electrode)
Wild type		6
SO_0997	Transcription cis-regulatory region binding	6
aroB	3-dehydroquinate synthase activity	1
SO_4522	Unkown	5.5
aggC	ABC-type transporter activity	4.5
recR	Metal ion binding	None
menD	Menaquinone biosynthetic	1
SO_3333	Unkown	6.5
SO_4688	Glycosyltransferase	8
yfbQ	Pyridoxal phosphate binding	None
SO_3449	Unknown	4
SO_4520	4 iron, 4 sulfur cluster binding	2
mtnC	Magnesium ion binding	4.13
SO_4681	Glycosyl transferase	5.3
yejM	Sulfuric ester hydrolase	None
cspD	Nucleic acid binding	3.2
hcr	Flavin adenine dinucleotide	3.5
yhcC	4 iron, 4 sulfur cluster	3.57
sirD	Menaquinol oxidase	5
SO_4806	Iron ion binding	2.19
SO_A0141	Unknown	5
mtrC	Electron transfer	1.6
SO_1720	Unknown	6.4
SO_2076	Unknown	6.6
nudF	Metal ion binding	7
hslU	ATP hydrolysis activity	4

We also analyzed the high current production mutants The result is shown in Figure 5-8A, the overlap 5 mutants show that mutants have higher EET ability than the wild type. There only 2 mutants appeared at 10 hours and 24 hours, not the maximum slope, those 2 mutants were kept at a high EET rate for all times so that the maximum slope is normal but the current is higher. 47 mutants appeared at the maximum slope and 24 hours current overlap, which suggests those 47 mutants have a high slope after 10 hours, and after 24 hours current is very high. 31 mutants only appeared at the maximum slope, which may be due to some small noises, because the very small noise will change the maximum slope a lot. 183 mutants only appeared at 24 hours current, as we have seen, the current production can be limited by the lactate concentration, even at the high OD_{600}, the current decreased after the electron donor was consumed. 183 mutants showed high current at 24 hours, maybe some genes in the charge of nutrition distribution, more lactate was used to transfer electrons to the electrode rather than other metabolism or growth.

Additionally, we used Gene Ontology to analyze the 5 genes which can improve the current production.

The results showed some amino acid metabolism pathways can enhance the current production.

The gene list shown in table 2 shows high current production. To further confirm the reliability of the high throughput system and anomaly detection. We picked up 5 mutants and then used the traditional electrochemical reactor to verify. Results showed 3 mutants of 5 mutants have higher current production than the wild type.

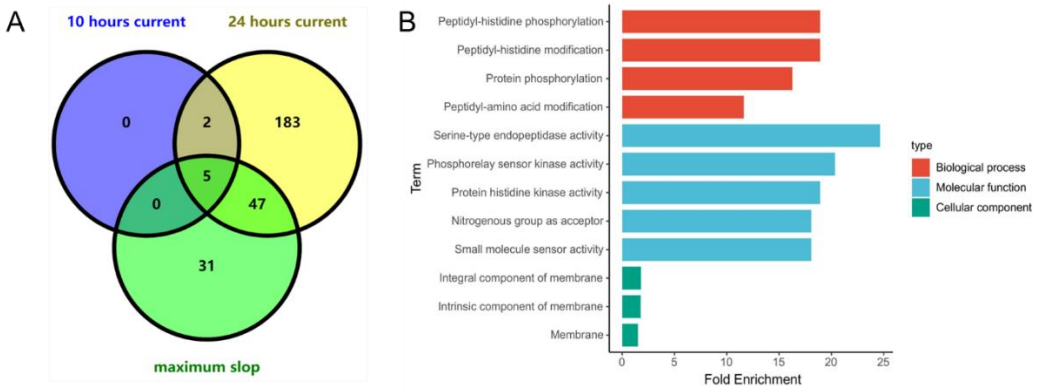

Figure 5-8 Analysis of high current mutants.

(A) Venn diagram showing overlap of genes among three parameters. (B) Gene function clusters of 5 low current production genes.

Table 2 mutants that show high current production

Gene name	Function	Current production (μA)(ITO electrode)
Wild type		6
SO_4488	Histidine phosphorylation	6
pdhR	Transcriptional repressor of Pyruvate metabolism	7.8
SO_A0048	Serine-type endopeptidase activity	8.95
SO_2975	Unknown	7
SO_4366	Unknown	6

5.4 Conclusion

To better understand the EET mechanism and control the EET process, the whole mutant library gene screening is a direct way. In the present study, we developed a high throughput system combined with anomaly detection to narrow down genes which are related to EET. Results showed 25 mutants over 1000 mutants showed a low current production and it was confirmed by the traditional electrochemical reactor, which had similar results. Additionally, 5 mutants showed high current production, which is related to some amino acid metabolism.

Reference

Baym, M., Shaket, L., Anzai, I. A., Adesina, O., & Barstow, B. (2016). Rapid construction of a whole-genome transposon insertion collection for Shewanella oneidensis by Knockout Sudoku. *Nature Communications*, *7*(1), 13270. https://doi.org/10.1038/ncomms13270

Deutschbauer, A., Price, M. N., Wetmore, K. M., Shao, W., Baumohl, J. K., Xu, Z., Nguyen, M., Tamse, R., Davis, R. W., & Arkin, A. P. (2011). Evidence-based annotation of gene function in Shewanella oneidensis MR-1 using genome-wide fitness profiling across 121 conditions. *PLoS Genetics*, *7*(11), e1002385. https://doi.org/10.1371/journal.pgen.1002385

Hernandez, M. E., & Newman, D. K. (2001). Extracellular electron transfer. *Cellular and Molecular Life Sciences CMLS*, *58*(11), 1562-1571. https://doi.org/10.1007/PL00000796

Logan, B. E., Hamelers, B., Rozendal, R., Schröder, U., Keller, J., Freguia, S., Aelterman, P., Verstraete, W., & Rabaey, K. (2006). Microbial Fuel Cells: Methodology and Technology. *Environmental Science & Technology*, *40*(17), 5181-5192. https://doi.org/10.1021/es0605016

Microbial Fuel Cells—Challenges and Applications. (2006). *Environmental Science & Technology*, *40*(17), 5172-5180. https://doi.org/10.1021/es0627592

Chapter 6 General conclusion and future prospects

6.1 Conclusion

In the present study, limitations of extracellular electron transfer have been investigated in the model bacteria *Shewanella oneidensis* MR-1. In this thesis, the study has a large range which is from developing the high throughput electrochemical system to studying the molecular mechanism of flavin enhancement.

Chapter 1 is a general introduction, the basic background was given in this chapter, and the latest research in this field was summarized. Although, extracellular electron transfer was studied a lot, the robustness of bound flavin and genome in model strain bacteria *Shewanella onidensis* MR-1 for current production are still not clear. In this study, 4 strategies were used to address and identify this problem.

Since the fluctuation of potential and solution balance always occurred in the bioelectrochemical system, the stability of current production is unclear. Chapter 2, data science emerges as a promising approach for studying and optimizing complex multivariable phenomena, such as the complex interaction between microorganisms and electrodes. However, there have been limited reports on a bioelectrochemical system that can produce a reliable database to date. Herein, we developed a high-throughput platform with low deviation to apply 2-D Bayesian estimation for electrode potential and redox-active additive concentration to optimize microbial current production (I_c). A 96-channel potentiostat represents <10% standard deviation for maximum I_c. 576 time-I_c profiles were obtained in 120 different electrolyte and potentiostatic conditions with two model electrogenic bacteria, *Shewanella* and *Geobacter*. Acquisition functions showed the highest performance per concentration for riboflavin over a wide potential range in *Shewanella*. The underlying mechanism was validated by electrochemical analysis with mutant strains lacking outer-membrane redox enzymes. We anticipate that the combination of data science and high-throughput electrochemistry will greatly accelerate breakthroughs for carbon-neutral electrochemical technologies.

As we used the high throughput electrochemical to acquire the best performance of the current production enhancement factor by flavin. In chapter 3, we continue to study the molecular mechanism of flavin for enhancing the EET ability of *Shewanella oneidensis* MR-1. Flavin enhances the current production by binding with the outer membrane cytochromes has been proved, however, under some conditions, flavin cannot exhibit the best performance. Herein, the heme redox state inside of outer membrane cytochromes was proved to be a vital factor to affect flavin binding with OMCs. Flavin

lose the ability for increasing the current production when alternative electron acceptors were used for specific oxidizing the heme centers, which suggests that flavin exert the best performance should be in the reduced state of the heme center and keeping the electrode as the sole electron acceptor in MFCs.

Chapter 4 shows the importance of membrane potential on extracellular electron transfer. Membrane potential was considered an indicator for extracellular electron transfer. Herein, we demonstrated the importance of membrane potential on extracellular electron transfer. After the cell membrane was depolarized, the ability of extracellular electron transfer was impaired. However, the EET ability was enhanced by the membrane hyperpolarized. Besides, the proton transporter rhodopsin can enhance the EET ability by the light-activated. Apart from the direct effect, flavin binding with OMCs also can be affected by the membrane potential. The depolarization of the cell membrane also dissociates the flavin with outer membrane cytochromes. This study indicated the extracellular respiration bacteria survival mechanism under different potential environments.

Chapter 5 showed the application of high throughput electrochemical system. To better understand the EET mechanism, it is necessary to explore genes that relate to the EET. Previously due to technical limitations, it is impossible to screen the whole mutant library. In this study, we developed a high-throughput system with anomaly detection to screen the whole mutant library of *Shewanella oneidensis* MR-1. The result showed only 25 over 1000 mutants have lower current production than the wild type, and 5 mutants have higher current production. Besides, the analysis of anomaly genes indicates extracellular electron transfer is related to some biological process. We also used the traditional method to verify the result. In this study, we developed a high throughput system combined with anomaly detection, which greatly narrowed the range for screening genes that limit EET.

In this thesis, we develop a high-throughput method with high reliability to analyze the optimal performance of intermediaries to improve the EET rate. Flavins showed a high range of enhancing current yield. To further analyze the potentiating effect of flavin, it was found that the redox state of heme within the outer membrane cytochrome that controls flavin binding was found. In addition, the membrane potential was found that control the EET rate and flavin binding. Last, we use the high throughput system combined with anomaly detection to screen EET-related genes from the whole mutant library of *Shewanella oneidensis* MR-1. Our studies from the instrument development to the fundamental mechanism aim to explain more about extracellular electron transfer.

6.2 Future prospects

Electrochemical measurement has been investigated for many years, however, currently, the high throughput system applied to the study of extracellular electron transfer is still immature. From our study, we developed a high-throughput system, it breaks the bottleneck of the current electrochemical system. That high throughput system combined with the data sciences for the study of bioelectrochemistry will hugely increase the efficiency of the fundamental study of extracellular electron transfer. Besides, mutant library screening by the high throughput system can provide new insight into the extracellular electron transfer like the coupled metabolism with EET or important genes which control EET rate. For that, we can better understand or utilize EET.

Flavin is a promising additive to enhance the microbial fuel cells (MFCs) power output, the factors which affect semiquinone formation has been explored, and the redox state of heme is a key factor to affect flavin binding, which suggests under the real MFCs system, electron acceptor should not be contained. Besides, the membrane potential also was proved to control flavin disassociation, which broadens the horizon for understanding the EET mechanism, and the potential survival mechanism of microbes employing extracellular electron transfer was revealed.

Acknowledgment

When I write this part, it means that my doctoral dissertation is almost finished, and my Ph.D. is about to graduate. My moods are really complicated, and I can't even describe it in words.

I want to express my sincere gratitude to my supervisor Prof. Okamoto Akihiro. He is the best scientist in my heart. He is really careful thought on the research. When I was confused by some scientific problems. He always gives me useful and pretty solutions. He is really patient and kind, he always explains a problem clearly even though I have asked many times. His attitude towards research deeply affects me, it needs me to learn using all my life. From project design to paper writing, He guides me all the time. I really apricate it that he can provide me with a chance for doctoral study and advanced equipment in the laboratory.

I would like to express my sincere gratitude to my labmates (Ms. Luo Dan, Ms. Ho Chialun, Ms. Yan Kangmin, Ms.Uematsu Miwa, Ms. Yamguchi Chiharu, Dr. Deng Xiao, Dr. Divya Naradasu, Dr. Long Xizi, Dr. Waheed Miran, Dr. Gaku Imamura, Mr. Ihara Souta, and technicians, postdocs in our lab). They are really kind and helped me a lot.

I wish to thank Dr. Dairi Tohru and Dr. Hidenori Noguchi, thanks for giving me some useful suggestions.

I want to thank for National Institute for Materials Science to provide me with NIMS junior fellowship, and thanks to Hokkaido University for providing me with an opportunity for doctoral study.

I want to thank my friends Mr. Cheng Yuanzhao and Dr. Guan Jiawei, and friends in NIMS, I learned a lot from you. I want to thank my parents, grandma, and my sister, I can face the future bravely with your constant love, and I want to be the real man they expect, I'm really grateful that they raised me and taught me a lot.

Last, I would like to thank myself, what you suffer is a real treasure for your future. Never forget the intention, and never give up.

Huang Wenyuan

Ferbrary 2023

Tsukuba Japan